Influence of the structure of the orientation preference map on the responses of V1 neurons

by

James M. Schummers

B.A., Neuroscience
Oberlin College, 1995

Submitted to the Department of Brain and Cognitive Sciences in Partial Fulfillment of the Requirements for the Degree of

Doctor of Philosophy In Neuroscience

at the

Massachusetts Institute of Technology

September 2003

Signature of Author: _____
Department of Brain and Cognitive Sciences
4 September 2003

Certified by: _____
Mriganka Sur
Department Head
Sherman Fairchild Professor of Neuroscience
Thesis Supervisor

Accepted by: _____
Earl K. Miller
Picower Professor of Neuroscience
Chairman, Department Graduate Committee

Influence of the structure of the orientation preference map on the responses of V1 neurons

by

James M. Schummers

Submitted to the Department of Brain and Cognitive Sciences in Partial Fulfillment of the Requirements for the Degree of Doctor of Philosophy in Neuroscience

ABSTRACT

The large majority of inputs to primary visual cortex (V1) neurons arise from the dense local projections of neighboring neurons. Although several proposals have been made, it is not known what role these connections play in shaping the response properties of V1 neurons. It was reasoned that the influence of local inputs on orientation tuning should be different at different locations in the orientation map, because the available data suggest that the orientation composition of the local connections varies with location in the map. In particular, near pinwheel centers, neurons of varying orientation preferences are likely to be connected, whereas far from pinwheel centers, the local connections are likely to only connect similarly tuned neurons. To approach this issue, the responses of neurons at pinwheel centers, and in orientation domains have been compared. The subthreshold responses are found to have much broader orientation tuning near pinwheel centers, reflecting the broader orientation specificity of local connectivity. However, the broad subthreshold inputs are filtered out by the spike threshold and strong inhibition, such that spike tuning is similar at all locations in the orientation map. Spike tuning in pinwheel neurons is found to be sharp during the entire timecourse of the response, suggesting that the mechanism that sharpens the broad inputs is rapid and stable. The broad connectivity near pinwheel centers also leads to correlated firing between pairs of neurons with widely different orientation preferences. Thus, the local inputs to a V1 neuron depend on its location in the orientation map, but the inputs are filtered to produce sharp orientation tuning, regardless of the selectivity of the inputs.

Thesis Supervisor: Mriganka Sur

Title: Sherman Fairchild Professor of Neuroscience

ACKNOWLEGEMENTS

Thanks to:

Mriganka for all of his support, encouragement and trust

My committee – Earl, Matt and Sacha

Jorge – the perfect collaborator and great friend

Jeetu for teaching me the ropes early on, and everything since

The rest of the Sur lab members, past and present for all of the discussions, collaborations, and good times

Javid and Sayan for going through all this with me

Gadi for all the coffee and discussions

HHMI for supporting me

Christine , Casey, Jen, Tara, and a long list of other administrators in the Sur lab that made things go smoothly

Adrienne for being in my life

My parents for their love and support

George Wright and Denny Smith for inspiration in my early years

Table of Contents

Chapter 1: Introduction

General introduction

A key problem in understanding the functioning of brain circuits is to describe the relationship between structure and function at the level of neurons. That is to say, what is the relationship between the inputs to a neuron, and the functionally relevant behavior (electrical activity) it produces? In cortex, this can be an extremely difficult relationship to establish, due to the enormous number of connections, and the complexity of the cortical circuits. In higher order 'association' areas the complex inter-connectivity of inter- and intra-areal connections makes the task of defining both the inputs to, and the function of, a neuron exceedingly difficult. In primary sensory cortical areas, the task is somewhat more tractable, because there is a reproducible mapping between the cortical response, and inputs from peripheral sensory organs.

Several general principles of sensory cortical representation have emerged which have been found to apply across sensory modalities. Sensory neurons are thought to extract different features of the stimulus and process them relatively independently of each other. This principle can be seen experimentally as the selectivity of neural responses; sensory neurons are tuned along specific dimensions in stimulus feature space (eg somatotopic location, acoustic frequency or line orientation). Further, neurons sharing similar tuning for a particular stimulus feature are grouped spatially, forming continuous "maps" of stimulus features across cortical space. Maps of sensory features provide excellent conditions to study the relationship between inputs and outputs. Because of the orderly arrangement of both the functional response properties, and the anatomical projections from subcortical nuclei, the behavior of individual neurons can be compared to the population responses of the cortical region in which they sit.

Maps of stimulus features have perhaps been most extensively studied in the visual cortex. In the primary visual cortex (V1), neurons respond selectively to such stimulus features as edge orientation, spatial frequency, ocular dominance, retinal position and direction of movement, and preference for each of these stimulus features is mapped across the cortical surface (Hubel and Wiesel, 1962; Hubener et al., 1997). The cortical population response to a stimulus of any particular orientation consists of patches (300-500 μm) of high responsivity spaced at regular intervals across the cortex, termed orientation domains (Bonhoeffer and Grinvald, 1991; Blasdel, 1992). The orientation domains representing all orientations converge at singularity points, termed

pinwheel centers. Pinwheel centers are tiled at regular intervals across the cortical surface, with the spokes that connect them containing neurons that prefer a single orientation. Anatomical tracer studies have shown that the orientation domains for each orientation are reciprocally connected by a network of long-range (>1mm) horizontal connections (Gilbert and Wiesel, 1989; Bosking et al., 1997; Kisvarday et al., 1997; Yousef et al., 1999; Yousef et al., 2001). The orientation map provides an excellent opportunity to study the relationship between anatomical connections and response properties. Due to the regular progression of population response properties, which can be readily mapped with optical imaging techniques, and the extensive literature describing the anatomical connections between neurons across the orientation map (see below), both the pattern of connectivity and response properties can be approximated fairly well. Thus, by recording the response properties of individual neurons in detail, within the framework of the population response and connectivity in which they are embedded can potentially provide deep insight into the determination of functional properties by structural arrangements. Further, the pinwheel structure of the orientation map provides the opportunity to study the behavior of neurons at diverse locations in the map, where the functional layout follows different patterns.

Layout of the introduction

This thesis is aimed at studying two conceptually reciprocal issues: the influence of the pinwheel structure on the response properties of individual neurons located at different locations within the map, and the integration of synaptic inputs by visual cortical neurons, which can be dissociated by studying neurons at different locations within the orientation map. Optical imaging of the layout of orientation preference map and several electrophysiological techniques have been combined (Mari o et al., 2003) in order to ask how the response properties of neurons are related to the inputs they receive, which in turn depends on their position within the orientation preference map.

Background information related to the issues examined in this thesis is broken into two main topics, discussed below. *Mechanisms of orientation selectivity in V1*: the results of the experiments described in this thesis do not directly address the mechanisms responsible for the transformation of un-oriented receptive fields in the visual thalamus (LGN) to the oriented receptive fields in V1. Nonetheless, the issues related to the mechanisms of orientation selectivity have largely shaped the direction of research in the field, and provide a useful backdrop to many of the issues discussed

throughout the thesis. *Anatomical connectivity underlying orientation maps*: to a large extent, this thesis will attempt to examine the physiological manifestations of connectivity between neurons within the orientation map. There exists a large literature on the anatomical connectivity related to orientation selectivity in V1. This thesis will complement these anatomical studies by exploring the physiological significance of the patterns of anatomical connections in relation to the orientation map. Indeed the orientation map in V1 provides a rare opportunity to make a strong evaluation of the functional structure-function relationships related to the neural representation of sensory stimuli.

Mechanisms of orientation selectivity

The emergence of orientation selectivity in the responses of V1 neurons has been examined extensively for several decades, but no consensus has been reached as to the mechanism(s) responsible. Three classes of models have been proposed, and each has received some experimental support, thus giving rise to considerable controversy. The 'feed-forward model' proposes that the selectivity of a first order cortical neuron arises linearly as a consequence of a collinear arrangement of the receptive fields of the thalamic neurons which drive it (Hubel and Wiesel, 1962). The 'cross-inhibition model' proposes that the net thalamic input to a cortical neuron is largely unselective, and the responses to 'non-optimal' orientations are cancelled by inhibitory inputs from other cortical neurons with orthogonal preferred (Sillito, 1975; Morrone et al., 1982; Bonds, 1989). The 'recurrent model' proposes that there is a mild orientation bias in the thalamic input to a cortical neuron, which becomes amplified by excitatory local cortical inputs from other neurons in the same cortical column, which are assumed to share the same orientation preference (Ben-Yishai et al., 1995; Douglas et al., 1995; Somers et al., 1995; Carandini and Ringach, 1997).

There is now substantial empirical evidence that the feed-forward thalamic input to a V1 neuron is indeed specifically aligned along the axis of its preferred orientation, and that this bias is sufficient to confer *some* orientation selectivity on V1 neurons (Chapman et al., 1991; Reid and Alonso, 1995). However, while this bias can account for the preferred orientation of a cell, it is not clear whether it is sufficient to account for the sharpness of tuning (Volgushev et al., 1996; Gardner et al., 1999, though see Lampl et al., 2001). Analysis of the dynamics of V1 cell responses has demonstrated that the subthreshold and spiking responses to a flashed bar or grating develop with time, often

becoming sharper during the first 20-50 msec (Volgushev et al., 1995; Ringach et al., 1997; Shevelev et al., 1998), consistent with a cortical mechanism which amplifies and/or suppresses responses to particular orientations.

Experiments intended to disable the recurrent cortical inputs to simple cells, by either cooling or shocking the cortex, have found that the remaining synaptic inputs, presumed to be thalamic in origin, are sufficient to generate orientation selective responses (Ferster et al., 1996; Chung and Ferster, 1998). However, numerous other experiments that have manipulated the activity of the local and/or long-range cortical network, pharmacologically, or with visual manipulations, *have* found changes in the orientation selectivity of V1 neurons (Sillito, 1975; Morrone et al., 1982; Eysel et al., 1990; Gilbert and Wiesel, 1990; Knierim and van Essen, 1992; Crook et al., 1997; Toth et al., 1997; Crook et al., 1998; Dragoi et al., 2000; Schuett et al., 2001).

Intracellular recordings of the subthreshold synaptic activity underlying the visual response have the potential to test predictions made by these models, because they allow the measurement of both excitatory and inhibitory inputs to a neuron. Unfortunately, several reports of intracellular studies have provided conflicting results. Ferster and colleagues (Ferster, 1986, 1987; Anderson et al., 2000) found that inhibition is strongest at the preferred orientation. Furthermore, Nelson et al (1994) found that blocking inhibition did not change orientation tuning (Nelson et al., 1994). On the other hand, other groups found this to be true for only some neurons, but also found many neurons for which inhibition was strongest at non-optimal orientations (Volgushev et al., 1993; Pei et al., 1994; Volgushev et al., 1995; Monier et al., 2003). This lack of a consistent pattern of epsps and ipsps has led to the proposal that V1 neurons may not all generate orientation selectivity by the same mechanism (Vidyasagar et al., 1996). Additional support for this hypothesis comes from analysis of the transformation from epsp to spike, which has shown diversity in this relationship as well (Volgushev et al., 2000). Thus, despite strong evidence in its support, the feed-forward model fails to account for the results of numerous studies, indicating strongly that cortical mechanisms play an important role in shaping the response properties of V1 neurons. It remains unclear however what the relative contributions of excitation and inhibition are, and to what extent variability of reported mechanisms reflects a true diversity of mechanisms employed by different neurons.

The study of the initial emergence of selectivity in first order, thalamic-recipient, simple cells has consumed the field for the last several decades. It has been largely

assumed that the responses of non-thalamic-recipient cells derive simply from feed-forward "vertical" inputs, as originally proposed by Hubel and Wiesel (1962). There is some support for the "vertical" propagation from layer IV simple cells to layer II/III complex cells (Chapman et al., 1991; Alonso and Martinez, 1998; Martinez and Alonso, 2001), but this data does not demonstrate a clean one-to-one transfer of orientation selectivity. Furthermore, there are numerous sources of inputs to super- and infra-granular layers, including local and long range intrinsic projections, callossal, and feedback projections from higher cortical areas. Regardless of the cellular mechanisms that generate selectivity in thalamic-recipient simple cells, the remainder of the inputs to simple cells (which constitute the majority) must maintain the selectivity of the cell. Similarly for complex cells, even if the selectivity is largely determined by vertical projections from simple cells, the selectivity must not be corrupted by the other inputs they receive, which are quite numerous, and derive from diverse sources.

Thus, the question of the generation of orientation selectivity for both first and second order V1 neurons, boils down to the question of how these neurons integrate their various inputs to yield sharply tuned spiking responses. Few studies have taken into account the structure of the orientation map to inform the analysis of the generation of orientation selectivity. However, information about the map location, together with known patterns of connectivity relative to the map, can provide both constraints and clues to nature of the process. By recording the activity of neurons at different map locations, one can potentially gain additional insight into the integration of inputs and the shaping of response tuning.

Orientation maps and intrinsic V1 connectivity

Little work to date has attempted to incorporate information about the structure of the orientation map into models of orientation selectivity (though see McLaughlin et al., 2000). Yet, the orientation map creates a fundamental inhomogeneity in the nature of the recurrent inputs impinging on V1 neurons. The orientation map is characterized by pinwheel centers, around which all orientations are represented radially, situated periodically between orientation domains, across which the preferred orientation changes smoothly and gradually (Bonhoeffer and Grinvald, 1991; Blasdel, 1992). It is thought that horizontal connections serve as the anatomical substrate for this organization of functional responses, based largely on the finding that long-range projections form patchy terminal fields, which preferentially connect domains sharing the

same orientation preference (Gilbert and Wiesel, 1989; Bosking et al., 1997; Kisvarday et al., 1997). The similar developmental timecourse of long-range projections and the orientation map lends support to this hypothesis (Durack and Katz, 1996). However, short range projections are spatially isotropic, and do not appear to be constrained by the architecture of the orientation (Malach et al., 1993; Bosking et al., 1997; Kisvarday et al., 1997; Yousef et al., 2001). Thus, the orientation representation of the local inputs to a neuron most likely depends on the location in the map, raising the question of whether neurons in heterogeneous portions of the map (near pinwheel centers) are sharply tuned for orientation. If local recurrent connections play a significant role in determining the response properties of neurons, as they do in both the 'cross-inhibition model' and the 'recurrent model', one would expect differences in the orientation tuning of neurons in different map locations. Even if the feed-forward model is essentially correct, differences in the tuning properties might be expected, because the local cortical inputs, which provide a significant portion of the drive to both simple and complex cells, would differ greatly. Maldonado et al (1997) compared the tuning curves of neurons in pinwheel centers with those in orientation domains, and found no difference.

Figure 1 shows a representation of a reasonable estimate of the orientation representation likely to provide inputs to two neurons, one at a pinwheel center and one in the center of an orientation domain. Panel A show an orientation map with two circles (400 μm radius) centered on a pinwheel center (left) and an orientation domain (right). Anatomical and physiological evidence suggests that the region enclosed in these circles is likely to provide the majority of intrinsic inputs to each cell (Hata et al., 1991; Malach et al., 1993; Weliky et al., 1995; Bosking et al., 1997; Roerig and Chen, 2002; Tucker and Katz, 2003). As can be seen in panel B, this architecture results in completely different selectivity in the local inputs impinging on neurons at pinwheel centers and orientation domains. Despite this difference, the firing rate tuning curves of neurons located at these two locations are almost indistinguishable (panel C). Thus, a fundamental question that remains to be answered, is what differences are there in the response properties of neurons located at different locations of the map which reflect the differences in local inputs at these map locations?

Thesis aims

Therefore, this thesis will be aimed at investigating the processing of oriented stimuli by neurons at different locations within the orientation preference map in cat V1.

Network and analytical models of orientation tuning have assumed all neurons to be identical units, with identical inputs (though shifted to the preferred orientation of each cell). Thus, the mechanisms generating orientation tuning have generally been treated as identical for all neurons. The patterns of connectivity, derived from anatomical studies, indicate that this is not an accurate description of the situation in vivo. Similarly, most electrophysiological studies have attempted to describe the prototypical neuron, and derive mechanisms responsible for orientation tuning from "average" neural behavior. However, studies that have explicitly attempted to look for diversity in the orientation tuning of individual neurons have found large diversity in the orientation tuning behavior. Intracellular recordings of the orientation selectivity of membrane potential responses have led two groups to propose that there may be a diversity of mechanisms responsible for orientation tuning (Vidyasagar et al., 1996; Monier et al., 2003). It has only recently received attention that the pinwheel structure of the orientation preference map may be an important source of diversity responsible for these differences (McLaughlin et al., 2000; Shelley et al., 2002; Kang et al., 2003). However, this possibility has yet to be tested experimentally.

Three specific hypotheses will be tested in this thesis. 1) The synaptic inputs to V1 neurons largely represent the orientation representation in the local patch of cortex surrounding them. The synaptic inputs to neurons near pinwheel centers will therefore be more broadly tuned than the inputs to neurons located far from pinwheel centers (in orientation domains). 2) Dynamic changes in orientation selectivity over the timecourse of the visual response will be more common, and more pronounced in neurons situated near pinwheel centers. 3) The correlated firing of pairs of neurons, which is presumed to result from common synaptic inputs, will also reflect the orientation representation of the putative common local inputs, which should differ as a function of location in the orientation map.

REFERENCES

Alonso JM, Martinez LM (1998) Functional connectivity between simple cells and complex cells in cat striate cortex. Nat Neurosci 1:395-403.

Anderson JS, Carandini M, Ferster D (2000) Orientation tuning of input conductance, excitation, and inhibition in cat primary visual cortex. J Neurophysiol 84:909-926.

Ben-Yishai R, Bar-Or RL, Sompolinsky H (1995) Theory of orientation tuning in visual cortex. Proc Natl Acad Sci U S A 92:3844-3848.

Blasdel GG (1992) Orientation selectivity, preference, and continuity in monkey striate cortex. J Neurosci 12:3139-3161.

Bonds AB (1989) Role of inhibition in the specification of orientation selectivity of cells in the cat striate cortex. Vis Neurosci 2:41-55.

Bonhoeffer T, Grinvald A (1991) Iso-orientation domains in cat visual cortex are arranged in pinwheel- like patterns. Nature 353:429-431.

Bosking WH, Zhang Y, Schofield B, Fitzpatrick D (1997) Orientation selectivity and the arrangement of horizontal connections in tree shrew striate cortex. J Neurosci 17:2112-2127.

Carandini M, Ringach DL (1997) Predictions of a recurrent model of orientation selectivity. Vision Res 37:3061-3071.

Chapman B, Zahs KR, Stryker MP (1991) Relation of cortical cell orientation selectivity to alignment of receptive fields of the geniculocortical afferents that arborize within a single orientation column in ferret visual cortex. J Neurosci 11:1347-1358.

Chung S, Ferster D (1998) Strength and orientation tuning of the thalamic input to simple cells revealed by electrically evoked cortical suppression. Neuron 20:1177-1189.

Crook JM, Kisvarday ZF, Eysel UT (1997) GABA-induced inactivation of functionally characterized sites in cat striate cortex: effects on orientation tuning and direction selectivity. Vis Neurosci 14:141-158.

Crook JM, Kisvarday ZF, Eysel UT (1998) Evidence for a contribution of lateral inhibition to orientation tuning and direction selectivity in cat visual cortex: reversible inactivation of functionally characterized sites combined with neuroanatomical tracing techniques. Eur J Neurosci 10:2056-2075.

Douglas RJ, Koch C, Mahowald M, Martin KA, Suarez HH (1995) Recurrent excitation in neocortical circuits. Science 269:981-985.

Dragoi V, Sharma J, Sur M (2000) Adaptation-induced plasticity of orientation tuning in adult visual cortex. Neuron 28:287-298.

Durack JC, Katz LC (1996) Development of horizontal projections in layer 2/3 of ferret visual cortex. Cereb Cortex 6:178-183.

Eysel UT, Crook JM, Machemer HF (1990) GABA-induced remote inactivation reveals cross-orientation inhibition in the cat striate cortex. Exp Brain Res 80:626-630.

Ferster D (1986) Orientation selectivity of synaptic potentials in neurons of cat primary visual cortex. J Neurosci 6:1284-1301.

Ferster D (1987) Origin of orientation-selective EPSPs in simple cells of cat visual cortex. J Neurosci 7:1780-1791.

Ferster D, Chung S, Wheat H (1996) Orientation selectivity of thalamic input to simple cells of cat visual cortex. Nature 380:249-252.

Gardner JL, Anzai A, Ohzawa I, Freeman RD (1999) Linear and nonlinear contributions to orientation tuning of simple cells in the cat's striate cortex. Vis Neurosci 16:1115-1121.
Gilbert CD, Wiesel TN (1989) Columnar specificity of intrinsic horizontal and corticocortical connections in cat visual cortex. J Neurosci 9:2432-2442.
Gilbert CD, Wiesel TN (1990) The influence of contextual stimuli on the orientation selectivity of cells in primary visual cortex of the cat. Vision Res 30:1689-1701.
Hata Y, Tsumoto T, Sato H, Tamura H (1991) Horizontal interactions between visual cortical neurones studied by cross-correlation analysis in the cat. J Physiol 441:593-614.
Hubel DH, Wiesel TH (1962) Receptive fields, binocular interaction and functional architecture of the cat's visual cortex. J Physiol 160:106-154.
Hubener M, Shoham D, Grinvald A, Bonhoeffer T (1997) Spatial relationships among three columnar systems in cat area 17. J Neurosci 17:9270-9284.
Kang K, Shelley M, Sompolinsky H (2003) Mexican hats and pinwheels in visual cortex. Proc Natl Acad Sci U S A 100:2848-2853.
Kisvarday ZF, Toth E, Rausch M, Eysel UT (1997) Orientation-specific relationship between populations of excitatory and inhibitory lateral connections in the visual cortex of the cat. Cereb Cortex 7:605-618.
Knierim JJ, van Essen DC (1992) Neuronal responses to static texture patterns in area V1 of the alert macaque monkey. J Neurophysiol 67:961-980.
Lampl I, Anderson JS, Gillespie DC, Ferster D (2001) Prediction of orientation selectivity from receptive field architecture in simple cells of cat visual cortex. Neuron 30:263-274.
Malach R, Amir Y, Harel M, Grinvald A (1993) Relationship between intrinsic connections and functional architecture revealed by optical imaging and in vivo targeted biocytin injections in primate striate cortex. Proc Natl Acad Sci U S A 90:10469-10473.
Mari o J, Schummers J, Sur M (2003) [Combination of new electrophysiological and imaging techniques in the study of primary visual cortex function]. Rev Neurol 36:944-950.
Martinez LM, Alonso JM (2001) Construction of complex receptive fields in cat primary visual cortex. Neuron 32:515-525.
McLaughlin D, Shapley R, Shelley M, Wielaard DJ (2000) A neuronal network model of macaque primary visual cortex (V1): orientation selectivity and dynamics in the input layer 4Calpha. Proc Natl Acad Sci U S A 97:8087-8092.
Monier C, Chavane F, Baudot P, Graham LJ, Fregnac Y (2003) Orientation and direction selectivity of synaptic inputs in visual cortical neurons: a diversity of combinations produces spike tuning. Neuron 37:663-680.
Morrone MC, Burr DC, Maffei L (1982) Functional implications of cross-orientation inhibition of cortical visual cells. I. Neurophysiological evidence. Proc R Soc Lond B Biol Sci 216:335-354.
Nelson S, Toth L, Sheth B, Sur M (1994) Orientation selectivity of cortical neurons during intracellular blockade of inhibition. Science 265:774-777.
Pei X, Vidyasagar TR, Volgushev M, Creutzfeldt OD (1994) Receptive field analysis and orientation selectivity of postsynaptic potentials of simple cells in cat visual cortex. J Neurosci 14:7130-7140.
Reid RC, Alonso JM (1995) Specificity of monosynaptic connections from thalamus to visual cortex. Nature 378:281-284.
Ringach DL, Hawken MJ, Shapley R (1997) Dynamics of orientation tuning in macaque primary visual cortex. Nature 387:281-284.

Roerig B, Chen B (2002) Relationships of local inhibitory and excitatory circuits to orientation preference maps in ferret visual cortex. Cereb Cortex 12:187-198.
Schuett S, Bonhoeffer T, Hubener M (2001) Pairing-induced changes of orientation maps in cat visual cortex. Neuron 32:325-337.
Shelley M, McLaughlin D, Shapley R, Wielaard J (2002) States of high conductance in a large-scale model of the visual cortex. J Comput Neurosci 13:93-109.
Shevelev IA, Eysel UT, Lazareva NA, Sharaev GA (1998) The contribution of intracortical inhibition to dynamics of orientation tuning in cat striate cortex neurons. Neuroscience 84:11-23.
Sillito AM (1975) The contribution of inhibitory mechanisms to the receptive field properties of neurones in the striate cortex of the cat. J Physiol 250:305-329.
Somers DC, Nelson SB, Sur M (1995) An emergent model of orientation selectivity in cat visual cortical simple cells. J Neurosci 15:5448-5465.
Toth LJ, Kim DS, Rao SC, Sur M (1997) Integration of local inputs in visual cortex. Cereb Cortex 7:703-710.
Tucker TR, Katz LC (2003) Spatiotemporal patterns of excitation and inhibition evoked by the horizontal network in layer 2/3 of ferret visual cortex. J Neurophysiol 89:488-500.
Vidyasagar TR, Pei X, Volgushev M (1996) Multiple mechanisms underlying the orientation selectivity of visual cortical neurones. Trends Neurosci 19:272-277.
Volgushev M, Vidyasagar TR, Pei X (1995) Dynamics of the orientation tuning of postsynaptic potentials in the cat visual cortex. Vis Neurosci 12:621-628.
Volgushev M, Vidyasagar TR, Pei X (1996) A linear model fails to predict orientation selectivity of cells in the cat visual cortex. J Physiol 496:597-606.
Volgushev M, Pernberg J, Eysel UT (2000) Comparison of the selectivity of postsynaptic potentials and spike responses in cat visual cortex. Eur J Neurosci 12:257-263.
Volgushev M, Pei X, Vidyasagar TR, Creutzfeldt OD (1993) Excitation and inhibition in orientation selectivity of cat visual cortex neurons revealed by whole-cell recordings in vivo. Vis Neurosci 10:1151-1155.
Weliky M, Kandler K, Fitzpatrick D, Katz LC (1995) Patterns of excitation and inhibition evoked by horizontal connections in visual cortex share a common relationship to orientation columns. Neuron 15:541-552.
Yousef T, Toth E, Rausch M, Eysel UT, Kisvarday ZF (2001) Topography of orientation centre connections in the primary visual cortex of the cat. Neuroreport 12:1693-1699.
Yousef T, Bonhoeffer T, Kim DS, Eysel UT, Toth E, Kisvarday ZF (1999) Orientation topography of layer 4 lateral networks revealed by optical imaging in cat visual cortex (area 18). Eur J Neurosci 11:4291-4308.

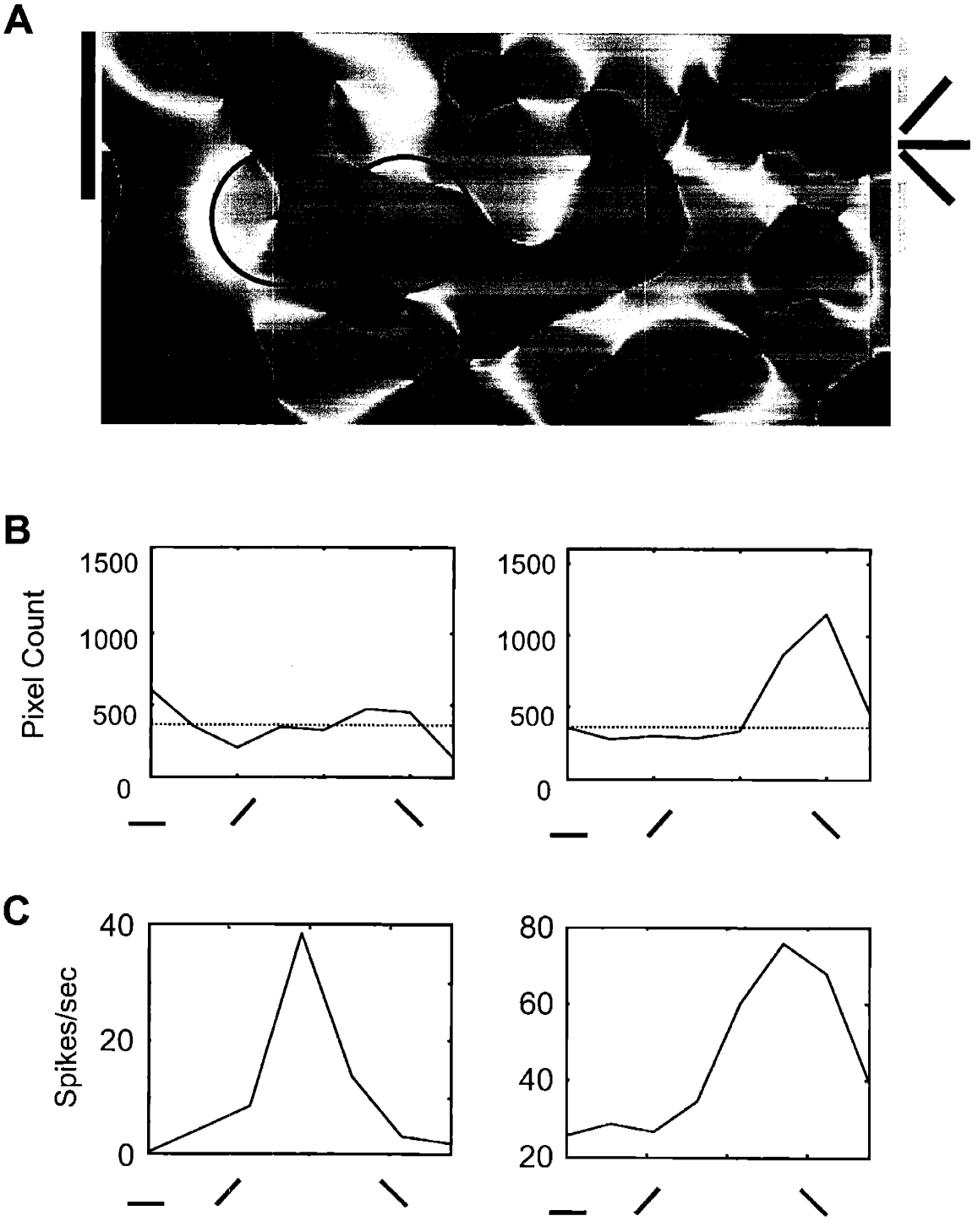
A
B
Pixel Count
1500
1000
500
0
1500
1000
500
0
C
Spikes/sec
40
20
0
80
60
40
20

Figure 1. Estimate of the local inputs to pinwheel centers and orientation domains. **A.** Orientation map, with estimated local input regions for two sites (one pinwheel and one orientation domain). The orientation preference of each pixel is pseudo-colored according to the code depicted to the right. Scale bar represents 1mm. **B.** Selectivity of the estimated inputs to the two neurons located at the positions indicated in **A**, calculated as the pixel counts in each bin falling within the circles in **A**. **C.** Firing rate tuning curves computed from neurons recorded at the two sites in **A**.

Chapter 2: Synaptic integration by V1 neurons depends on location within the orientation map

ABSTRACT

Neurons in the primary visual cortex (V1) are organized into an orientation map consisting of orientation domains, arranged radially around 'pinwheel centers' at which the representations of all orientations converge. Using a combination of optical imaging of intrinsic signals and intracellular recordings, the synaptic inputs and spike outputs of neurons located near pinwheel centers or in orientation domains were estimated. Neurons near pinwheel centers showed large membrane potential responses to all stimulus orientations but spike responses to only a narrow range of orientations. Across the map, the selectivity of membrane potential responses covaries with the selectivity of orientations in the local cortical network, while the selectivity of spike outputs does not. Thus, the input-output transformation performed by V1 neurons is powerfully influenced by the local structure of the orientation map.

INTRODUCTION

Primary visual cortex (V1) is the first level in the visual pathway in which neurons show pronounced selectivity for the orientation of a visual stimulus (Hubel and Wiesel, 1962). Discerning which inputs are responsible for this selectivity remains a challenge. V1 neurons receive feed-forward excitatory inputs, local intracortical excitatory and inhibitory inputs, as well as long-range connections. Defining and distinguishing the role of the specific inputs to cortical neurons is a formidable task due to the multiple connections they make and the variety of networks they constitute. In particular, the role of local intracortical connections in generating orientation selectivity has been debated for decades (Vidyasagar et al., 1996; Sompolinsky and Shapley, 1997; Ferster and Miller, 2000).

Mechanisms generating orientation selectivity

There now exists substantial evidence that orientation selectivity in thalamic-recipient V1 simple cells is conferred largely by the spatial structure of the simple receptive field, which is constructed linearly from a row of aligned thalamic inputs (Chapman et al., 1991; Reid and Alonso, 1995; Lampl et al., 2001). There is also evidence that second order (non-thalamic-recipient) V1 neurons inherit the orientation preference of the first order neurons via feedforward connections within their column (Alonso and Martinez, 1998; Martinez and Alonso, 2001). However, in both first- and second-order neurons, the influence of intracortical inputs remains unexplained. It is estimated that a minority of synaptic inputs to first-order neurons arises from thalamocortical sources (Reid and Alonso, 1995; Ferster et al., 1996; Chung and Ferster, 1998). The rest of the synaptic inputs, mainly arising from within the local cortical network, are burdened with maintaining the selectivity established by thalamocortical afferents. Outside of layer IV, the majority of synaptic inputs also arise from within the local cortical circuit. A complete description of orientation selectivity will ultimately require an understanding of not only how selectivity emerges in first-order neurons, but also how it is maintained by the myriad other synaptic inputs that impinge on cortical neurons. For instance, there are numerous demonstrations that altering the local cortical network can alter the selectivity of nearby neurons (Gilbert and Wiesel, 1990; Crook et al., 1991; Knierim and van Essen, 1992; Crook et al., 1997; Levitt and

Lund, 1997; Toth et al., 1997; Dragoi et al., 2000; Schuett et al., 2001). These studies suggest that inputs from within the local cortical network may have profound effects on visual responses, but a basic understanding of the rules of the influences of these connections on visual responses is still lacking.

Orientation map structure and local inputs

In order to address the role of the cortical network in shaping the responses of V1 neurons, it is important to consider the functional architecture of V1, which should influence the nature of cortical inputs to a neuron. Orientation columns are arranged into a map with a radial, 'pinwheel' configuration (Bonhoeffer and Grinvald, 1991; Blasdel, 1992). That is, neurons sharing similar orientation preference are grouped together in 'orientation domains', across which preferred orientation changes slowly and continuously, that are arranged radially around 'pinwheel centers', at which the representation of all orientations converge. Despite this diversity in the local structure of the functional map, available data suggest that the extent of local connections is relatively uniform across the orientation map (Malach et al., 1993; Yousef et al., 2001). Thus, it is likely that the functional connectivity within the local cortical circuit varies considerably between locations in the orientation map, such that near pinwheel centers neurons have local connections with neurons with all orientation preferences (Das and Gilbert, 1999), whereas far from pinwheel centers, connectivity is restricted to neurons sharing similar orientation preferences. Few studies to date have incorporated information about the heterogeneous local structure of the orientation map, which would predict heterogeneity in the cortical inputs to V1 neurons (though see McLaughlin et al., 2000; Dragoi et al., 2001; Wielaard et al., 2001).

Diversity of orientation tuning properties

In fact, there exist clues in the literature that there may indeed be substantial diversity in both the excitatory and inhibitory inputs that single V1 neurons receive. Intracellular studies have shown that the initial response to a flashed bar of the non-preferred orientation can lead to hyperpolarization in some neurons, a small depolarization in others, and a combination of the two in still others (Volgushev et al., 1993). This diversity of inhibitory influence on response tuning has led to the proposal that there may be multiple mechanisms for the generation of orientation selectivity

(Vidyasagar et al., 1996). In a recent study (Anderson et al., 2000) in which conductance measurements were used by the authors to argue for the feed-forward model, about one third of cells shown have substantial increases in conductance for non-preferred, including orthogonal stimulus orientations, suggesting inhibitory influences at a range of orientations. Analysis of the dynamics of responses to rapidly flashed gratings has also shown diversity in the magnitude and timing of both enhancement and suppression of spike responsiveness (Volgushev et al., 1995; Ringach et al., 1997; Ringach et al., 2002). Furthermore, careful studies of the contribution of the spike threshold to orientation tuning have shown that the degree to which this non-linearity sharpens selectivity varies considerably across the population (Carandini and Ferster, 2000; Volgushev et al., 2000). The experiments in this Chapter were designed to assess whether such diversity in the inputs and non-linearities which contribute to the orientation selectivity of V1 neurons might be related to the diversity in the orientation composition of the local cortical network created by the pinwheel structure of the orientation map in V1.

MATERIALS AND METHODS

Animal preparation

Experiments were performed on adult cats (2-3 kg) of either sex according to procedures that were approved by MIT's Animal Care and Use Committee and conformed to NIH guidelines. Animals were prepared for imaging and recording according to procedures that have been described (Rao et al., 1997; Dragoi et al., 2000). Briefly, animals were anesthetized (1-1.5 % isofluorane in 70:30 N_2O and O_2), paralyzed with vercuronium bromide (0.2 mg/kg/hr) in a 50-50 mixture of lactated Ringer's solution and 5% dextrose, and artificially respired. Expired CO_2 was maintained at 4%; anesthesia was monitored continuously. A craniotomy and durotomy were performed over area 17, and a stainless steel chamber was mounted on the skull. The chamber was filled with agar (~2.0% in saline), covered with a circular coverglass and coated with viscous silicone oil.

Physiological recordings

An orientation map was first obtained by optical imaging of intrinsic signals. Full-field, high contrast square-wave gratings (0.5 cycle/deg, 2 cycles/sec) of 4 orientations,

drifting in each of 2 directions were presented using STIM (courtesy of Kaare Christian, Rockefeller University) on a 17 inch CRT monitor placed at a viewing distance of 30 cm. Images were obtained using a slow-scan video camera (Bischke CCD-5024, Japan), equipped with a tandem macro-lens arrangement, and fed into a differential amplifier (Imager 2001, Optical Imaging Inc, NY). The cortex was illuminated with 604 nm light, and the focus was adjusted to ~500 μm below the cortical surface during imaging. Care was taken to obtain reference images of the surface vasculature several times over the course of the imaging session to detect any shift of the cortex relative to the camera, and increase the accuracy of electrode penetrations.

Intracellular whole-cell recordings were subsequently obtained at locations that were aligned to the angle map by reference to images of the surface vasculature. A bilateral pneumothorax was performed and a canula inserted into the cisterna magna to minimized brain movement. Patch pipettes (tip diameter ~2 μm; 12-20 MOhms) containing (in mM) Kglu: 120.0, NaCl: 5.0, ATP: 2.0, GTP: 0.2, Hepes: 40.0, EGTA: 11, CaCl: 1.0, MgCl: 1.0, were lowered into the cortex at sites specifically targeted to pinwheel centers and to orientation domains (locations intermediate between pinwheel centers). Tight seals were obtained by gentle suction and intracellular access was gained by increased suction and slight vibration of the pipette tip. Recordings were made in bridge mode with manual bridge balance and capacitance neutralization. Signals were amplified, digitized at 6-8 kHz (Axoclamp 2A, Axon Instruments, Union City, CA) and stored to disk on a computer running Pclamp software. Analysis was performed with custom routines written in Matlab (Mathworks, Natick, MA). Data acquisition and visual stimulus computers were synchronized by a master computer running CORTEX (NIH). Stimuli were drifting full-field, high contrast, square-wave gratings (0.3-0.7 cycles/deg, 2-5 cycles/sec) of 8 orientations generated by a computer running STIM and presented on a 17 inch CRT monitor at a distance of 30 cm. Each stimulus was presented 5-7 times for 1-2 seconds. Trials with a blank screen of uniform intermediate gray were also randomly interleaved to provide an estimate of unstimulated, background activity levels. Neurons were accepted for analysis if they had action potentials that were at least 15 mV in amplitude and showed stable resting membrane potentials for a duration of recording adequate for 5 trials of each stimulus orientation.

Analysis

Single-condition maps were obtained by dividing the summed activity maps of each orientation by the 'cocktail blank'. Smoothed single condition maps were summed vectorially to produce orientation angle maps. Orientation angle maps were further smoothed for display purposes only.

Spikes were identified and extracted from membrane potential traces by setting a threshold for the first derivative (slope) of the trace, counting the time of crosses as spike times, and linearly interpolating between the points surrounding the spike waveform. Membrane potential and firing rate responses were taken as the mean response over the first second of stimulus presentation, after subtraction of baseline levels. Cells were classified as simple or complex based on the F1/F0 ratio of the spiking responses to drifting gratings (Skottun et al., 1991). To facilitate more ready comparison with the orientation angle map data, which does not include direction information, only the responses to the optimal direction were analyzed. The Orientation Selectivity Index (OSI) was calculated as in Dragoi et al (Swindale, 1998);

$$OSI = \sqrt{\left(\sum_{i=1}^{n} R(\theta_i)\cos(2\theta_i)\right)^2 + \left(\sum_{i=1}^{n} R(\theta_i)\sin(2\theta_i)\right)^2} \Big/ \sum_{i=1}^{n} R_i$$

it is a continuous measure with values ranging from 0 (unselective) to 1 (perfectly selective). The Modulation Index (MI) was calculated as a measure of the relative response to the optimal orientation and the orientation orthogonal to it: $MI = (R_{opt}-R_{orth})/R_{opt}$ It is identical to the Selectivity Index used by others (eg (Volgushev et al., 2000), but we chose not to use this nomenclature to avoid confusion with the OSI. The OSI and SI values were calculated by the same formulas on the distributions of pixels found in the local input region for the analysis in Fig 5. All measures were computed using the mean response values. Statistical comparisons of distributions of these measures were made with the Student's t-test. Membrane potential traces were smoothed for display purposes only; all analysis was performed on unsmoothed traces. Visually evoked changes in input conductance were calculated based on previous work (Anderson et al., 2000). The complete set of visual stimuli was presented while the cell

was subjected to 3-4 levels of constant current injection. The membrane potential traces (after careful removal of spikes) of all trials for each condition were averaged. The input resistance was corrected offline, as in (Anderson et al., 2000), by fitting a double exponential function to the membrane responses to a series of current steps. The inverse of the slope of the best linear fit of the current voltage relationship at each time sample was taken as the input conductance. The excitatory and inhibitory components of the conductance were extracted by solving a set of two equations at each time point.

(1) $G_{tot} = G_e + G_i + G_{rest}$

(2) $V = (G_e V_e + G_i V_i + G_{rest} V_{rest})/G_{tot}$

V_e and V_i were set to 0mV and –85mV. Small changes in these values did not dramatically change the results.

RESULTS

Whole cell patch recordings were made from neurons at known locations in the orientation map in order to estimate the orientation selectivity of both the synaptic inputs to, and spike outputs of, individual V1 neurons. Penetrations were targeted to either pinwheel centers, or far from them, close to the centers of orientation domains, with the aim to evaluate the selectivity of synaptic and spike responses as a function of map location.

In vivo whole cell recordings of visually evoked membrane potential responses

Figure 1 shows an example of the recordings, and the extraction of parameters used in the subsequent analysis. Figure 1A shows six trials of the raw membrane potential during the presentation of a drifting grating of preferred orientation and direction. Figure 1B shows the average membrane potential after the spikes have been removed, the individual trials have been averaged, and the trace has been smoothed. The average potential of the trace during the grating, minus the resting potential is termed the membrane potential response. Figure 1C shows the PSTH of the average firing rate, from which the spike response (average minus spontaneous) is extracted. All

subsequent analyses were performed on the membrane potential response and spike response, by measuring their magnitude as a function of stimulus orientation.

Comparison of pinwheel and orientation domain neuron responses

Figure 2 shows the responses of a simple cell and a complex cell that are typical of those found far from pinwheel centers, in orientation domains. The simple cell in Figure 2A-D shows a large depolarization to a narrow range of stimulus orientations, and a spike response to a similarly narrow range of orientations. Because simple cell responses follow the luminance modulation of a drifting grating stimulus (Movshon et al., 1978; Skottun et al., 1991), the mean response (F0) and the temporal modulation of the response with each cycle of the grating (F1) are plotted separately (Figure 2C-D). The membrane potential shows a strong, mostly depolarizing, response to each phase of the grating of optimal or near-optimal orientation. The modulations of the membrane potential ride on a small baseline depolarization that is also orientation selective. Stimuli progressively away from the preferred orientation lead to responses that show progressively less modulation and reduced net depolarization. Thus, the tuning curves for both the mean membrane potential and spike responses (Figure 2C), and of the temporal modulation of these responses (Figure 2D), are narrowly tuned, and responses fall to zero for stimuli orthogonal to the optimal. Figure 2E-G shows the responses of a complex cell, also recorded within an orientation domain. As is typical of complex cells (Skottun et al., 1991), the cell does not show temporal modulation of its response to each phase of the drifting grating but instead a general elevation in response to gratings at and near its preferred orientation. Again, this cell shows strong depolarization and spike responses only near its preferred orientation, with no significant response to the orthogonal orientation. Thus, both simple and complex cells located in orientation domains show a strong membrane potential response only for a limited range of stimulus orientations, and this selectivity is reflected in their spike responses.

Figure 3 demonstrates responses from a simple cell and a complex cell that are typical of cells near pinwheel centers. These neurons demonstrate strikingly different profiles of subthreshold responses compared to neurons in orientation domains. The simple cell shown in Fig 3A-D has a robust depolarization to all orientations. The F1 component of the membrane potential response is narrowly tuned (Figure 3D), most likely due to the receptive field structure of simple cells. The response modulation rides on a relatively large baseline depolarization which is prominent at all stimulus

orientations, including those orthogonal to the preferred orientation. The mean depolarization to the orthogonal orientation is roughly half as large as that to the preferred orientation, and thus the tuning curve of the membrane potential response has a large offset (Figure 3C). The spike response of the cell generally follows the modulated component of the membrane potential, largely ignoring its baseline component, and is therefore sharply tuned for orientation. The complex cell in Figure 3E-G also shows a depolarization in response to all stimulus orientations. Similar to the simple cell of Figure 3C, the membrane potential tuning curve of this neuron (Figure 3G) has a large offset in that an orthogonal stimulus evokes a depolarization which is nearly half the amplitude of the response to the preferred stimulus. The spike tuning curve has a much smaller offset, indicating that non-preferred stimuli evoke little spiking activity. It is noteworthy that the spike responses of these pinwheel neurons do not follow the membrane potential particularly faithfully. This may be the result of averaging several repetitions of the stimulus (Anderson et al., 2000) or of differences in the temporal micro-structure of the fluctuations in membrane potential for different stimulus orientations, which has recently been shown to dramatically affect spike generation in visual cortical neurons (Volgushev et al., 2002). Regardless of the mechanism, these cells generate significantly more spikes for the preferred orientation, despite relatively similar average depolarization in response to several orientations. Thus, these examples indicate that both simple and complex cells located near pinwheel centers receive synaptic inputs over a broad range of stimulus orientations, although not all of these inputs are represented in the spike outputs.

A total of 27 cells were recorded, including 15 in orientation domains (4 simple and 11 complex) and 12 near pinwheel centers (5 simple and 7 complex). Orientation selectivity (see below) did not differ significantly between simple and complex cells at either location, so these cells were combined for subsequent analysis. Neurons were sampled across all layers; the distributions of recording depths were similar between the pinwheel and orientation domain cells groups (data not shown). Across the population, there was a consistent difference between the orientation selectivity of the membrane potential responses in neurons located in orientation domains and those near pinwheel centers. The average tuning curves of the spike rate are indistinguishable between pinwheel cells and orientation domain cells (Figure 4A), as described previously (Maldonado et al., 1997; Dragoi et al., 2001). However, the average tuning curves of the membrane potential responses are clearly different (Figure 4B); the tuning curve of the

pinwheel cells is shallower, with a larger offset, than that of the orientation domain cells. To enable quantitative comparisons of tuning between the two populations, two indices of orientation selectivity were calculated (Methods). A comparison of the Orientation Selectivity Index (OSI; Figure 5C) reveals that whereas the distribution of firing rate OSIs is similar between the two groups ($p > 0.4$), the membrane potential OSIs are significantly lower in the pinwheel population ($p < 0.03$). A comparison of the Modulation Index (MI; Figure 4D) also shows that the values for spike responses are similar ($p > 0.1$) whereas the values for membrane potential responses are significantly lower in the pinwheel neurons ($p < 0.03$). However, the distributions of tuning curve half-widths (data not shown) are not statistically different between neurons at pinwheel centers and orientation domains, for either the spike rate ($p > 0.9$) or the membrane potential response ($p > 0.4$). Thus, these quantitative comparisons confirm the impression from the average tuning curves that the difference between the two populations of neurons is not in the responses at and around the preferred orientation (as measured by the HW), but whether the full range of stimulus orientations drives synaptic inputs to the cell (as measured by the OSI) and particularly whether orthogonal stimuli evoke larger subthreshold depolarizations in pinwheel neurons (as reflected in the MI).

Sub-threshold response selectivity related to the local structure of the orientation map

The orientation map does not consist only of neurons in pinwheel centers and orientation domains, but rather there is a continuum of the diversity of orientations found in the local region surrounding any point in the map. In order to relate the tuning of responses more directly to the local orientation map structure, the selectivity of the orientation representation surrounding each recording site was characterized using the same selectivity measures used for the cellular responses. If local connections contribute a significant portion of the synaptic drive to V1 neurons, the differences in the membrane potential responses of the neurons might be traced to differences in the orientation representation within their local circuit. Based on anatomical tracer injection studies of local synaptic connectivity (Malach et al., 1993; Bosking et al., 1997; Kisvarday et al., 1997; Yousef et al., 2001), the majority of potential local inputs to a neuron were estimated to arise from a circular region of radius 400 μm. The orientation distribution within this "local input region" was compared to the selectivity of the synaptic inputs to a neuron, as estimated by the membrane potential response, at each recording site.

For each cell, the orientation distribution of pixels in the local input region was calculated from the orientation angle map (in 22.5 degree bins). The dashed circles in Figures 2(B, F) and 3 (B, F) show the regions used in this analysis for these four cells. We characterized these pixel distributions using the same indices (OSI and MI) that we used to characterize the tuning curves of the neurons. Figure 5A-D shows the scatter plots of these measures for the local input region against those for the firing rate and membrane potential responses. It is noteworthy that the OSI values calculated from the local map do not overlap for the populations designated as pinwheel or domain (squares and circles, respectively). There is a continuous distribution of these indices across the map (data not shown), and the two groups capture the extremes of the distribution. There is no significant correlation between the selectivity of the firing rate and the selectivity of the local input region, as assessed by either of the measures (Figure 5C-D). Thus, the local map structure is a poor indicator of the selectivity of spike responses. However, there is a significant correlation between the OSI and MI values of the membrane potential responses and of the local input region (Figure 5A-B), indicating that the orientation representation in the local cortical network is related to the selectivity of the membrane potential responses of a neuron at all locations in the cortex. These analyses were also performed for local input regions with radii from 200-700 μm (data not shown); correlations were strong up to ~400 μm, above which they became less robust, indicating that the selectivity of membrane potential responses is most closely related to the structure of the *local* cortical map.

Synaptic conductances underlying membrane potential responses

Recordings of membrane potential in response to a visual stimulus provide a first pass estimate of the synaptic inputs underlying the visual response. However, any given membrane voltage can arise from any number of combinations of excitatory and inhibitory synaptic inputs (under the assumption that all changes in membrane potential are of synaptic origin). The underlying assumption of the previous analysis is that the visually evoked changes in the membrane potential provide a reasonable measure of the total synaptic activity at all of the neuron's synapses. However, due to the inherent ambiguity of the source of measured changes in membrane potential, this assumption may not always hold. For instance, small response to orthogonal orientations in orientation domain neurons could theoretically result from precisely balanced excitatory and inhibitory synaptic inputs, rather than from very little synaptic input. Because the

conclusions of this chapter rely on the assumption that the membrane potential response magnitude is a reasonable estimate of the magnitude of synaptic inputs activate by the stimulus, it is necessary to verify that the synaptic conductances underlying the membrane potential response are also more sharply tuned in domain neurons than in pinwheel neurons.

Synaptic conductances cannot be directly measured with in vivo whole cell recording. However, under the appropriate experimental conditions, they can be estimated from the input conductance, based on knowledge of the reversal potentials of the ions that underlie synaptic currents. A method to derive estimates of the visually evoked changes in conductance has recently been developed and applied to V1 neurons in vivo (Borg-Graham et al., 1996; Borg-Graham et al., 1998; Hirsch et al., 1998). By recording visually evoked membrane potential responses to the same stimulus during injection of constant current of several sizes, the total input conductance of the cell can be derived at each time point as the inverse of the slope of the I-V curve computed from the injection currents and measured membrane potential response. Furthermore, under the assumptions that 1) visually evoked changes in input conductance are of synaptic origin, and 2) that the interaction between inhibitory and excitatory conductances is linear, the excitatory and inhibitory components of the total conductance can be extracted (Borg-Graham et al., 1998; Anderson et al., 2000; Monier et al., 2003).

Figure 6 shows the measurements of synaptic conductance for an example neuron. Panel A shows the membrane potential responses to eight stimulus orientations, spanning 180 degrees. Each stimulus was presented under three levels of current injection, color coded as in the legend. Each trace is the average of four trials, after the spikes have been removed by interpolation. During the preferred grating stimulation, there is a robust depolarization, which is similar in shape, but varies in amplitude for the three currents. The input conductance at each point in time is the inverse of the slope of the line that best fits the three voltages; thus if the three curves become closer, there is an increase in the input conductance. The total input conductance is plotted for each stimulus orientation in panel B. For this neuron, there is a robust increase at the preferred orientation, but not during the orthogonal. This suggests that the small membrane depolarizations at the orthogonal most likely do not result from balanced inhibition and excitation, but rather from a lack of synaptic input.

The orientation tuning of visually evoked changes in input conductance was studied in a population of six orientation domain neurons and eight pinwheel center neurons that met strict criteria for inclusion. The average tuning curves of the two populations are shown in Figure 7. The tuning curves of firing rate, Membrane potential and G_{tot} are plotted in Figure 7A-C respectively. As in the neurons described above, the firing rate tuning curves are almost indistinguishable, but the membrane potential tuning curves are less selective in pinwheel neurons, due largely to the offset of the tuning curve, which is roughly twice as large in the pinwheel population. The tuning curves of G_{tot} reflect the behavior exhibited by the two example neurons in Figure 6. There is a relatively small increase in conductance near the orthogonal orientation in orientation domain neurons, but there is substantially more in pinwheel neurons. Thus, the total synaptic input is more broadly tuned for neurons near pinwheel centers, mostly because of elevated flanks of the tuning curve.

Measurements of input conductance have the added feature that the synaptic currents underlying the responses can be estimated, thus constraining the potential synaptic processes responsible for the membrane potential responses. Changes in the magnitude of the membrane potential responses resulting from current injection are assumed to arise from the manipulation of the driving forces of the ions that mediate synaptic potentials. Using approximations of the reversal potentials of the ions most likely to mediate the synaptic potentials, it is possible to extract estimates of the excitatory and inhibitory components of the conductance response by solving the set of two equations (see METHODS). Figure 8 shows the tuning curves of the extracted excitatory (G_e) and inhibitory (G_i) conductances for the population. Both inhibitory and excitatory conductances are more broadly tuned for pinwheel center neurons. Inhibition is greatest relative to excitation at the orthogonal orientation, especially in the pinwheel center neurons. This suggests that inhibition may be a crucial factor in regulating the membrane potential response in pinwheel neurons, and could potentially help explain the transformation from broad membrane potential tuning to sharp firing rate tuning seen in these cells.

DISCUSSION

The data presented in this chapter indicate that the orientation specificity of synaptic inputs to V1 neurons correlates with the orientation specificity of the

surrounding local cortical network; however, the different patterns of synaptic input are transformed differently, such that the selectivity of spike responses is similar, regardless of map location. This result demonstrates that the input-output transformation performed by neurons in V1 is influenced by the orientation representation in their local neighborhood and hence by their location in the orientation map. The most obvious interpretation of this result is that the inhomogeneity in the selectivity of inputs to result from the inhomogeneity in the orientation composition of the local cortical neighborhood. The difference in membrane potential tuning between pinwheel and orientation domain neurons could, in principle, arise from an inhomogeneity in the inputs arising from any source. However, in light of data suggesting that the local connections are less orientation specific near pinwheel centers (Yousef et al., 2001), and absent any evidence for inhomogeneity in the thalamocortical projection, the cortical interpretation of the data is more plausible. Furthermore, the finding that the selectivity of inputs correlates well with the selectivity in the local cortical representation argues strongly for the local cortical connections as the source of the difference in inputs between pinwheel and orientation domain locations.

Integration of local inputs

A possible explanation for the different input-output transformations at different map locations is that the spike threshold plays an important role. Indeed, previous studies have shown diversity in the magnitude of sharpening caused by the spike threshold (Anderson et al., 2000; Carandini and Ferster, 2000; Volgushev et al., 2000). The present results suggest the possibility that the diversity may be accounted for by position in the orientation map. It is clear from comparison of Figures 4A and 4B that neurons near pinwheel centers undergo a more severe sharpening in the transformation of synaptic inputs to spike outputs. The central portion of the membrane potential tuning curves (the 'tip of the iceberg') is similar between pinwheel and orientation domain neurons, and this is the portion of the tuning curves which is translated into spikes. It is the flanks of the membrane potential tuning curves, which lie below the spike threshold, that are different between pinwheel and orientation domain neurons.

An important question which naturally arises is why the flanks of the tuning curves are elevated compared to those of orientation domain neurons, and how they are kept below threshold, and thus removed from the spiking tuning curves. A simple explanation of the relationship between the selectivity of the synaptic inputs and the map

representation is that neurons sum inputs from the local network in a relatively linear fashion; the area of cortex representing a particular orientation that lies within the local integration range of a neuron will determine the magnitude of the membrane potential response to that orientation. However, for several reasons, it is unlikely that V1 neurons integrate inputs entirely linearly. First, a look at the data reveals that the absolute magnitude of the maximum response is not different between pinwheel and orientation domain neurons (9.4 +/- 1.9 mV vs. 8.3 +/- 0.9 mV), as would be expected if responses of neurons were linearly related to the area of cortex activated by the stimulus. If neurons were linearly summing local inputs, the depolarization in response to the preferred orientation would be expected to be much larger for orientation domain neurons, because the amount of cortex representing that orientation is much larger than for neurons near pinwheel centers. Furthermore the sum of the responses to all orientations is ~50% larger for pinwheel neurons (data not shown). This is also inconsistent with the linear interpretation, because the absolute area of the local input region is, by definition, identical. Another issue is the nature of the influence of the spike threshold on the input-output transformation performed by V1 neurons. Two possibilities exist to explain the influence of the spike threshold. The threshold may always sit high enough relative to the magnitude of synaptic depolarization that only the central portion of the tuning curve can cross it and lead to an increase in firing rate. Alternatively, the threshold could also vary with map position, so as to regulate the portion of the tuning curve which leads to spikes. Further studies will be required to distinguish these two possibilities.

A more fundamental reason to doubt this simple linear relationship is that V1 neurons receive large amounts of inhibition (both hyperpolarizing and shunting), which can effectively cancel or mask excitatory inputs (Borg-Graham et al., 1998; Hirsch et al., 1998; Martinez et al., 2002; Martinez-Conde et al., 2002). One possibility is that in pinwheel neurons, inhibition is crucial to keeping responses to non-optimal orientations below threshold. The analysis of conductance changes is consistent with this hypothesis. The responses of pinwheel neurons at orthogonal orientations are composed of both excitation and inhibition. The ratio of inhibitory to excitatory conductance is higher at orthogonal orientations, which might explain the lack of spikes. It is also possible that the responses to near-optimal orientations are preferentially amplified by the spike-generation process, due to differences in the temporal structure of fluctuations in the membrane potential (Volgushev et al., 2002; Azouz and Gray, 2003).

Thus, several possible mechanisms could account for the observed tuning curves and further experiments will be required to distinguish between them.

Generation and maintenance of orientation selectivity

The dependence of synaptic integration on map location may help to resolve the relative importance of feedforward (thalamocortical) and recurrent (intracortical feedback) inputs in shaping the orientation tuning of V1 neurons (Somers et al., 1995; Ferster et al., 1996; Sompolinsky and Shapley, 1997; Anderson et al., 2000). Although these experiments do not directly address the generation of orientation selectivity in first-order thalamic-recipient cells, it is noteworthy that the major result holds for both simple and complex cells. In this respect, the results do not discriminate between models of the mechanism for the initial generation of orientation selectivity in first-order thalamic-recipient V1 neurons. However, the majority of the response of simple cells (Ferster et al., 1996), and the propagation of orientation selectivity to complex cells (Alonso and Martinez, 1998; Chance et al., 1999; Martinez and Alonso, 2001), depend on intracortical connections. Regardless of the mechanism which confers the initial selectivity, cortical inputs must ultimately play an important role in shaping the responses of all V1 neurons. A recent report suggests that recurrent inputs may have different roles in producing orientation selectivity at different stages (layers) of the cortical microcircuit (Martinez et al., 2002). The data presented in this chapter are sampled from all cortical depths, but the cells were not labeled, so the laminar positions are unknown. Future studies will be required to examine any interaction between laminar location and position with regard to the orientation map. That issue aside, the data suggest that the local cortical inputs have potentially different orientation composition at different locations in the map and the mechanisms which ultimately shape orientation selective spike responses may be different as well. Specifically, responses to non-preferred orientations are large, but remain sub-threshold, in neurons near pinwheel centers.

A number of experiments have demonstrated that manipulation of the cortical network can reveal these subthreshold inputs. For example, it has been shown that short-term shifts in the preferred orientation induced by pattern adaptation are much more prominent near pinwheel centers (Dragoi et al., 2001). This is presumably allowed by the strong subthreshold inputs, which are shown here to be much closer to threshold near pinwheel centers. It has also been shown that the selectivity of a neuron can be reduced by local inactivation of a cortical site ~500 μm away if the orientation preference

of the inactivation site is orthogonal to that of the recorded cell, but not if the inactivation site is iso-oriented with the recorded cell (Crook et al., 1997). Although these recordings were done without knowledge of the orientation map location, it is likely that sites at which an orthogonal domain is located within 500 μm will be rather near a pinwheel center. These results, together with those presented here, imply strongly that orientation selectivity is actively, and dynamically, maintained through a balance of the magnitude of the inputs at non-preferred orientations relative to the spike threshold. This balancing act is particularly important, and particularly susceptible to alteration of inputs, for neurons at or near pinwheel centers.

Note: Portions of the data reported in this chapter have been previously published (Schummers et al., 2002).

REFERENCES

Alonso JM, Martinez LM (1998) Functional connectivity between simple cells and complex cells in cat striate cortex. Nat Neurosci 1:395-403.

Anderson JS, Carandini M, Ferster D (2000) Orientation tuning of input conductance, excitation, and inhibition in cat primary visual cortex. J Neurophysiol 84:909-926.

Azouz R, Gray CM (2003) Adaptive coincidence detection and dynamic gain control in visual cortical neurons in vivo. Neuron 37:513-523.

Blasdel GG (1992) Orientation selectivity, preference, and continuity in monkey striate cortex. J Neurosci 12:3139-3161.

Bonhoeffer T, Grinvald A (1991) Iso-orientation domains in cat visual cortex are arranged in pinwheel- like patterns. Nature 353:429-431.

Borg-Graham L, Monier C, Fregnac Y (1996) Voltage-clamp measurement of visually-evoked conductances with whole- cell patch recordings in primary visual cortex. J Physiol Paris 90:185-188.

Borg-Graham LJ, Monier C, Fregnac Y (1998) Visual input evokes transient and strong shunting inhibition in visual cortical neurons. Nature 393:369-373.

Bosking WH, Zhang Y, Schofield B, Fitzpatrick D (1997) Orientation selectivity and the arrangement of horizontal connections in tree shrew striate cortex. J Neurosci 17:2112-2127.

Carandini M, Ferster D (2000) Membrane potential and firing rate in cat primary visual cortex. J Neurosci 20:470-484.

Chance FS, Nelson SB, Abbott LF (1999) Complex cells as cortically amplified simple cells. Nat Neurosci 2:277-282.

Chapman B, Zahs KR, Stryker MP (1991) Relation of cortical cell orientation selectivity to alignment of receptive fields of the geniculocortical afferents that arborize within a single orientation column in ferret visual cortex. J Neurosci 11:1347-1358.

Chung S, Ferster D (1998) Strength and orientation tuning of the thalamic input to simple cells revealed by electrically evoked cortical suppression. Neuron 20:1177-1189.

Crook JM, Eysel UT, Machemer HF (1991) Influence of GABA-induced remote inactivation on the orientation tuning of cells in area 18 of feline visual cortex: a comparison with area 17. Neuroscience 40:1-12.

Crook JM, Kisvarday ZF, Eysel UT (1997) GABA-induced inactivation of functionally characterized sites in cat striate cortex: effects on orientation tuning and direction selectivity. Vis Neurosci 14:141-158.

Das A, Gilbert CD (1999) Topography of contextual modulations mediated by short-range interactions in primary visual cortex. Nature 399:655-661.

Dragoi V, Sharma J, Sur M (2000) Adaptation-induced plasticity of orientation tuning in adult visual cortex. Neuron 28:287-298.

Dragoi V, Rivadulla C, Sur M (2001) Foci of orientation plasticity in visual cortex. Nature 411:80-86.

Ferster D, Miller KD (2000) Neural mechanisms of orientation selectivity in the visual cortex. Annu Rev Neurosci 23:441-471.

Ferster D, Chung S, Wheat H (1996) Orientation selectivity of thalamic input to simple cells of cat visual cortex. Nature 380:249-252.

Gilbert CD, Wiesel TN (1990) The influence of contextual stimuli on the orientation selectivity of cells in primary visual cortex of the cat. Vision Res 30:1689-1701.

Hirsch JA, Alonso JM, Reid RC, Martinez LM (1998) Synaptic integration in striate cortical simple cells. J Neurosci 18:9517-9528.
Hubel DH, Wiesel TH (1962) Receptive fields, binocular interaction and functional architecture of the cat's visual cortex. J Physiol 160:106-154.
Kisvarday ZF, Toth E, Rausch M, Eysel UT (1997) Orientation-specific relationship between populations of excitatory and inhibitory lateral connections in the visual cortex of the cat. Cereb Cortex 7:605-618.
Knierim JJ, van Essen DC (1992) Neuronal responses to static texture patterns in area V1 of the alert macaque monkey. J Neurophysiol 67:961-980.
Lampl I, Anderson JS, Gillespie DC, Ferster D (2001) Prediction of orientation selectivity from receptive field architecture in simple cells of cat visual cortex. Neuron 30:263-274.
Levitt JB, Lund JS (1997) Contrast dependence of contextual effects in primate visual cortex. Nature 387:73-76.
Malach R, Amir Y, Harel M, Grinvald A (1993) Relationship between intrinsic connections and functional architecture revealed by optical imaging and in vivo targeted biocytin injections in primate striate cortex. Proc Natl Acad Sci U S A 90:10469-10473.
Maldonado PE, Godecke I, Gray CM, Bonhoeffer T (1997) Orientation selectivity in pinwheel centers in cat striate cortex. Science 276:1551-1555.
Martinez LM, Alonso JM (2001) Construction of complex receptive fields in cat primary visual cortex. Neuron 32:515-525.
Martinez LM, Alonso JM, Reid RC, Hirsch JA (2002) Laminar processing of stimulus orientation in cat visual cortex. J Physiol 540:321-333.
Martinez-Conde S, Macknik SL, Hubel DH (2002) The function of bursts of spikes during visual fixation in the awake primate lateral geniculate nucleus and primary visual cortex. Proc Natl Acad Sci U S A 99:13920-13925.
McLaughlin D, Shapley R, Shelley M, Wielaard DJ (2000) A neuronal network model of macaque primary visual cortex (V1): orientation selectivity and dynamics in the input layer 4Calpha. Proc Natl Acad Sci U S A 97:8087-8092.
Monier C, Chavane F, Baudot P, Graham LJ, Fregnac Y (2003) Orientation and direction selectivity of synaptic inputs in visual cortical neurons: a diversity of combinations produces spike tuning. Neuron 37:663-680.
Movshon JA, Thompson ID, Tolhurst DJ (1978) Receptive field organization of complex cells in the cat's striate cortex. J Physiol 283:79-99.
Rao SC, Toth LJ, Sur M (1997) Optically imaged maps of orientation preference in primary visual cortex of cats and ferrets. J Comp Neurol 387:358-370.
Reid RC, Alonso JM (1995) Specificity of monosynaptic connections from thalamus to visual cortex. Nature 378:281-284.
Ringach DL, Hawken MJ, Shapley R (1997) Dynamics of orientation tuning in macaque primary visual cortex. Nature 387:281-284.
Ringach DL, Bredfeldt CE, Shapley RM, Hawken MJ (2002) Suppression of neural responses to nonoptimal stimuli correlates with tuning selectivity in macaque V1. J Neurophysiol 87:1018-1027.
Schuett S, Bonhoeffer T, Hubener M (2001) Pairing-induced changes of orientation maps in cat visual cortex. Neuron 32:325-337.
Skottun BC, De Valois RL, Grosof DH, Movshon JA, Albrecht DG, Bonds AB (1991) Classifying simple and complex cells on the basis of response modulation. Vision Res 31:1079-1086.
Somers DC, Nelson SB, Sur M (1995) An emergent model of orientation selectivity in cat visual cortical simple cells. J Neurosci 15:5448-5465.

Sompolinsky H, Shapley R (1997) New perspectives on the mechanisms for orientation selectivity. Curr Opin Neurobiol 7:514-522.
Swindale NV (1998) Orientation tuning curves: empirical description and estimation of parameters. Biol Cybern 78:45-56.
Toth LJ, Kim DS, Rao SC, Sur M (1997) Integration of local inputs in visual cortex. Cereb Cortex 7:703-710.
Vidyasagar TR, Pei X, Volgushev M (1996) Multiple mechanisms underlying the orientation selectivity of visual cortical neurones. Trends Neurosci 19:272-277.
Volgushev M, Vidyasagar TR, Pei X (1995) Dynamics of the orientation tuning of postsynaptic potentials in the cat visual cortex. Vis Neurosci 12:621-628.
Volgushev M, Pernberg J, Eysel UT (2000) Comparison of the selectivity of postsynaptic potentials and spike responses in cat visual cortex. Eur J Neurosci 12:257-263.
Volgushev M, Pernberg J, Eysel UT (2002) A novel mechanism of response selectivity of neurons in cat visual cortex. J Physiol 540:307-320.
Volgushev M, Pei X, Vidyasagar TR, Creutzfeldt OD (1993) Excitation and inhibition in orientation selectivity of cat visual cortex neurons revealed by whole-cell recordings in vivo. Vis Neurosci 10:1151-1155.
Wielaard DJ, Shelley M, McLaughlin D, Shapley R (2001) How simple cells are made in a nonlinear network model of the visual cortex. J Neurosci 21:5203-5211.
Yousef T, Toth E, Rausch M, Eysel UT, Kisvarday ZF (2001) Topography of orientation centre connections in the primary visual cortex of the cat. Neuroreport 12:1693-1699.

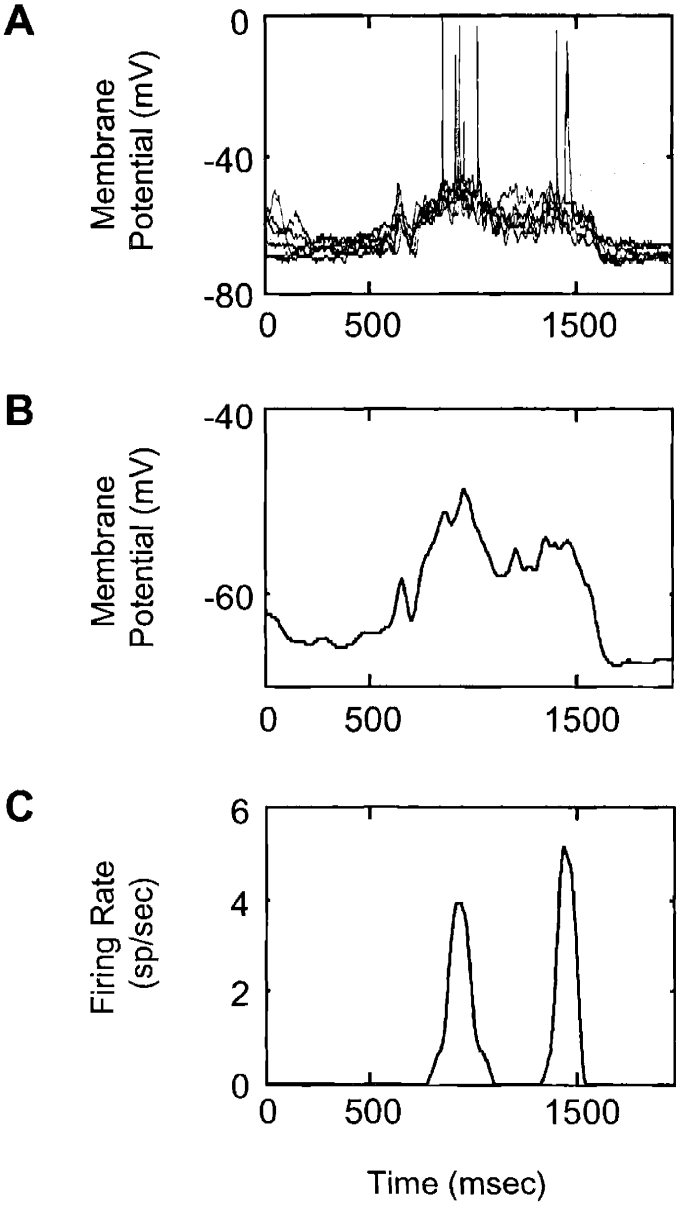
A
Membrane Potential (mV)
0
-40
-80
0
500
1500
B
Membrane Potential (mV)
-40
-60
0
500
1500
C
Firing Rate (sp/sec)
6
4
2
0
0
500
1500
Time (msec)

Figure 1. Representative example of whole cell recording **A**. Six traces of raw membrane potential in response to a drifting grating stimulus. Some action potentials are chopped due to sampling frequency; in fact the action potentials overshot zero. The stimulus was turned on at 500 msec, and turned off at 1500 msec. **B**. Average membrane potential after the spikes were removed by interpolation, the five trials were averaged, and the trace was smoothed with a sliding boxcar. The difference between the average membrane potential during the stimulus period minus the resting potential (membrane potential during blank stimulus or before stimulus appearance) is extracted and termed the membrane potential response. In this case the response is 10 mV. **C**. PSTH of the average rate of the spikes extracted from **A**. As in **B**, the spike response is extracted by subtracting the baseline from the average across the entire stimulus period; in this case, 2 spikes/sec.

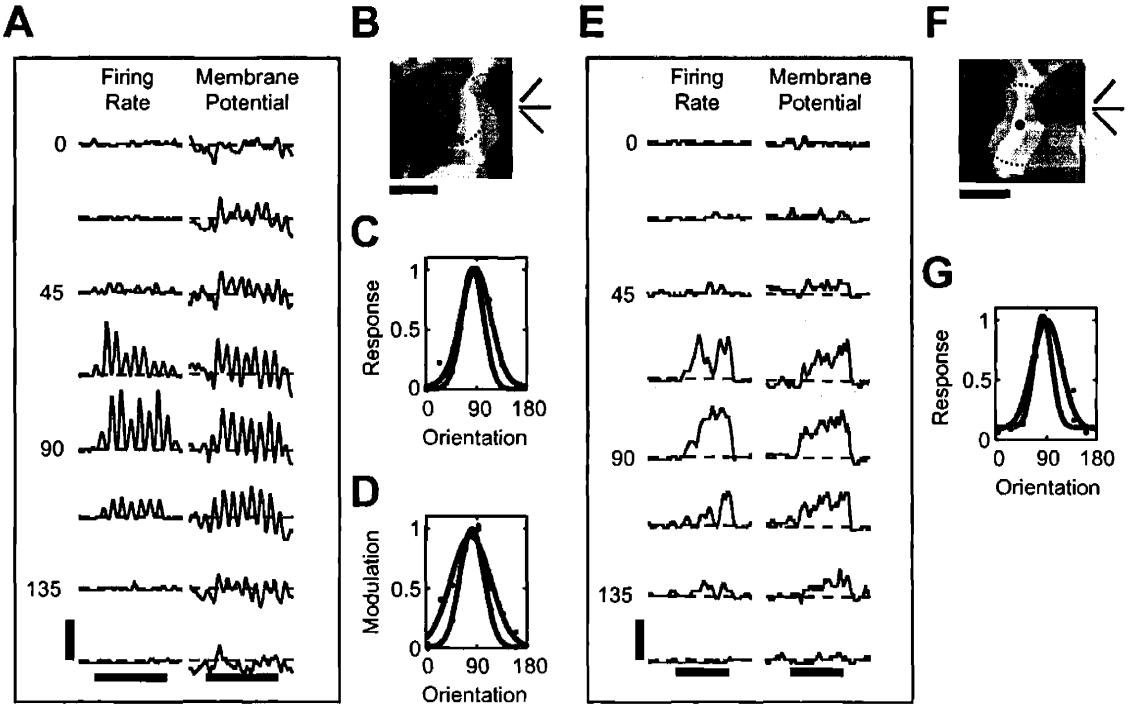
A
Firing Rate
Membrane Potential
0
45
90
135
I
B
C
Response
1
0.5
0
0 90 180
Orientation
D
Modulation
1
0.5
0
0 90 180
Orientation
E
Firing Rate
Membrane Potential
0
45
90
135
I
F
G
Response
1
0.5
0
0 90 180
Orientation

Figure 2. Responses of a simple and a complex cell recorded in orientation domains **A.** The responses of a simple cell recorded at the location marked by the dot in the orientation angle map (shown in **B**). The spike response (left column) and membrane potential response (right column) of the neuron to drifting gratings of eight orientations, spanning 180 degrees, are shown. In this figure and in subsequent figures, red is used to represent spike (firing rate) responses, whereas blue is used to represent membrane potential responses. Each trace is the average of five repetitions of a grating stimulus with the orientation shown to the left of the trace. The dashed red and blue lines represent the average resting spike rate and membrane potential, respectively. Black bar below the bottom traces show the time of the grating stimulus. Vertical scale bar represents 8 spikes/sec or 10 mV; horizontal scale bars represent 2 sec. **B.** Orientation angle map taken from the region of cortex surrounding the recording site. The color of each pixel codes for the optimal orientation at that pixel, as indicated in the color bars at the top right. The same color code applies to all orientation maps shown throughout. The dotted circle denotes a local region of the map of radius 400 μm centered on the recorded cell (see text for details). Scale bar here and in subsequent figures represents 0.5 mm. **C.** Tuning curves of the amplitude of synaptic (blue) and spike (red) responses, taken as the average across the duration of the stimulus presentation (the F0 component of the response). Here, and in subsequent examples, the lines correspond to a gaussian estimate of the tuning curve which was fit to the data points, shown as small circles. The responses to a uniform gray screen of the same mean luminance as the grating stimulus were defined as baseline and were subtracted from the average firing rate and membrane responses. All tuning curves are normalized and aligned to 90 degrees for ease of comparison. **D.** Tuning curves of the amplitude of modulation, in response to each phase of the stimulus grating (the F1 component of the response). **E.** Spike and membrane potential responses of a complex cell recorded in an orientation domain (as shown in **F**). Vertical scale bar represents 8 spikes/sec or 10 mV; horizontal scale bars represent 2 sec. **G.** Tuning curves of the average amplitude of the spike and membrane potential responses.

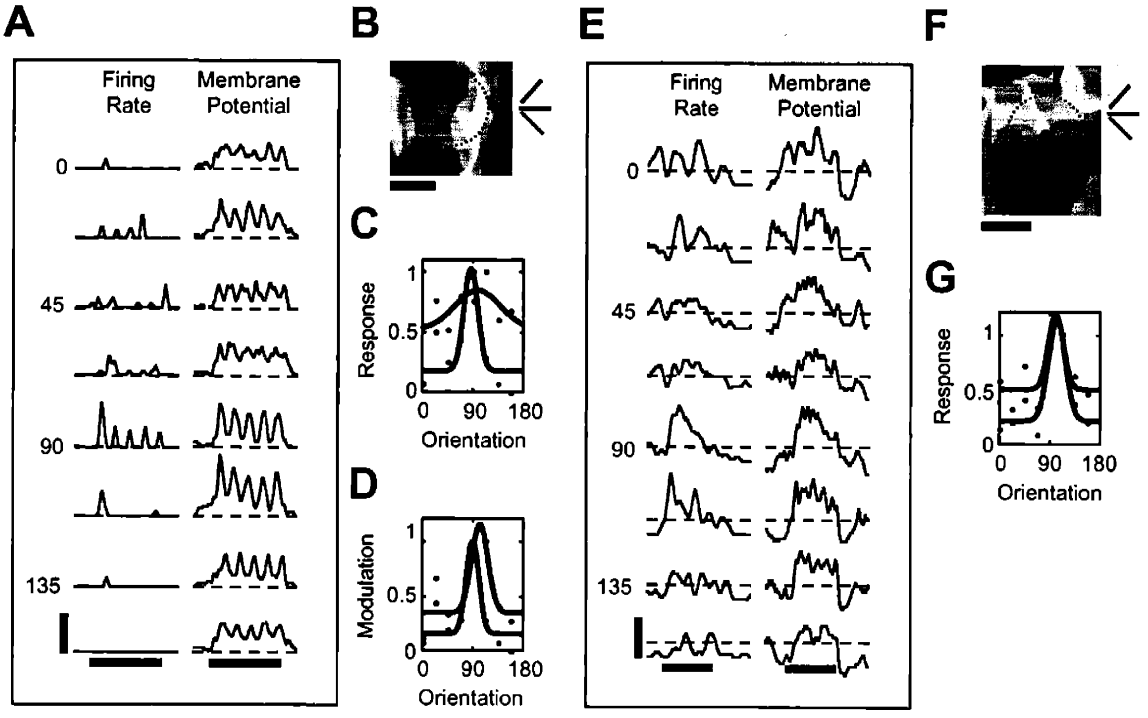
A
Firing Rate
Membrane Potential
0
45
90
135
B
C
Response
1
0.5
0
0 90 180
Orientation
D
Modulation
1
0.5
0
0 90 180
Orientation
E
Firing Rate
Membrane Potential
0
45
90
135
F
G
Response
1
0.5
0
0 90 180
Orientation

Figure 3. Responses of a simple and a complex cell recorded near pinwheel centers **A-D**. Responses of a simple cell recorded at the location marked by the dot in the orientation angle map (shown in **B**). Vertical scale bar represents 3 spikes/sec or 8 mV; horizontal scale bars represent 2 sec. All conventions in panels **A-D** are the same as in **Figure 2**. **E-G**. Responses of a complex cell recorded at a pinwheel center (as shown in F). Vertical scale bar represents 5 spikes/sec or 7 mV; horizontal scale bars represent 1 sec. All conventions in **Figure 3** are the same as in **Figure 2**.

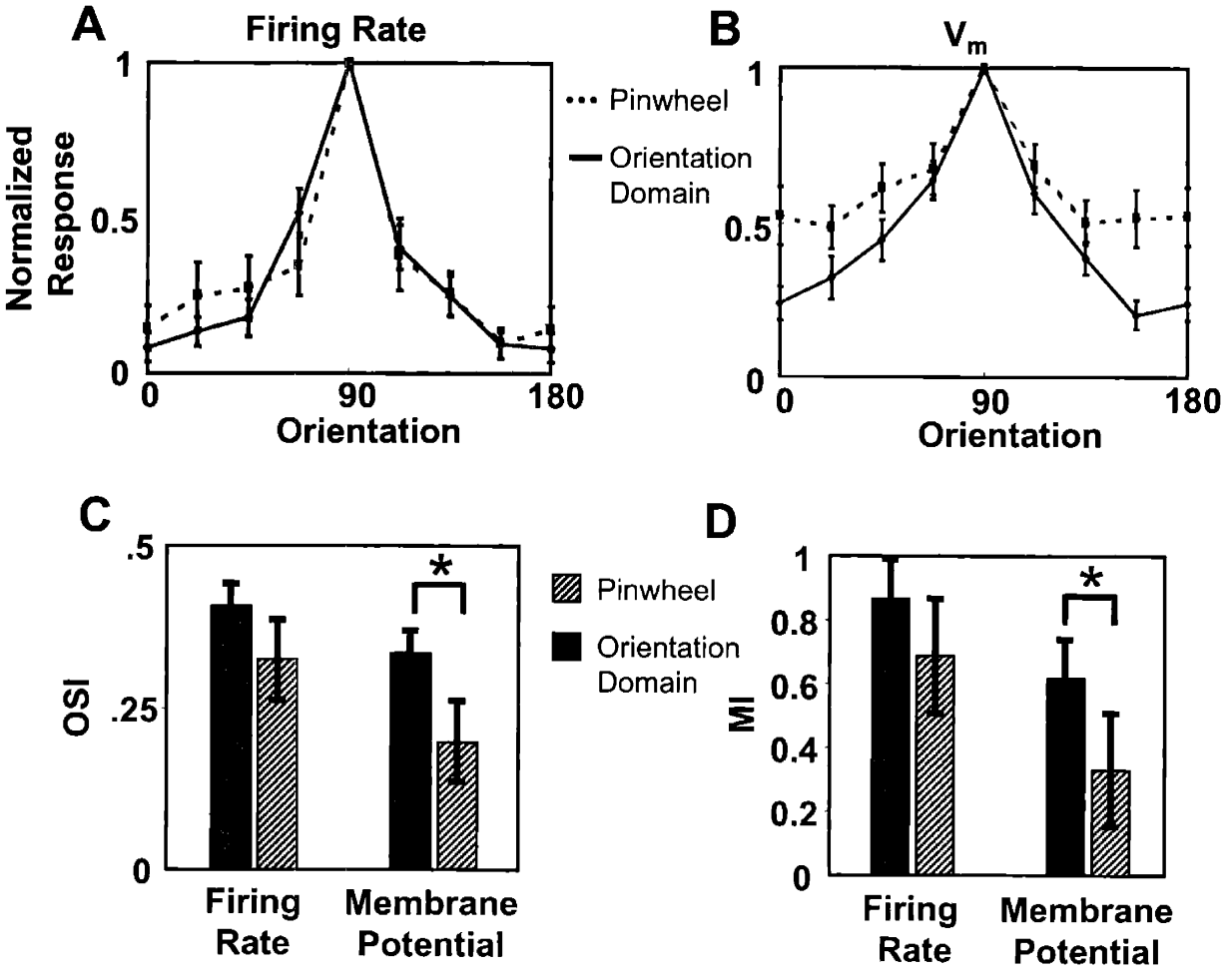
A
Firing Rate
Normalized Response
1
0.5
0
0
90
180
Orientation
Pinwheel
Orientation Domain
B
V_m
1
0.5
0
0
90
180
Orientation
C
OSI
.5
.25
0
*
Firing Rate
Membrane Potential
Pinwheel
Orientation Domain
D
MI
1
0.8
0.6
0.4
0.2
0
*
Firing Rate
Membrane Potential

Figure 4. Pinwheel cells have less selective synaptic inputs across the population of cells. **A.** Average tuning curves (+/- SEM) of the firing rate responses for the sample of pinwheel neurons (n = 12) and orientation domain neurons (n = 15). Tuning curves were normalized, and aligned to the peak response before averaging. **B.** Average tuning curves of the membrane potential responses of the same pinwheel and orientation domain neurons. Curves were normalized and aligned to the peak response. **C, D.** Bar plots showing the average values of the Orientation Selectivity Index (OSI) and Modulation Index (MI) of the firing rate and membrane potential tuning curves from the population of neurons, grouped according to recording location (orientation domain or pinwheel). * represents statistically significant difference of population means (Student's t-test; $p<.05$).

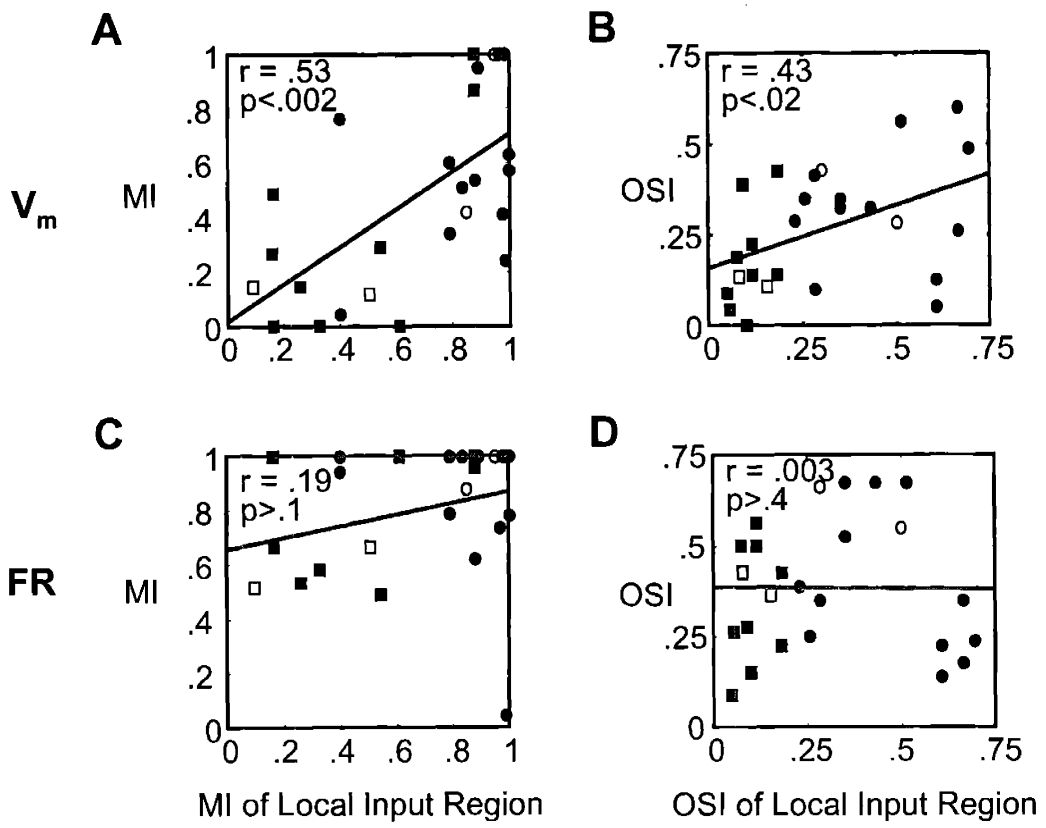
A
B
C
D
V_m
FR
MI
OSI
r = .53
p<.002
r = .43
p<.02
r = .19
p>.1
r = .003
p>.4
0
.2
.4
.6
.8
1
.25
.5
.75
MI of Local Input Region
OSI of Local Input Region

Figure 5. Local map orientation representation correlates with the selectivity of membrane potential responses, but not spike responses. **A** Scatter plot of the Modulation Index (MI) values of the membrane potential responses and the MI values of the local input region for each recording site. Squares indicate recording sites at pinwheels while circles indicate sites at orientation domains. Open points represent the cells shown in **Figures 2 and 3**. Lines in this and all plots indicate the least-squares linear fit to the data. Correlation coefficients and associated p values are indicated. **B** Scatter plot of the OSI values of the membrane potential response and the local input region of the map. **C** and **D** Scatter plots of the MI and OSI values of the spike responses and the local input region.

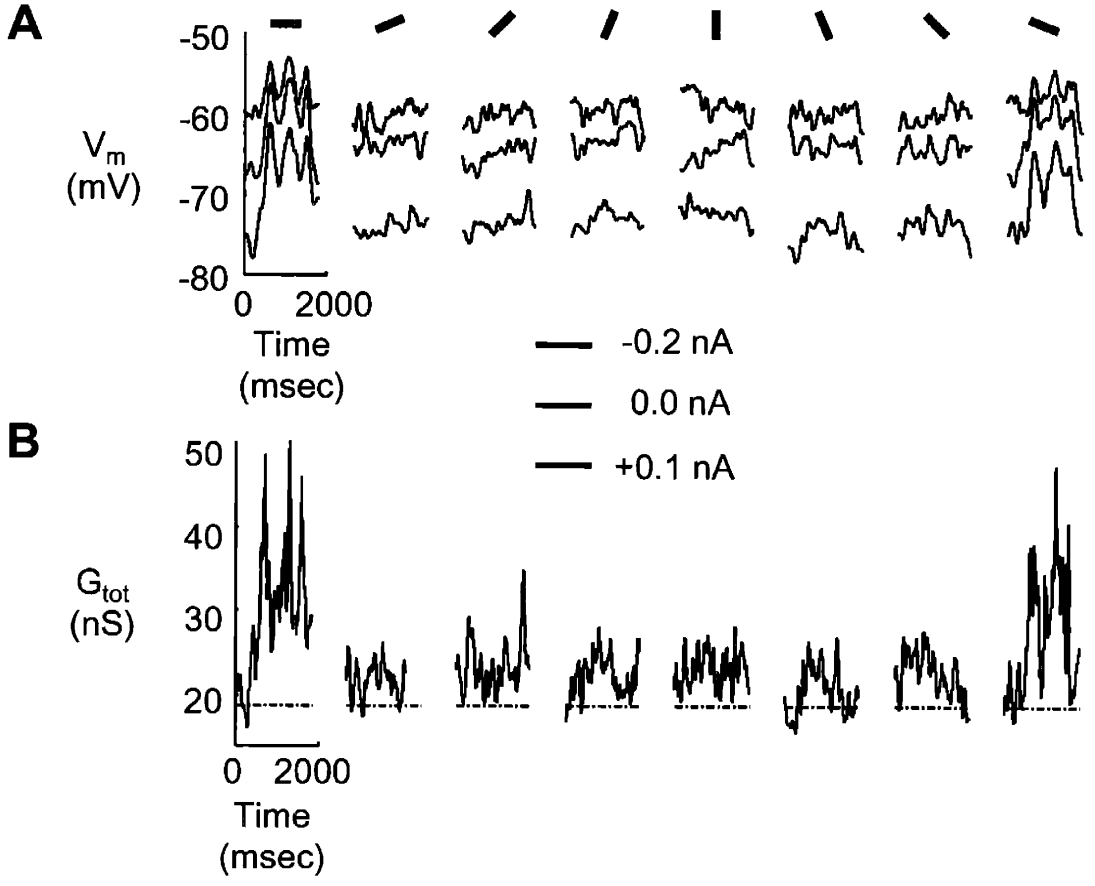
A
-50
-60
-70
-80
V_m
(mV)
0
2000
Time
(msec)
-0.2 nA
0.0 nA
+0.1 nA
B
50
40
30
20
G_{tot}
(nS)
0
2000
Time
(msec)

Figure 6. Example of the measurement of input conductance. **A**. V_m traces of the responses of an example cell to eight stimulus orientations (indicated by the bars above each plot) in the presence of three levels of constant current injection (color coded as indicated in the legend). All of the plots are on the same scale as indicated in the left-most panel. The stimulus was present from 300 to 1300 msec. **B**. The input conductance derived from the V_m responses shown in **A**. All of the plots are on the same scale as indicated in the left-most panel. The dashed line represents the mean input conductance during the blanks stimulus presentation.

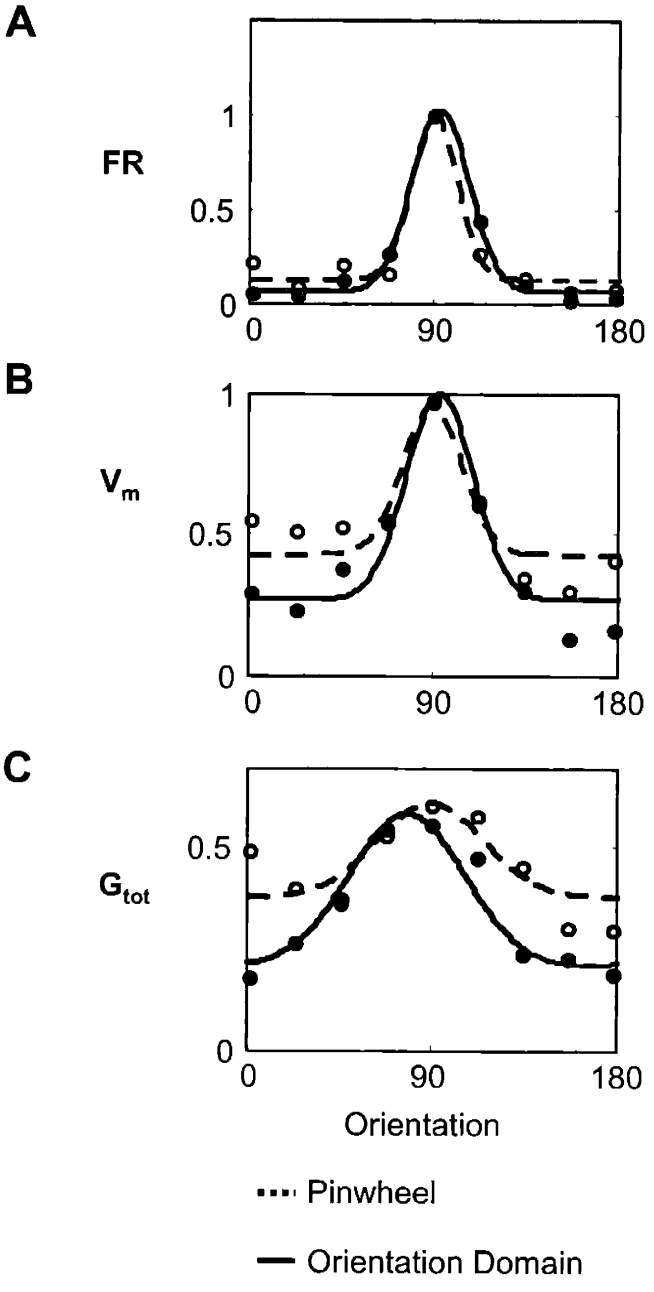
A
FR
1
0.5
0
0
90
180
B
V_m
1
0.5
0
0
90
180
C
G_{tot}
0.5
0
0
90
180
Orientation
Pinwheel
Orientation Domain

Figure 7. Average tuning curves of changes in FR, membrane potential and input conductance. **A**. The average aligned firing rate tuning curves for a population of pinwheel center (n = 8) and orientation domain (n = 6) neurons. The circles (open = pinwheel; closed = domain) are the actual data points, and the continuous curves (dashed = pinwheel; solid = domain) are the Gaussian fits to the data. The values of each curve were normalized to range between 1 for the maximal response, and 0 for no response. **B**. The tuning curves for membrane potential response. **C**. The tuning curves of the average change in input conductance (G_{tot}). The scaling and labeling conventions are the same in **B** and **C** as in **A**.

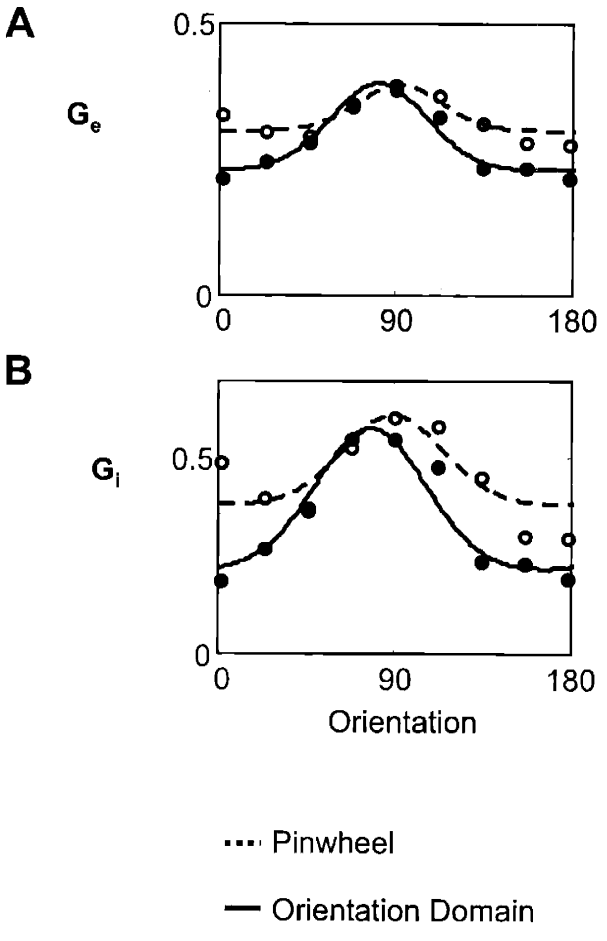
A
G_e
0.5
0
0
90
180
B
G_i
0.5
0
0
90
180
Orientation
Pinwheel
Orientation Domain

Figure 8. Average tuning curves of changes in inhibitory and excitatory conductances. **A**. The average aligned G_e tuning curves for the same populations of pinwheel and orientation domain neurons shown in **Figure 7**. The circles (open = pinwheel; closed = domain) are the actual data points, and the continuous curves (dashed = pinwheel; solid = domain) are the Gaussian fits to the data. The values of each curve were normalized to range between 1 for the maximal response, and 0 for no response. **B**. The average aligned G_i tuning curves for the same populations of pinwheel and orientation domain neurons shown in **Figure 7**. The circles (open = pinwheel; closed = domain) are the actual data points, and the continuous curves (dashed = pinwheel; solid = domain) are the Gaussian fits to the data. The values of each curve were normalized to range between 1 for the maximal response, and 0 for no response

Chapter 3: Dynamics of Orientation Selectivity in V1

ABSTRACT

Numerous studies have examined the temporal dynamics of orientation selectivity in V1 neurons. There is no consensus regarding the timecourse of orientation selectivity; some studies have found large changes in the orientation tuning curves during the response, whereas others have found no such changes. Given the diversity in the orientation tuning of the inputs to V1 neurons (Chapter 2), it was hypothesized that neurons situated near pinwheel centers would be more likely to show large changes in orientation tuning properties over time. However, regardless of location in the orientation preference map, cat V1 neurons extremely rarely showed changes in orientation preference, or multiple peaks in their tuning curves. It is therefore concluded that despite the diversity of synaptic inputs to neurons near pinwheel centers, the tuning properties of spike responses are tightly regulated throughout the duration of the response, and do not evolve significantly with time.

INTRODUCTION

Previous studies of orientation dynamics

Numerous studies have investigated the temporal evolution, or dynamics, of the orientation selectivity of responses of V1 neurons. This analysis is generally performed by presenting an oriented stimulus (bar or grating) for a brief period of time (16-200 msec) over the receptive field of a neuron, and measuring the response of the neuron over a sequence of time windows covering the duration of the response. Thus, the selectivity can be evaluated at multiple times relative to the stimulus onset. The rationale of such an approach is that the numerous sources of synaptic input that contribute to the response may be separable in time, and the influence of each may therefore be relatively more prominent at different periods of the response. In particular, this type of analysis has been used in attempts to distinguish between feed-forward (thalamocortical) and recurrent (intracortical) inputs, and thus to estimate the role of each in the generation of orientation selectivity. The reasoning in such studies has been that if the orientation selectivity is generated by the convergence of LGN inputs, the neuron should be equally selective during the initial response as it is at the time of peak response. Conversely, if orientation selectivity arises from specific intracortical amplification (or suppression) of responses to some orientations, the initial period of the response should be less selective than later time points. It has been with this general framework in mind that several groups have analyzed the response dynamics of V1 neurons.

Unfortunately, the results, and their interpretation, have been inconsistent across different reports. Some studies have demonstrated that the tuning curves derived from early portions of the visual response are quite different from those derived from later in the response, whereas others have found that orientation selectivity is relatively constant throughout the duration of the visual response. A number of differences in the stimulus, species, recording method and analysis may have contributed to differences in the conclusions drawn, but an analysis of these differences does not provide a clear picture of which factors may be critical to seeing or not seeing complex orientation dynamics.

Time-slice analysis

Several studies have analyzed the timecourse of orientation selectivity of extracellular spike responses to flashed stimuli, using the "time-slice" analysis. In these studies, an oriented stimulus is flashed over the RF for 100-200 msec, and orientation tuning curves are constructed from spike counts in contiguous, ~10 msec, time windows. One group, recording in awake behaving monkeys, found that the orientation selectivity generally does not improve dramatically over the timecourse of the response (Celebrini et al., 1993). The authors interpreted these results as support for a feedforward mechanism of orientation selectivity, because the orientation tuning curves were fully selective at the earliest measurable timepoint. However, the temporal resolution of the analysis was low, and was probably inadequate to resolve the influence of feedforward and feedback influences on response selectivity. Another group, in a series of papers reporting results from cat V1, found that a large portion of cells have dramatic changes in features of the orientation tuning curves over the timecourse of responses (Shevelev et al., 1993). They grouped cells into several classes of orientation dynamics: seeker neurons – those that gradually changed preferred orientation with time, inverters – those that showed a fairly sudden inversion of the tuning curve, and stable cells – those that did not have substantial changes in preferred orientation with time. They did not analyze changes in the selectivity over time, only changes in preferred orientation. They also noted that the proportion of seekers and inverted was dramatically larger when the level of anesthesia was reduced.

Intracellular experiments

Two groups have examined the evolution of the orientation selectivity of membrane potential responses, using intracellular recordings in cat V1 neurons. Volgushev et al (Volgushev et al., 1995) have recorded intracellularly from neurons in anaesthetized cat V1 using flashed light bars. The first general feature of their data is that for most cells, bars of any orientation elicited an initial depolarization with similar latencies. Thus, tuning curves derived from the initial response (~30-50 msec), showed a general elevation (above baseline), and broad selectivity as estimated by half-width at half-height (HW). This behavior was observed in both simple and complex cells, although the proportion of different types of cells was not reported. The response to the optimal orientation often had a faster rise time – as a result at the very earliest times, the

cell could be highly selective, then become less selective as the responses to non-optimal orientations arose, only to become more selective again, as the responses to non-optimal orientations rapidly declined, likely due to delayed inhibition. This behavior was not universal, however; some neurons had much slower responses to the non-optimal orientations, such that the tuning curves gradually became less selective.

Across their population, they found that the majority of cells had at least one period (5 msec window) during which the selectivity was broader than that of the integrated response, as would be measured with typical analysis techniques. The majority of cells also had at least one time slice when the selectivity was higher than the integral. There was a general trend for neurons with less selective integrated responses to have a larger divergence in the minimum and maximum selectivity during the course of the response. They also found that the time of maximal selectivity coincided with the time of maximal response magnitude in only half of their cells.

The data in this report also demonstrate an interesting aspect of the responses to flashed stimuli. In some cells (close to 20%), multiple distinct peaks (depolarizations) were observed; the first generally occurred between 30-50 msec, and the second generally between 100-140 msec after stimulus onset. In all such cases, the second peak was more selective than the first. The interval between the peaks may, or may not have included hyperpolarization beyond the resting potential, but was generally more hyperpolarized for non-optimal orientations, such that the tuning curves had lower, or negative, baselines (or offsets), during these periods. The authors attribute such hyperpolarizations to intracortical inhibitory inputs, and the secondary peaks to reverberatory cortical activity.

A more recent study has taken an almost identical approach, but come to substantially different conclusions. Gillespie et al (Gillespie et al., 2001) recorded intracellularly from anaesthetized cat V1 neurons, while presenting a rapid (10-25 Hz) series of randomly oriented sine gratings limited to the neurons' receptive field. As in Volgushev et al, the data was analyzed by calculating tuning curves from the membrane potential measured in successive small (5 msec) windows after the stimulus onset. Four parameters of each tuning curve were extracted by Bayesian estimation of a gaussian model of the tuning curve (orientation, HW, amplitude and offset). Such analysis yields probability distribution functions (pdfs) for each of the parameters, for each time slice, and the cross-correlation of two such pdfs, taken from "early" and "later" time slices was used to create confidence intervals on the likelihood that the modes of the two pdfs are

different. Unlike in Volgushev et al, who scanned the entire response period for maximal differences in the tuning curves, Gillespie et al chose only two time slices, from the earliest response time and the peak response time, to perform these comparisons. They found that 2 of 20 cells had significantly broader tuning curves at the peak than at the onset, and only one cell had a significantly different preferred orientation at the later time slice. An inspection of their data indicates that 5/20 decreased selectivity by more than 10 degrees, and 4/20 increased the selectivity by more that 10 degrees. Thus, nearly half of their cells did show large changes in selectivity, but only 2 of them (both increasing HW) met the criteria for significance. According to the authors, this is due to the fact that early in the response, when the responses are relatively small relative to noise, the pdfs are broad, and thus the burden of meeting significance is much more difficult to carry. The authors admit that they discarded four cells which had multimodal pdfs for any of the parameter/time slice combinations. It may well be, given these arguments, that the data of Gillespie et al and Volgushev et al are fairly similar, but more stringent tests of significant differences, and selective choice of only "clean" cells, may have led the authors to different conclusions. They found that 6/20 cells had significantly lower offsets at the peak, and 3/20 had significantly higher offsets. However, when they compared the time of maximal hyperpolarization with the earliest response, they found that 10/20 cells had a significantly hyperpolarized offset during the later period of the response. They attribute this to orientation-non-specific inhibition, which serves to shift the entire tuning curve, without altering "orientation selectivity" per se.

Unfortunately, an issue that is particularly relevant to the question of response development, and would have addressed the issues raised in Volgushev et al more directly, is the development of the offset over time. In particular, it would be interesting to know whether the offset *rose* significantly during the early part of the response. This would be an indication, as shown by Volgushev et al, that early in the response, neurons respond to all orientations strongly, and that it is selective suppression/amplification of the responses to particular orientations which gives a neuron its final selectivity. (The example shown in their Figure 2a in fact gives an indication that the cells in their population may indeed be behaving in this manner, as reported in Volgushev et al.)

Optical imaging experiments

One study has studied the dynamics of orientation selectivity at the population level using optical imaging of voltage changes across the surface of cat area 18 using

voltage-sensitive dyes (Sharon and Grinvald, 2002). The authors concluded that the dynamics of orientation selectivity in the superficial (non thalamic recipient) layers support a model of orientation selectivity arising from both feedforward and recurrent sources. They found that the HW of selectivity was fully developed at the earliest moments of the response, although they are careful to note that the temporal resolution of their recordings precludes distinguishing a very rapid sharpening (within the first 10 msec of the response) from initial fully sharp responses. However, they found that other measures of selectivity did increase over the first 20-30 msec of the response, especially the modulation depth (ratio of the response to the preferred orientation and the orthogonal). The peak selectivity index (defined as the modulation depth divided by the product of the HW and the non-selective offset) was reached at ~55 msec. Interestingly, this time point correlated with a deceleration in the response, which was followed by a re-acceleration. The deceleration was larger for the orthogonal stimulus, and thus the modulation depth was larger during the deceleration period. Thus, although the HW of the tuning curve does not appear to narrow over the course of the response, the overall selectivity, the relative response magnitude to the preferred and orthogonal stimuli shows a rapid increase during the initial portion of the response. Furthermore, this increase in the modulation depth may result from a suppressive mechanism which is more pronounced for orthogonal than preferred orientations.

Reverse-correlation experiments

Recent studies in macaque V1 have analyzed response dynamics using a novel reverse-correlation technique. In these experiments, gratings are presented continuously, with the orientation changing rapidly, and randomly, so that V1 neurons are continuously stimulated. During this protocol, the cells are in a continual high state of excitation, with the timing of fluctuations in excitation, and therefore spike initiation, varying as a function of the preceding stimulus orientation history. Thus, the orientation selectivity can be assessed as the probability distribution of stimulus orientation proceeding spiking by τ msec, where τ represents the offset between stimulus and spike. The evolution of the probability distribution (in orientation), with increasing τ can provide a good measure of the response dynamics of a cell. This analysis has the advantage over the previous methods that the stimulus changes faster than the integration time of V1 neurons, and thus it measures the "impulse response" of the neurons, rather than the "step response".

Three recent studies have employed this technique to characterize the dynamics of V1 neurons. Ringach et al (Ringach et al., 1997b) found that the orientation selectivity of many anaesthetized macaque V1 neurons changed dramatically over the timecourse of the response (30-120 msec). In half of their neurons found outside of the input layers, neurons showed shifts, or inversions of the preferred orientation. Such "multimodal" dynamics were interpreted as an indication of recurrent processing, suggesting that feedforward inputs cannot fully explain the orientation selectivity of V1 neurons. However, results from the same group, as well as two others, indicate that such dramatic dynamics are relatively rare (Dragoi et al., 2002; Mazer et al., 2002; Ringach et al., 2003). Mazer et al assessed changes in selectivity by testing the time separability of orientation tuning. They found that at most 5% of cells had inseparable orientation dynamics. A second study by Ringach and colleagues did not emphasize shifts or inversions of tuning curves, but rather focused on Mexican hat profiles, which they found in a large portion of cells (Ringach et al., 2003). They found different timecourses of three components of tuning curves – the enhancement of firing, the selective suppression for some orientations, and the global suppression, as measured by a decrease in the offset of the entire tuning curve. The authors conclude that tuning curves are constructed by a combination of all three features, each with a different timecourse. They emphasize the importance of spike suppression, presumably indicative of synaptic inhibition, in sculpting orientation selectivity. Experiments by Dragoi et al in awake monkey V1 did not find substantial changes in orientation preference or selectivity during the course of response (Dragoi et al., 2002). They did, however, find that orientation preference can be shifted by pattern adaptation, and they argued that this result supports a role for intracortical processing in shaping orientation selectivity.

Taken together, the previous studies of orientation dynamics paint a cloudy picture of the timecourse of orientation selectivity in V1 neurons. The diversity of results regarding this issue, in light of recent results indicating diversity in the mechanisms that generate orientation selectivity (Martinez et al., 2002; Monier et al., 2003), suggest that many factors, including laminar location, position relative to pinwheel centers, species and anesthetic state, may influence the orientation dynamics of V1 neurons. This Chapter will describe experiments aimed at clarifying some of these issues by measuring the response dynamics of neurons with known laminar and orientation map location. In particular, the hypothesis of these experiments is that neurons situated

close to pinwheel centers are likely to demonstrate more complex orientation dynamics than neurons in orientation domains due to the more diverse orientation representation in the local cortical region surrounding them.

METHODS

Animal preparation

All experiments were performed in adult female cats, in accordance with protocols approved by the MIT CAC and NIH guidelines. Details of animal surgery and recording techniques were as described in Chapter 2.

Visual stimuli

Visual stimuli were generated offline using routines written in Matlab, and played in movie mode in Cortex v 5.5, in two computer mode. Stimuli were presented on a 17 inch CRT monitor placed at a distance of 57 cm from the eyes, running with a vertical refresh rate of 60 or 100 Hz. The luminance values were linearized by adjusting the color lookup tables based on the measured output of the monitor using a photometer. Drifting gratings were presented in a 10 x 10 dva window, centered on the aggregate RF of the recorded neurons. Gratings were high contrast, spatial frequency was .25-.5 cycles/deg, temporal frequency was 2 cycles/sec and the orientation resolution was 22.5 degrees. Each trial consisted of 2 sec of grating, with a blank gray screen of intermediate gray during the intervening 1.5 sec interval.

The reverse-correlation stimulus consisted of a series of gratings, the orientation and spatial phase of which was pseudorandomly chosen every 20 or 30 msec (2 or 3 video frames). Thirty-four movies were generated, each 100 frames long, and frames were chosen from 16 orientations, 4 spatial phases and 4 blanks, for a total of 68 possible frames, drawn with equal probability. Each trial was 2 sec long, and each movie was repeated 10-30 times, for a total stimulus duration of at least 11 minutes of visual stimulus, and 500 presentations of each stimulus condition. The accuracy of the timing of the stimulus was carefully tested, because even very small errors in timing could dramatically corrupt the reverse-correlation analysis. During initial testing, the stimulus was presented to a high temporal resolution photoresistor (rise time << 1 msec), placed on the monitor over the display. An elongated "receptive field" was created on the face of the photoresistor, by masking all but an elongated strip with black

tape. The output of the photoresistor was amplified and acquired identically to the neuronal recordings. Reverse-correlation analysis of these "spikes" showed very sharp orientations selectivity, confirming the temporal fidelity of the stimulus presentation, and the accuracy of the analysis procedures. During neural recording, the stimulus was created with a small square in the far corner of the grating, which alternated between white and black on each stimulus frame. The photoresistor was placed over this square, fed through the data acquisition hardware and software simultaneously with the neural signals. Furthermore, the vertical sync output from the PC to the CRT monitor was also acquired. The neural spike times could therefore be synchronized to the precise time of stimulus presentation with 1 msec resolution, equal to the spike time-stamping resolution.

Reverse-correlation analysis

The reverse-correlation procedure is conceptually very simple (see Figure 1). For each τ, the distribution of stimulus conditions preceding the spikes is tabulated. This is equivalent to correlating the stimulus with spike counts across a range of offsets. For the present experiments, the procedure was performed for τs from –20 to 145, every msec. The four phases were averaged, yielding distributions over orientation, which for the sake of simplicity will be called tuning curves throughout the thesis. For each τ, the value for the blank condition was subtracted from the tuning curves. Each tuning curve was then aligned to peak at 90 degrees, for ease of comparison, and normalized by dividing the tuning curves at all τs by the maximum value at any τ. This scales all the tuning curves such that the upper bound is 1 (the max response at the optimal τ), and thus any positive value is a decimal of this value. Negative values, on the other hand are unbounded, though they still represent the fraction of the maximum positive value. Since suppression is almost always smaller than enhancement, almost all cells have values lower than –1. Singular value decomposition (SVD) was implemented in Matlab, as in Mazer et al (2002). The amount of variance captured by the first singular value (as a fraction of the total) is reported. This value indicates how much of the variance, in all the values of the 2-D matrix of time and orientation can be accounted for by a linear combination of two functions (in orientation and time). If a fixed tuning curve were multiplied by a temporal response function, the value would be 1. Deviations from the

prototypical tuning curve, other than scaling, such as shifts, broadening, etc, would decrease the value.

RESULTS

To examine the dynamics of orientation selectivity in V1, RFs were stimulated with a protocol based on the subspace-reverse-correlation technique (Ringach et al., 1997a). The basic approach is similar to previous reverse-correlation protocols that have been used to map receptive fields in earlier visual areas. Instead of using white noise stimuli, oriented gratings were used in order to drive V1 neurons more effectively, and also to allow the responses to be mapped in orientation space. The approach involves presenting a series of rapidly, randomly changing gratings to the receptive field of a neuron while recording its spikes. The cross-correlation of the spike train with the stimulus sequence, over a series of delays (τs) yields the transfer-function or filtering operation being performed by the neuron's receptive field. Another way to look at the operation is the following: for each spike, the stimulus present τ msec previous is assigned to that spike. Summing over all spikes, the probability distribution of stimulus orientation occurring τ msec before the occurrence of a spike is generated. Taken over a series of τs, one can estimate the relative probabilities of different orientations eliciting spikes as a function of time. For the purposes of this work, each probability distribution function will be treated exactly as an orientation tuning curve of stimulus-evoked spike counts, taken in the traditional PSTH manner.

Evolution of the orientation tuning curve

The dynamics of orientation selectivity have not previously been reported in cat V1 neurons using the reverse-correlation technique. The basic features of the responses in the population were similar to those previously reported using similar protocols in macaque monkey V1 neurons (Ringach et al., 1997b; Dragoi et al., 2002; Mazer et al., 2002; Ringach et al., 2003). "Tuning curves" were taken at τs ranging from -20 msec (before stimulus onset), up to times exceeding the response duration (150-250 msec), in steps of 1-10 msec (Figure 2). As expected from previous studies of response latency, the tuning curves at τs <25 msec were generally flat, indicating that the stimulus

had not yet influenced the firing probability of the neuron. Beginning at τs between 25-50 msec orientation selectivity began to emerge. The selectivity at each value of τ was assessed using the OSI, and significant selectivity was determined by setting a threshold of OSI values equal to the mean plus three times the SD of the OSI values taken at τs less than 25 msec. This is a similar criterion to that used by Mazer et al, except that this measures the circular variance, rather than the linear variance, which makes more sense, because orientation selectivity is a circular measure.

Figure 2 shows the timecourse of responses from a typical example cell. Panel A shows the tuning curves at each successive τ, from 15 at the bottom to 125 at the top. During the early part of the response (τ = 30 to τ = 45), the base increases, indicating that all orientations elicit a response above baseline. Then, at τ = ~50, there is a sharp drop in the base, which falls well below baseline, indicating that the non-optimal orientations are suppressing firing, while orientations at and around the preferred continue to elicit an increase in probability of firing. It is interesting that this reversal of the base occurs during the peak of selectivity. Early in the response, the selectivity is determined strictly by an enhancement of firing, whereas in the later portion of the response, both enhancement and suppression of firing sculpt the selectivity. This can be seen clearly in the "psth" plots shown in panel B. The response is shown for each orientation individually (the impulse response, or the height of the tuning curve bin for one orientation, as a function of time). The preferred orientation (90) never drops below zero (the solid line), whereas the non-preferred orientations show a small initial positive peak (enhancement), followed by a small negative peak (suppression).

Across the population of cells (n = 93), the average time of the first significantly selective tuning curve was 34.3 +/- 4.3 msec (Figure 3). This is consistent with findings in monkey, and is somewhat faster than reports based on standard stimulus techniques, most likely due to the temporal smearing of responses which comes from calculating the tuning curves with higher temporal resolution than that of the stimulus refresh rate (as noted by Mazer et al). Responses could also be faster in the reverse-correlation regime because neurons throughout the visual pathway are continually stimulated, and thus closer to threshold, which could decrease latency. The average time of the peak selectivity was 55.8 +/- 3.2 msec, which is again similar to monkey data. Other estimates of the peak time of the impulse response of cat V1 neurons using different stimuli are also fairly low, compared to the peak time of the step response (Alonso et al., 2001). In general, the temporal profile of selectivity was similar across the entire population; the

selectivity increased rapidly after onset, peaked for a short period of time (<10 msec), and then decayed back to a flat, untuned curve. The largest variability in timecourses came during the declining phase of the response (τs greater than ~60 msec). Some neurons were only selective for short durations (<30 msec), whereas others continued to be selective for τs up to 150 msec. Of the later group, there was a subpopulation that didn't decay smoothly back to baseline, but rather had an inflection, or even a second peak in selectivity at τs of ~100-125 msec.

Suppression of firing by non-optimal orientations

The orientation tuning curves used to analyze the orientation tuning of V1 neurons are in fact probability distributions, not firing rate tuning curves, as are typically used to describe the steady-state orientation tuning of V1 neurons. One question that therefore arises in this analysis is how to define an appropriate level of baseline probability against which to compare the bins in the tuning curves. In standard steady-state experiments, it is typical to interleave trials in which the "stimulus" is a blank gray screen of the same mean luminance as the grating stimuli, and take the firing rate during such trials as the baseline, or spontaneous firing level of the neuron. In the reverse-correlation paradigm, the spontaneous level of firing is not indeed the baseline activity of the neuron, as most neurons demonstrate generally elevated firing during the stimulus presentation on a timescale much larger than the individual "stimuli". Blank frames were interleaved in the stimulus sequence to serve as a measure of the level of spiking induced by a stimulus with no features to which the neurons are tuned. Previous reverse-correlation studies have measured the baseline with either such a blank or with a grating with spatial parameters far from those which excite the V1 neurons (Bredfeldt and Ringach, 2002; Ringach et al., 2003). Using the response to the blank gray screen, it is possible to assign the firing probabilities measured with the reverse-correlation procedure both positive and negative values. These values can best be described as "enhancement" and "suppression" of firing probability, for positive and negative values, respectively. While it is tempting to think of these as excitation and inhibition, the synaptic mechanisms responsible for enhancement and suppression can not be clearly assigned with these measurements. Nonetheless, an examination of the levels of enhancement and suppression may be informative in describing tuning curves,

especially in the comparison of tuning curves which are shaped more or less by either of the two components.

Consistent with monkey V1 recordings, most cat V1 neurons showed robust suppression of firing probability following presentation of non-optimally oriented gratings Overall, 82% of neurons showed significant suppression for at least one τ and stimulus orientation. In a few cases, the magnitude of the suppression was similar to the magnitude of enhancement evoked by optimally oriented gratings. In general, the magnitude of suppression was weaker, but in many cases, this may have resulted from floor effects; for many neurons, the probability of firing following non-optimal orientations fell to close to zero. The magnitude of suppression was almost always maximal for orientations at, or close to, orthogonal to the preferred orientation (see below). In all neurons that met the criterion for significant tuning, enhancement was present, though suppression was only present in a subpopulation. The extent of significant suppression, in orientation space, was generally graded, but often covered almost all non-optimal orientations. The timecourse of the suppression was generally similar to that for enhancement, though the first evidence of suppression usually appeared 5-10 msec after enhancement was visible. Figure 4 shows examples of neurons demonstrating the range of suppression magnitude. The example in the middle column is the most representative of the behavior across the population: there is clear suppression, but it is much weaker than the enhancement. The gray background highlights the τs that exhibit clear suppression, from 55-75 msec. Figure 4B shows the "psth" view of the responses of the same three cells, with the timepoints of maximal suppression highlighted. In neurons that showed suppression, it followed a fairly stereotyped trajectory in time. Figure 5 show histograms of the size of the initial general enhancement (left) and the subsequent global suppression (right) to give an impression of their location in the distribution. The values for the three cells shown in Figure 4 are shown by the downward arrows. Unfortunately, it is difficult to definitively ascribe the suppression to particular synaptic mechanisms. In theory, suppression could result from active inhibition, withdrawal of excitation, or any of a large number of combinations of inhibition and excitation.

Comparison of simple and complex cells

Two basic classes of receptive fields have been described in V1 neurons: simple and complex. The two types are distinguished largely by the linearity of their spatial

transformation of visual input to spiking response (Hubel and Wiesel, 1962; Movshon et al., 1978). Linearity can be assessed by several means, all of which aim to ascertain the degree of spatial separation of the responses to light increment and light decrement, indicative of spatially offset "on" and "off" subfields within the receptive field. The classical method is to flash both light and dark spots (or small bars) over the extent of the RF and make independent x-y plots of the response to on and off stimuli. A lack of overlap is seen as an indication of RF linearity, and these fields are classified as simple. Conversely, any cell with overlapping on and off responses is classified as complex. A more recent, and more quantitative, method to determine linearity is to evaluate the temporal response to a drifting sine wave grating (Skottun et al., 1991). A linear transformation of this stimulus would be obtained if the RF were composed of multiple, spatially discrete subfields of alternating sign (on and off), of the same spatial interval as the grating. Thus, cells that approximate a linear transformation of this stimulus are termed simple, and others are termed complex. In practice, this is assessed by comparing the magnitude of the F1 Fourier component of the response (the response component at the temporal frequency of the stimulus) to the F0 component (mean, or DC component of the response). It should be noted that no V1 cell can respond completely linearly, because of the non-linearity imposed by the spike threshold, which doesn't allow nearly as much negative modulation (below baseline, or threshold) of the firing rate as positive modulation. Nonetheless, this method has proven to provide a robust separation of simple and complex cells, as classified by the classical method, and the threshold of the F1/F0 ratio is generally accepted to be at 1, with simple cells falling above 1, and complex cells below (Hubel and Wiesel, 1962; Movshon et al., 1978; Skottun et al., 1991).

Although the distinction between simple and complex cells is generally accepted, the importance (functional, or mechanistic) of the classification is less widely agreed upon. A common viewpoint is that simple cells are an intermediate stage in the visual hierarchy between LGN relay cells, and complex cells. Indeed, most simple cells are found in the input layers of V1 (IV and VI) (Gilbert, 1977), and there is evidence that simple cells send projections to complex cells in the same cortical column (Alonso and Martinez, 1998). As such, simple cells are the first stage at which orientation selectivity is generated, and they are presumed to pass the selectivity on to complex cells, and to the rest of the visual cortex.

It is therefore worthwhile to compare the dynamics of orientation selectivity in simple and complex cells to see whether differences in the timecourse of selectivity might be visible with the reverse-correlation analysis. Figure 6A shows the average timecourse of the OSI for the populations of simple and complex cells. Three features of the timecourse of the OSI are different between simple and complex cells. First, simple cells are more selective, seen as a higher peak OSI, as is true using standard steady state recordings, both in this population and in reports by others (Heggelund and Albus, 1978; Leventhal and Hirsch, 1978; Ringach et al., 2002). Second, the time of peak OSI is earlier for simple cells (44 vs 54 msec). Third, the baseline OSI is higher for simple cells. Otherwise, the evolution of selectivity is similar between the two cell classes. The earlier peak in selectivity in simple cells is consistent with the hierarchical description of information flow through V1, and is not surprising, given the wealth of anatomical and physiological data supporting this arrangement. It has recently been proposed that simple and complex cells represent the extremes of a continuum of linearity of integration, rather than distinct cell classes (Chance et al., 1999; Mechler and Ringach, 2002). To examine this issue, cells were grouped into four groups of the F1/F0 ratio (<. 4, .4-. 8, .8-1.2 and >1.2). Figure 6B shows the average OSI timecourse for these four groups. There is a gradual decrease in the time of peak OSI with increases in the F1/F0 ratio. This suggests that, at least as far as the timecourse of selectivity, the two cell classes may not be absolute, but rather ranges within a continuous range of response properties.

Dependence on cortical depth

Inputs from the LGN impinge mostly in layer IV, but also send projections to layer VI and lower layer III. Layer IV neurons in turn, send strong projections to layer II/III, which sends strong projections to layer V. It is therefore to be expected that the timecourse of responses should be slightly different in the different cortical layers. Evidence from monkey V1 indicates that there may be substantial differences in the orientation selectivity in the different layers (Ringach et al., 2002), although the laminar structure of monkey V1 is quite different from that of cat. Previous analysis of the laminar dependence of orientation dynamics in the macaque have found that the orientation selectivity in layer IV is stable, whereas many cells in other layers have multi-modal dynamics (Ringach et al., 1997b).

To test whether 1) the different "stages" of visual processing can be discerned with the reverse-correlation technique, and 2) whether multi-modal dynamics are layer specific, the dynamics of tuning properties were analyzed separately for different layers. Due to the uncertainty of exact laminar position with the current techniques, this was done by roughly grouping neurons estimated to be in the supergranular layers (<600 μm), the middle layers (600-1200 μm) and the infragranular layers (>1200 μm). The assignment to laminar groups is corroborated by an analysis of the F1/F0 ratio as a function of depth; the highest ratio of simple cells is found between 600-800 μm, providing support for the assignment of laminar location on the basis of microdrive depth readings (data not shown).

Figure 7 shows the average tuning curves and timecourses from the three laminar groups. Panel A shows the tuning curves at a series of τs, and panel B shows the "PSTH" plots for each orientations. As expected, given the general homogeneity of the timecourse of selectivity across the population, there are no dramatic differences among the groups. However, several subtle patterns can be discerned. First, the time of peak response is slightly earlier for cells in the middle layers than for the superficial and deep neurons. Second, the responses of middle layer neurons are slightly shorter, the responses of deep layer neurons are substantially longer, and the responses of superficial layer neurons are intermediate in duration. The mean peak time for middle layers is 50.5 msec, 5.5 msec earlier than the mean peak time for the superficial group, and 3.2 msec earlier than for the deep layers. The intermediate peak time for the deep layers is most likely because it comprises a mixture of layer VI, which receives direct LGN input, and layer V, which only receives multi-synaptic inputs from the LGN. Thus, the timing differences are generally consistent with the known circuitry, and suggest that the reverse-correlation procedure is capable of resolving small timing differences between neurons in different laminae.

Other than these differences in the timing of responses, the overall tuning characteristics of all three groups are fairly similar. The tuning widths, the OSI and the influence of suppression on tuning curves are all nearly indistinguishable for the three curves. There is no evidence of substantial changes in the tuning curve shape over time for any of the laminar groups. Overall, the analysis of orientation dynamics at different cortical depths indicates that other than differences in the timing of responses, the dynamics are rather homogeneous across cortical depths.

Mexican hat tuning curves

Mexican hat tuning curves are tuning curves with valleys on either side of the peak, and can be thought of as being composed of a linear addition of a narrow positive peak and a broad negative peak, each centered on roughly the same orientation. Ringach et al have reported that a significant portion of monkey V1 neurons have Mexican hat tuning curves during the decay phase of the response (Ringach et al., 2003). They argued that this was an indication of a broadly tuned suppressive mechanism, which has been proposed to play a role in shaping orientation selectivity in a number of models (Ben-Yishai et al., 1995; Somers et al., 1995; Carandini and Ringach, 1997).

To examine the propensity of cat V1 neurons to also behave in this way, the cells were examined for signs of Mexican hat profiles. Mexican hat tuning was not found to be prominent in the present data set. Only a few cells had what visually appeared to be a clear example of Mexican hat tuning at any point during the response. Histograms of the orientation with the minimum response at each τ are shown in figure 8A. It was expected that if a substantial portion of cells had Mexican hat tuning, there would be a second peak in the histograms, distinct from the peak at the orthogonal. Such a peak is not seen at any τ – the histogram always has a single peak at the orthogonal, which gradually falls off to close to zero at the preferred orientation. Evidence of individual cases of Mexican hat tuning that might be obscured in the population histograms was sought by searching for neurons which had minima significantly below the orthogonal response at the half decay point of the response, the timepoint which Ringach et al found to have the most clear Mexican hat tuning. Eighteen of 93 neurons had at least one point in the tuning curve more than 3 standard deviations below the orthogonal point at the half-decay time point in the response. Figure 8B shows the average tuning curves of the subpopulation of neurons that met this criterion. The average tuning curves of the other 75 neurons that failed to meet this criterion are shown for comparison. There is very little difference between the tuning for these two populations of cells, suggesting that most of these cases result from noise in the tuning curves, rather than an orientation selective suppressive mechanism.

It is possible that the timecourse of the selective suppressive mechanisms is different in cat than in monkey, and choosing a single timepoint might miss the Mexican hat tuning curves. To check for this, neurons were selected for which any consecutive 10 one msec bins after the response peak had a minimum response to orientations

intermediate between the preferred and orthogonal. Twenty-three of 93 neurons met this criterion, and their tuning curves were averaged. As can be seen in Figure 8C, the average tuning curve of this population has an extremely modest Mexican hat profile at τ=70. However, the average tuning curve of this subpopulation is barely distinguishable from the remaining population, and given that it was specifically selected based on this criterion, this does not seem to be compelling evidence for a specific Mexican hat profile. It is therefore unlikely that a substantial portion of cells have any orientation selective suppression of responses. Furthermore, it is unlikely that many neurons have secondary peaks because this would also result in tuning curve minima not occurring at the orthogonal.

Tuning curve inversions

Another nonlinearity reported in monkey V1 neurons is the inversion of tuning curves during the decay phase; the preferred orientation at later τs is orthogonal to that during the response peak. Potential cases of inversions were identified by searching for any ten consecutive bins during the decay phase with preferred orientation orthogonal to the preferred orientation at the response peak. Eighteen of 93 neurons met this criterion, and their average tuning curves are plotted in blue in Figure 9A. For comparison, the average tuning curves of the 75 neurons identified as "stable", having preferred orientation identical to the peak for at least ten consecutive msec, are plotted in red. It is fairly clear that, although the identified neurons met the fairly strict criterion, they do not, on average, have clear tuning orthogonal to that of the peak response. In fact, the average tuning curve is rather flat during the decay phase indicating that the neurons that were selected by the algorithm are those that are selective for only a short duration. The orthogonal preferred orientation during the decay is most likely the result of random noise in the tuning curves that are generally unselective.

Pinwheel vs orientation domain neurons

The major hypothesis of this chapter is that neurons situated near pinwheel centers will have different dynamics than neurons far from pinwheel centers. Previous reports have described neurons that show large shifts in preferred orientation with time, inversions of tuning curves at late timepoints, and multiple distinct peaks in their tuning curves. Given the larger range of orientations that send inputs to pinwheel center

neurons (see Chapter 2), it might be expected that they would be more likely to have such nonlinear dynamics, whereas neurons situated in the center of orientation domains would be incapable of such large shifts, because they only receive inputs over a narrow range of orientations. As described above, large nonlinearities in the dynamics of orientation tuning are extremely rare in the population. Nonetheless, the tuning curves of pinwheel center and orientation domain neurons were analyzed separately to determine if any subtle features of the tuning curves reveal the different inputs they receive.

Figure 10 shows the average tuning curves of the two populations over the timecourse of the response. For all τs up to 65 msec, the average tuning curves of the two populations are nearly indistinguishable. The only noticeable difference is that the peak of the tuning curve for orientation domain neurons has a slightly higher peak at τ = 45; This difference is quite small and short-lived, and because it occurs during the rapidly changing portion of the response it is difficult to resolve. Later in the response, between 75 and 105 msec, the non-optimal orientations are more suppressed in pinwheel neurons than in orientation domain neurons. The difference is relatively small, and comes at a time during the response when the tuning curves are relatively flat. These differences are seen more clearly in the "psth" plots shown in Figure 10B. The lower peak for the pinwheel neurons is clearly seen in the plot for the preferred orientation (90 degrees), and the two adjacent orientations. The peak of the pinwheel plot (red) never reaches the height of the orientation domain plot. Given the normalization procedure applied to these plots, the best explanation for this difference is that there is more spread in the time of the peak response in pinwheel neurons. Since each neuron is normalized to the maximum response at any τ, if all neurons peaked at the same time, the peak of the average plots would be definitionally one. Therefore, with this analysis, the absolute value of the average timecourse cannot be unambiguously as a difference in response magnitude.

The difference in late suppression is more clear. Neurons at both location show a general suppression, manifested at non-preferred orientations from τ = 55 to τ = 85, but from τ = 65 onward, the magnitude of the suppression is larger on average for neurons near pinwheel centers. The general suppression is hard to reconcile with a mechanism derived from inputs arising from the local network. Neurons in orientation domains receive inputs only from a narrow range of orientations; inputs from the local network should not be able to influence the firing rate (either up or down), in response to

orthogonal orientations. The general suppression must therefore come from some other source – either synaptic inputs from some other source, or intrinsic cellular mechanisms. The impulse response of many LGN neurons indeed shows a large negative component, that begins, on average ~25 msec after the peak of the positive component of the response. There exist cellular mechanisms for contrast normalization in V1 neurons. However, since the average contrast in the RFs is constant across time, and the contrast normalization mechanism is not orientation selective (Carandini and Heeger, 1994; Carandini and Ferster, 1997), contrast normalization should not follow the temporal profile of the suppression seen in the reverse-correlation recordings. It is therefore most likely that the general suppression originates in the impulse response function of the LGN inputs to the cortex. Figure 11 shows histograms of the initial elevation of the tuning curve (top), and the maximal suppression (bottom) for the pinwheel and orientation domain populations. There is no significant difference in the distribution of either.

One way to describe the dynamics of orientation selectivity is to examine the separability of orientation tuning and time. Separability is best quantified using singular value decomposition (SVD). For the current application, SVD uses a linear model of the interaction of orientation and time on the responses of a neuron. If orientation and time are completely separable, the first singular value should capture all of the variance of the orientation-time response. The magnitude of variance accounted for by the first singular value gives an indication of the degree to which the responses are determined by a linear interaction between a fixed orientation tuning curve, and a temporal kernel. SVD have been applied to reverse-correlation data from awake and anesthetized monkey V1, and the first singular value was found to account for ~85% of the variability of responses (Mazer et al., 2002). Applied to the current data, it was found that the first singular value accounted for 77% of the variance across the entire population. If tuning curves shifted, inverted, sharpened, or developed secondary peaks over time, separability would be lessened, and the first singular value would account for less of the variance of responses. SVD was therefore performed separately for pinwheel center neurons and orientation domain neurons, and the degree of linear separability was found to be the same for both populations (76% for pinwheel centers and 78% for orientation domain neurons). Thus, it is unlikely that pinwheel neurons have less linear orientation dynamics over time, either in magnitude or proportion.

Despite the general similarity of the average tuning dynamics in the pinwheel center and orientation domain neurons, it is possible that a subpopulation of neurons near pinwheel centers might show more complex orientation dynamics. Although the SVD analysis did not indicate any differences across the population, it cannot differentiate between non-specific noise and true non-linear interactions. Previous studies have identified several distinct classes of nonlinear dynamics present in V1 neurons, including Mexican hats, shifts, inversions and multiple peaks in tuning curves over time. One of the hypotheses of this chapter was that neurons located near pinwheel centers would be more likely to exhibit such dynamics. As described above, these features were not found in the data. The small number of cells that did meet the criteria for Mexican hat and inversion tuning dynamics were distributed proportionally between neurons in orientation domains and pinwheel centers (data not shown).

DISCUSSION

The results of the reverse-correlation experiments can be summarized as follows. First, the orientation tuning in most cells is characterized by non-specific enhancement, followed by tuning, and non-specific suppression. While variations are seen, this description provides an important general scheme for the timecourse of orientation tuning. Second, there is remarkable homogeneity in the generation of orientation selectivity across the population – the overall diversity of response dynamics is relatively low, compared to some previous results. Cases of inversions, double peaks and Mexican hat tuning curves are extremely rare. Third, there are slightly different response timecourses in different cortical layers, and between simple and complex cells. Thus, the reverse-correlation analysis can resolve small differences in the timing of responses. Fourth, there are only minor differences between the dynamics of neurons as a function of location relative to pinwheel centers in the orientation preference map.

Comparison with previous results

As described in the introduction of this chapter, previous studies of orientation dynamics have produced inconsistent results. Three groups have found large changes in the shape or position of the tuning curve with time, while five groups have found that tuning curves are more or less stable over time. The present recordings have reproduced the latter – tuning curves were extremely stable. It is difficult to surmise

what experimental differences might have lead to such different findings. Obvious parameters such as species, stimulus, recording method and analysis method fail to consistently group with the results. The present experiments provide the most comprehensive analysis of the factors of laminar and map position, and it can be safely concluded that the differences do not arise from different sampling along these dimensions. One possibility that remains relatively untested is an effect of anesthetic state on orientation dynamics (Verderevskaya and Shevelev, 1981, 1982; Shevelev et al., 1993). One group has reported that lightly anesthetized neurons are more likely to show drifts or inversions in preferred orientation over time. If this is true, it may partially explain some of the differences. However, the failure to see such behavior in awake monkeys (Dragoi et al., 2002; Mazer et al., 2002) suggests that this might indicate an artifact of intermediate anesthesia levels, rather than a suppression of shifts by anesthesia itself.

Across different stimulus and recording protocols, one major feature of orientation dynamics has been found consistently. The temporal modulation of the tuning curve offset, or pedestal, follows a similar profile in all reports in which it was explicitly examined: an initial increase in the offset, followed by a decrease below baseline. The present results confirm this aspect of tuning curve dynamics. Whether this behavior reflects mechanisms involved in producing orientation selectivity will be discussed below.

Suppression – inhibition or withdrawal of excitation?

The base, or pedestal, of the tuning curve shows a fairly stereotyped trajectory over time in most neurons. There is an initial enhancement, followed by a suppression. The initial enhancement is easily explained by broad excitatory inputs which are non-zero at the orthogonal orientation. Such inputs are commonly seen in steady state tuning curves, and are predicted by many models of orientation tuning. Suppression of firing could be the result of either removal of excitatory input or an increase in inhibition (or even a cellular reduction in the spike-generation mechanism). It is not possible to accurately determine the source of the suppression, but the evidence is consistent with two main possibilities. Direct measurements of visually-evoked synaptic conductances in V1 neurons suggest that synaptic inhibition is active on the timescale of the suppression (Borg-Graham et al., 1996; Borg-Graham et al., 1998; Hirsch et al., 1998; Anderson et al., 2000; Monier et al., 2003). Support for a thalamic source of the

suppression follows from studies of the impulse responses of LGN cells (Wolfe and Palmer, 1998; Alonso et al., 2001). Many X and Y cells have a biphasic impulse response, with a peaks followed by a trough, though for lagged cells, the order is reversed. The timecourse of the negative aspect of LGN inputs is roughly consistent with the timecourse of the suppression seen here. Thus, the suppression could result from decreased feedforward LGN drive.

Simple and complex cells

The dynamics of orientation selectivity revealed differences in the time to peak response between simple and complex cells. The simplest explanation for this finding is that simple cells receive strong direct thalamic inputs, whereas the majority of the drive to complex cells is at least one synapse removed from direct thalamic input. This is not surprising given that anatomical and cross-correlation studies have already provided strong support for such an arrangement. What is somewhat surprising is the graded relationship between response timing and the degree of linearity of spatial integration. The classical description holds that simple and complex cells form two distinct classes of neurons, without intermediate response types. It has recently been proposed that there is a continuous distribution of the spatial linearity of the inputs to V1 neurons, and that the two classes may be created by the effects of the spike threshold (Mechler and Ringach, 2002). These authors noted that the bimodal distribution of modulation ratio is not reflected in other response properties, across a large group of experiments, and thus may not reflect two distinct cell classes. It has been suggested that a cell may behave more or less linearly, depending on the levels of recurrent excitation it receives, and therefore simple and complex cells represent different operating regimes rather than cell types (Chance et al., 1999; Abbott and Chance, 2002). There is some experimental support for such a scenario, including the finding that specific pharmacological blockade of receptor subtypes and stimulus configurations can shift the behavior of a neuron to be more complex- or simple-like (Sillito, 1975; Rivadulla et al., 2001). Within this framework, the present results support a scheme in which the degree of response linearity reflects the relative proportion of drive provided by feedforward vs recurrent inputs. Neurons with a higher modulation ratio receive more of their drive from feedforward inputs, and therefore respond more rapidly; the opposite is true for neurons with low modulation ratio.

Laminar influences on orientation dynamics

The inputs to, and intrinsic connections within, different cortical layers are correspondingly different. Direct inputs from LGN relay cells are limited to layers IV, VI and lower layer III. Visually driven inputs to neurons outside of these layers is therefore necessarily delayed by at least one synapse, relative to the input layers. The exact laminar positions of the neurons described in this chapter were not histologically reconstructed, but laminar location could be reasonably approximated by the depth readings of the microdrive. The accuracy of this methods is corroborated by the consistently higher probability of finding simple cells between 600 and 1200 μm. The grouping used here was chosen such that the "superficial" neurons were safely above the extent of LGN arbors, and therefore not thalamically driven, the "middle" neurons were likely to be within the reach of the main LGN arbors that target layer IV, and the "deep" neurons were likely to be below this main LGN projection zone, but may have received some direct projections via collateral projections to layer VI. Although these groupings are necessarily rough approximations, the differences in response timing among the groups bear out the accuracy of the estimates.

The major difference found between neurons in different layers is the timing of responses. Neurons in the middle layers on average had peak responses several msec before those in the superficial or deep layers. The duration of responses was also shorter in the middle layers, and substantially longer in the deep layers. These differences are broadly consistent with the degree of thalamic input to the different layers; ie neurons in layers with more thalamic input respond faster. Of course, there are laminar differences in the proportions of simple and complex cells, and the present analysis cannot discern the influence of the two factors: cell type and laminar position. Unfortunately, the number of cells recorded does not allow a separate analysis of cell types in different layers. Regardless, the conclusion that more thalamic drive results in faster responses appears to hold.

Orientation dynamics relative to location in the orientation map

Taken at face value, the lack of difference between pinwheel center neurons and orientation domain neurons in the dynamics of orientation selectivity is not surprising. All previous studies of orientation selectivity relative to location in the orientation preference map have failed to find any difference in firing rate tuning curves near pinwheel centers

(Maldonado et al., 1997; Dragoi et al., 2001). It might have been expected that due to the continuous stimulation during the reverse-correlation stimulus protocol, neurons would be constantly depolarized and the otherwise subthreshold inputs would have been elevated above threshold, leading to broader tuning in this stimulus regime. It seems though that the filtering of inputs occurs prior to spike generation, regardless of the constant synaptic bombardment induced by the flashed grating stimulus. This is not surprising, given the assumption that responses at non-preferred orientations are comprised of a balance of excitation and inhibition. There is strong experimental support for a strong inhibitory component to visual responses to all orientations (Eysel et al., 1990; Borg-Graham et al., 1998), but see (Nelson et al., 1994). If synaptic inputs to non-preferred orientations are kept subthreshold by the shunting action of inhibition, suprathreshold tuning would remain sharp even in the face of continuous visually-evoked depolarization.

It was hypothesized that only neurons near pinwheel centers would be capable of shifts, double peaks and inversions of their tuning curves, because neurons in orientation domains simply do not have access to inputs over a large enough orientation range. However, no evidence was found for such changes in tuning curve shape in any substantial portion of the neurons recorded. Within the framework presented in this thesis, this is not altogether unexpected. If, in fact, the responses of V1 neurons are largely derived from the inputs from the local patch of cortex, there would be very few locations in the orientation map that would provide inputs consistent with these types of changes in the tuning curve shape. Furthermore, some inhomogeneity in the temporal properties of inputs would have to be postulated.

Conclusion

The major conclusion of the reverse-correlation experiment is that there are no substantial differences in the timecourse of orientation selectivity between neurons situated close to pinwheel centers and those in orientation domains. In general, there were very few cases of nonlinearities in the dynamics of orientation selectivity in the population of cat V1 neurons. The lack of differences related to the orientation preference map are probably not attributable to lack of temporal resolution or signal to noise ratio, because other well characterized difference between simple and complex cells, and between neurons in different cortical laminae could be reliably distinguished. Thus, the input-output transformation appears to be stable throughout the duration of the

response, such that the sharply tuned firing rate response is maintained despite the broad inputs that pinwheel neurons receive.

REFERENCES

Abbott LF, Chance FS (2002) Rethinking the taxonomy of visual neurons. Nat Neurosci 5:391-392.

Alonso JM, Martinez LM (1998) Functional connectivity between simple cells and complex cells in cat striate cortex. Nat Neurosci 1:395-403.

Alonso JM, Usrey WM, Reid RC (2001) Rules of connectivity between geniculate cells and simple cells in cat primary visual cortex. J Neurosci 21:4002-4015.

Anderson JS, Carandini M, Ferster D (2000) Orientation tuning of input conductance, excitation, and inhibition in cat primary visual cortex. J Neurophysiol 84:909-926.

Ben-Yishai R, Bar-Or RL, Sompolinsky H (1995) Theory of orientation tuning in visual cortex. Proc Natl Acad Sci U S A 92:3844-3848.

Borg-Graham L, Monier C, Fregnac Y (1996) Voltage-clamp measurement of visually-evoked conductances with whole- cell patch recordings in primary visual cortex. J Physiol Paris 90:185-188.

Borg-Graham LJ, Monier C, Fregnac Y (1998) Visual input evokes transient and strong shunting inhibition in visual cortical neurons. Nature 393:369-373.

Bredfeldt CE, Ringach DL (2002) Dynamics of spatial frequency tuning in macaque V1. J Neurosci 22:1976-1984.

Carandini M, Heeger DJ (1994) Summation and division by neurons in primate visual cortex. Science 264:1333-1336.

Carandini M, Ringach DL (1997) Predictions of a recurrent model of orientation selectivity. Vision Res 37:3061-3071.

Carandini M, Ferster D (1997) A tonic hyperpolarization underlying contrast adaptation in cat visual cortex. Science 276:949-952.

Celebrini S, Thorpe S, Trotter Y, Imbert M (1993) Dynamics of orientation coding in area V1 of the awake primate. Vis Neurosci 10:811-825.

Chance FS, Nelson SB, Abbott LF (1999) Complex cells as cortically amplified simple cells. Nat Neurosci 2:277-282.

Dragoi V, Rivadulla C, Sur M (2001) Foci of orientation plasticity in visual cortex. Nature 411:80-86.

Dragoi V, Sharma J, Miller EK, Sur M (2002) Dynamics of neuronal sensitivity in visual cortex and local feature discrimination. Nat Neurosci 5:883-891.

Eysel UT, Crook JM, Machemer HF (1990) GABA-induced remote inactivation reveals cross-orientation inhibition in the cat striate cortex. Exp Brain Res 80:626-630.

Gilbert CD (1977) Laminar differences in receptive field properties of cells in cat primary visual cortex. J Physiol 268:391-421.

Gillespie DC, Lampl I, Anderson JS, Ferster D (2001) Dynamics of the orientation-tuned membrane potential response in cat primary visual cortex. Nat Neurosci 4:1014-1019.

Heggelund P, Albus K (1978) Orientation selectivity of single cells in striate cortex of cat: the shape of orientation tuning curves. Vision Res 18:1067-1071.

Hirsch JA, Alonso JM, Reid RC, Martinez LM (1998) Synaptic integration in striate cortical simple cells. J Neurosci 18:9517-9528.

Hubel DH, Wiesel TH (1962) Receptive fields, binocular interaction and functional architecture of the cat's visual cortex. J Physiol 160:106-154.

Leventhal AG, Hirsch HV (1978) Receptive-field properties of neurons in different laminae of visual cortex of the cat. J Neurophysiol 41:948-962.

Maldonado PE, Godecke I, Gray CM, Bonhoeffer T (1997) Orientation selectivity in pinwheel centers in cat striate cortex. Science 276:1551-1555.

Martinez LM, Alonso JM, Reid RC, Hirsch JA (2002) Laminar processing of stimulus orientation in cat visual cortex. J Physiol 540:321-333.
Mazer JA, Vinje WE, McDermott J, Schiller PH, Gallant JL (2002) Spatial frequency and orientation tuning dynamics in area V1. Proc Natl Acad Sci U S A 99:1645-1650.
Mechler F, Ringach DL (2002) On the classification of simple and complex cells. Vision Res 42:1017-1033.
Monier C, Chavane F, Baudot P, Graham LJ, Fregnac Y (2003) Orientation and direction selectivity of synaptic inputs in visual cortical neurons: a diversity of combinations produces spike tuning. Neuron 37:663-680.
Movshon JA, Thompson ID, Tolhurst DJ (1978) Spatial summation in the receptive fields of simple cells in the cat's striate cortex. J Physiol 283:53-77.
Nelson S, Toth L, Sheth B, Sur M (1994) Orientation selectivity of cortical neurons during intracellular blockade of inhibition. Science 265:774-777.
Ringach DL, Sapiro G, Shapley R (1997a) A subspace reverse-correlation technique for the study of visual neurons. Vision Res 37:2455-2464.
Ringach DL, Hawken MJ, Shapley R (1997b) Dynamics of orientation tuning in macaque primary visual cortex. Nature 387:281-284.
Ringach DL, Shapley RM, Hawken MJ (2002) Orientation selectivity in macaque V1: diversity and laminar dependence. J Neurosci 22:5639-5651.
Ringach DL, Hawken MJ, Shapley R (2003) Dynamics of Orientation Tuning in Macaque V1: the Role of Global and Tuned Suppression. J Neurophysiol 26:26.
Rivadulla C, Sharma J, Sur M (2001) Specific roles of NMDA and AMPA receptors in direction-selective and spatial phase-selective responses in visual cortex. J Neurosci 21:1710-1719.
Sharon D, Grinvald A (2002) Dynamics and constancy in cortical spatiotemporal patterns of orientation processing. Science 295:512-515.
Shevelev IA, Sharaev GA, Lazareva NA, Novikova RV, Tikhomirov AS (1993) Dynamics of orientation tuning in the cat striate cortex neurons. Neuroscience 56:865-876.
Sillito AM (1975) The contribution of inhibitory mechanisms to the receptive field properties of neurones in the striate cortex of the cat. J Physiol 250:305-329.
Skottun BC, De Valois RL, Grosof DH, Movshon JA, Albrecht DG, Bonds AB (1991) Classifying simple and complex cells on the basis of response modulation. Vision Res 31:1079-1086.
Somers DC, Nelson SB, Sur M (1995) An emergent model of orientation selectivity in cat visual cortical simple cells. J Neurosci 15:5448-5465.
Verderevskaya NN, Shevelev IA (1981) Change in the receptive fields of the visual cortex of the cat in relation to the level of wakefulness. Neurosci Behav Physiol 11:563-569.
Verderevskaya NN, Shevelev IA (1982) Receptive fields of neurons in the cats visual cortex after a change of alertness level. Acta Neurobiol Exp 42:75-91.
Volgushev M, Vidyasagar TR, Pei X (1995) Dynamics of the orientation tuning of postsynaptic potentials in the cat visual cortex. Vis Neurosci 12:621-628.
Wolfe J, Palmer LA (1998) Temporal diversity in the lateral geniculate nucleus of cat. Vis Neurosci 15:653-675.

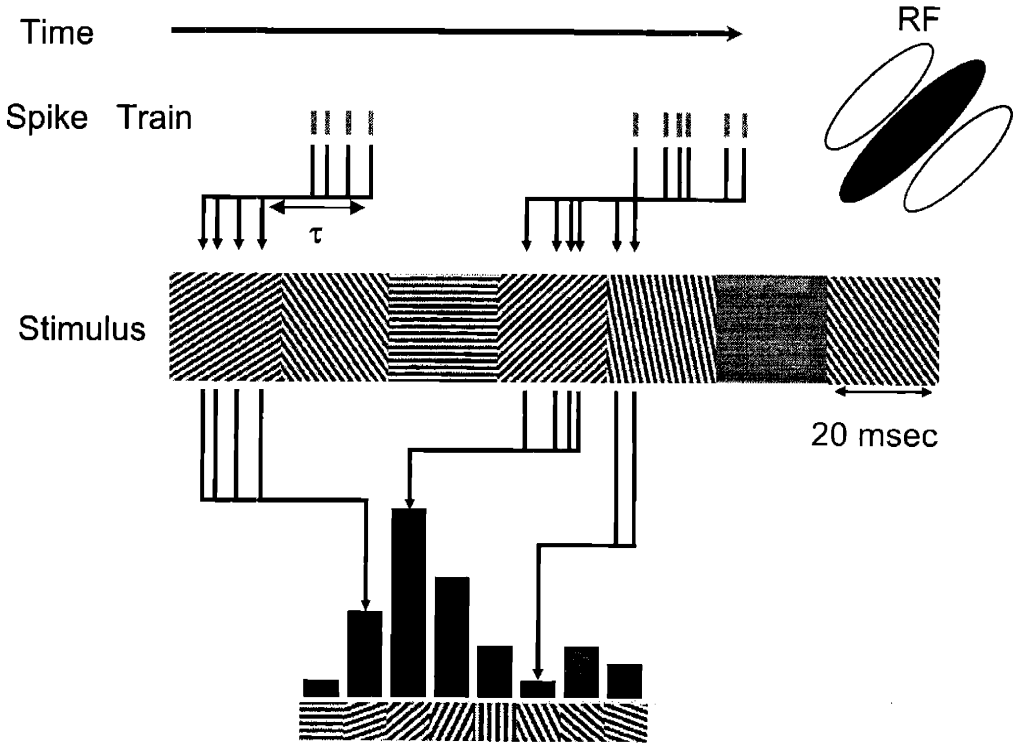
Time
RF
Spike Train
τ
Stimulus
20 msec

Figure 1 - Schematic representation of reverse-correlation in orientation space. As time proceeds from left to right, spikes times are recorded (red tick marks), in response to the random grating stimulus sequence. An example of a short segment of the stimulus is shown below – a new random orientation is presented every 20 msec. For a set value of τ, a histogram of the stimulus orientation present τ msec before each spike is computed. The schematic receptive field of the neuron is oriented at 45 degrees, so the majority of spikes are in response to gratings oriented near 45 degrees.

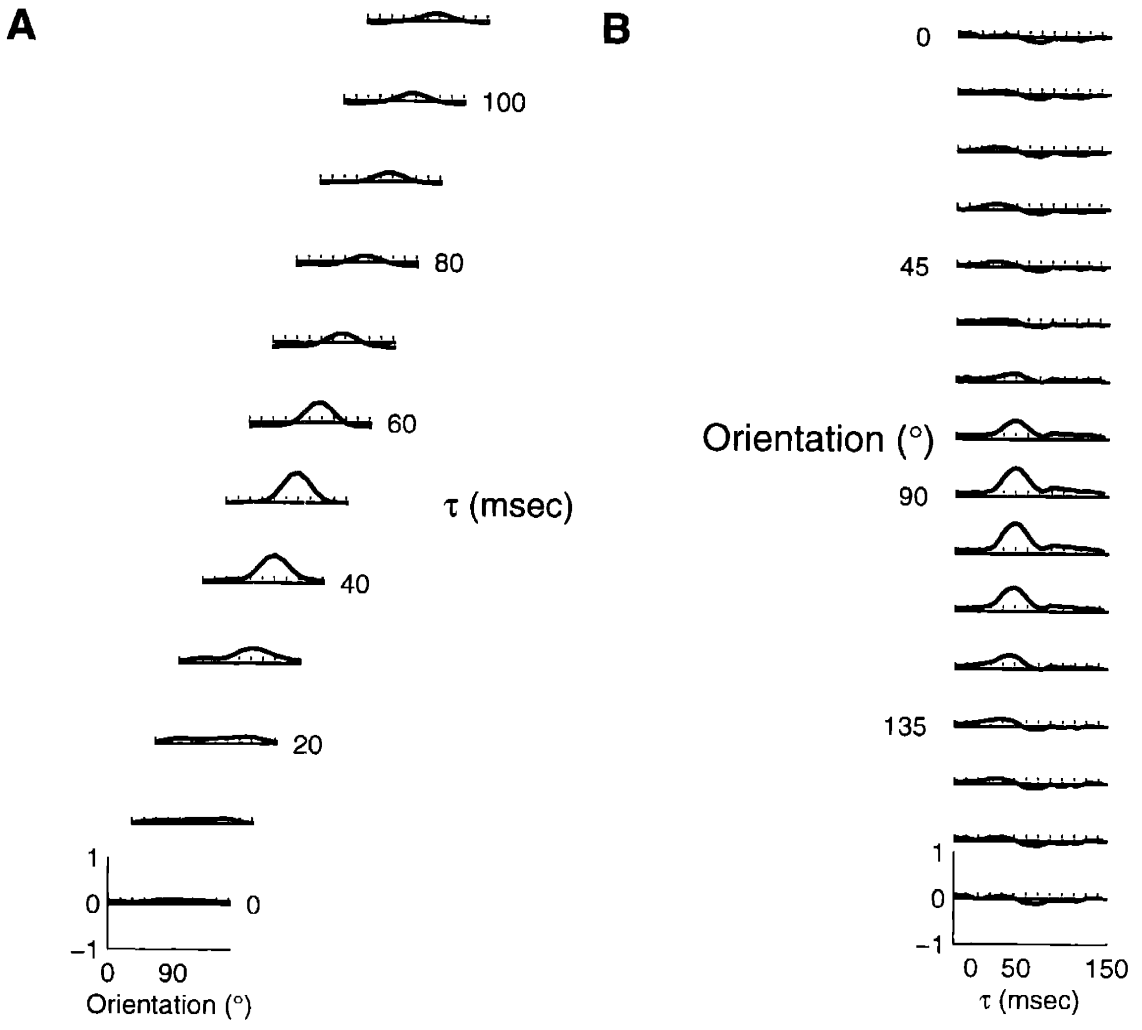
A
100
80
60
τ (msec)
40
20
1
0
−1
0
0 90
Orientation (°)
B
0
45
Orientation (°)
90
135
1
0
−1
0 50 150
τ (msec)

Figure 2 – Example of orientation dynamics. **A.** A series of tuning curves taken at τs ranging between 15 and 125 msec after stimulus onset, as indicated to the right of each plot. The height of the tuning curves at each orientation represent the normalized probability that a spike was fired, plotted between –1 and 1, as indicated by the scale for the bottom curve. The solid line represents zero, and the dashed line represents the mean + 2 SDs of the value during τs less than 20 msec. **B.** The timecourse of response for each orientation, from τ = -20 to τ = 145. The vertical scale and the position of the reference lines are identical to those in panel **A.**

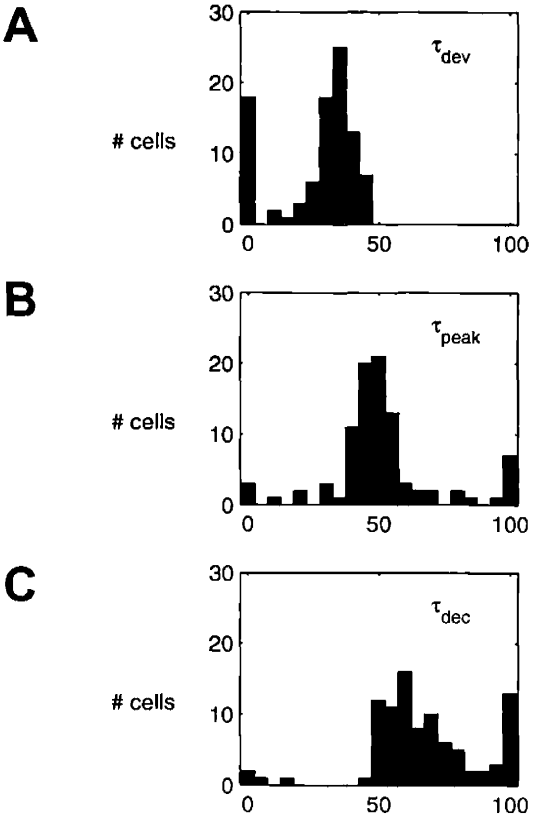
A
cells
30
20
10
0
0
50
100
τ_{dev}
B
cells
30
20
10
0
0
50
100
τ_{peak}
C
cells
30
20
10
0
0
50
100
τ_{dec}

Figure 3. Histograms of three indices of the timecourse of responses. The middle panel shows the time of peak response. The top panel shows the timepoint Tdev, at which the response is half the amplitude reached at Tpeak. The bottom panel shows the time point after the peak at which the tuning curve amplitude has fallen to half of the peak value.

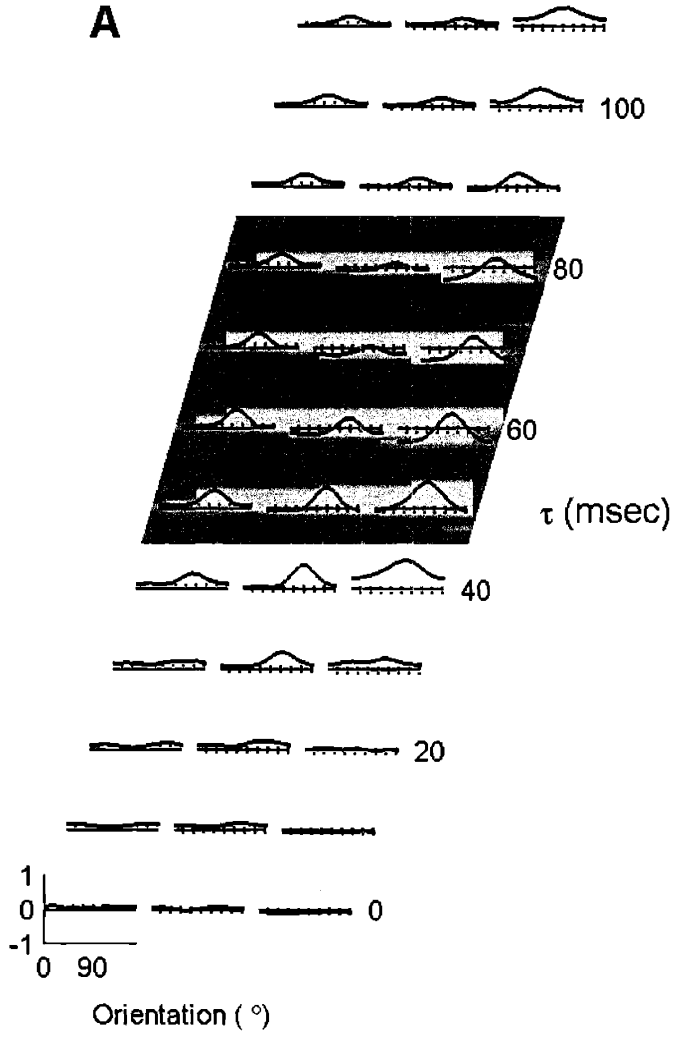
A
100
80
60
τ (msec)
40
20
1
0
-1
0
0 90
Orientation (°)

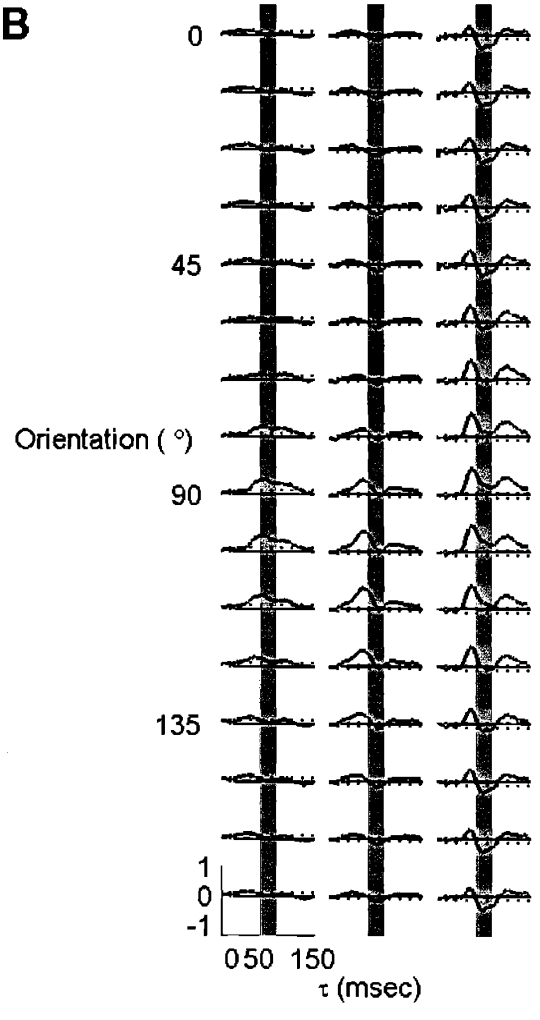
B
0
45
Orientation (°)
90
135
1
0
-1
050 150
τ (msec)

Figure 4 – Examples of responses suppression. **A.** The tuning curves at a series of τs are shown for three example neurons which illustrate the range of suppression seen in the population, from no suppression (left neuron), to dramatic suppression (right neuron). The conventions and scales are the same as in Figure 2. The gray patch highlights the τs during which the differences in suppression are most apparent. **B.** The timecourse of responses for the same three neurons as in panel **A**. The scale and the timepoints of the gray shading are identical to panel **A**.

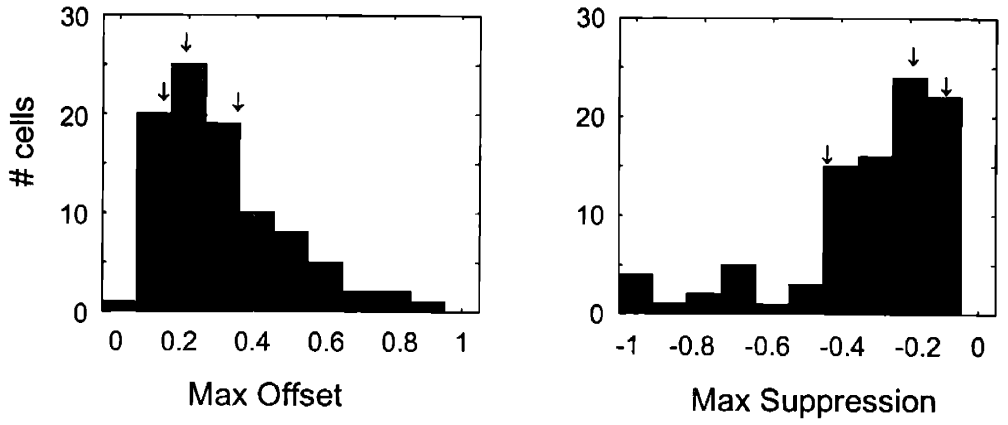
30
20
10
0
cells
0
0.2
0.4
0.6
0.8
1
Max Offset
30
20
10
0
-1
-0.8
-0.6
-0.4
-0.2
0
Max Suppression

Figure 5 -- Histogram of peak tuning curve offset and maximum suppression. The left panel shows the histogram of the maximum value reached by the orthogonal orientation, which represents the offset of the tuning curve. The three arrows indicate the values for the three example neurons shown in Figure 4. The right panel is a histogram of the minimum value in the tuning curve at the orthogonal, which measures the global suppression of the tuning curve. The three arrows point to the values for the three neurons in Figure 4.

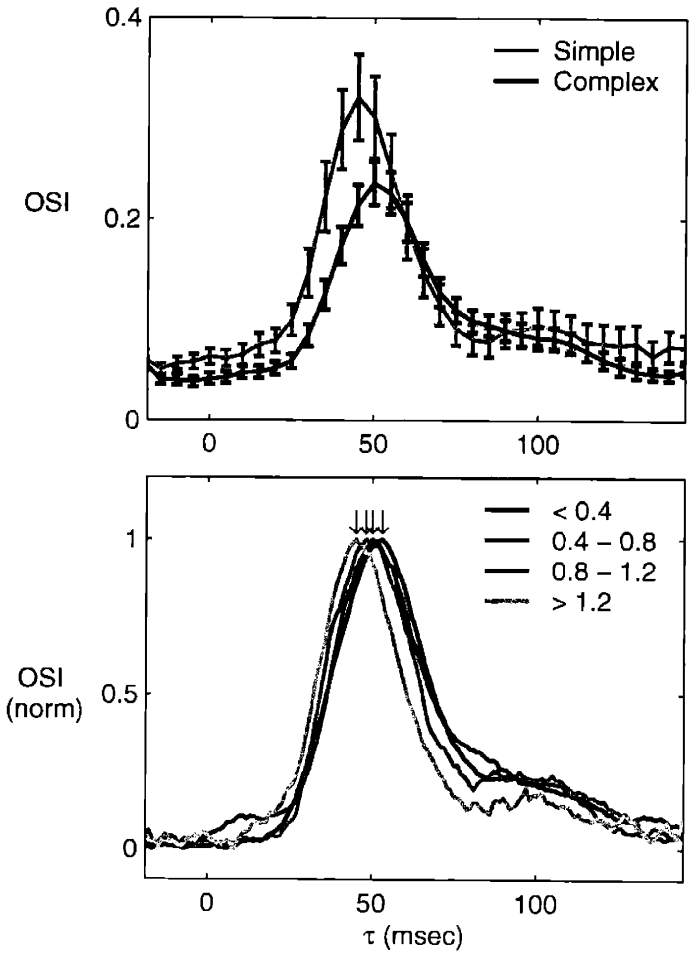
0.4
0.2
0
OSI
Simple
Complex
0
50
100
1
0.5
0
OSI
(norm)
< 0.4
0.4 – 0.8
0.8 – 1.2
> 1.2
0
50
100
τ (msec)

Figure 6 – Comparison of the timecourse of selectivity in simple and complex cells. **A.** The average +/- SEM of the OSI is plotted as a function of τ for the population of simple (n = 28) and complex cells (n = 65). **B.** The scaled average OSIs are plotted for four groups of neurons based on the F1/F0 ratio of their responses to drifting gratings. The arrows indicate the peak time for each curve

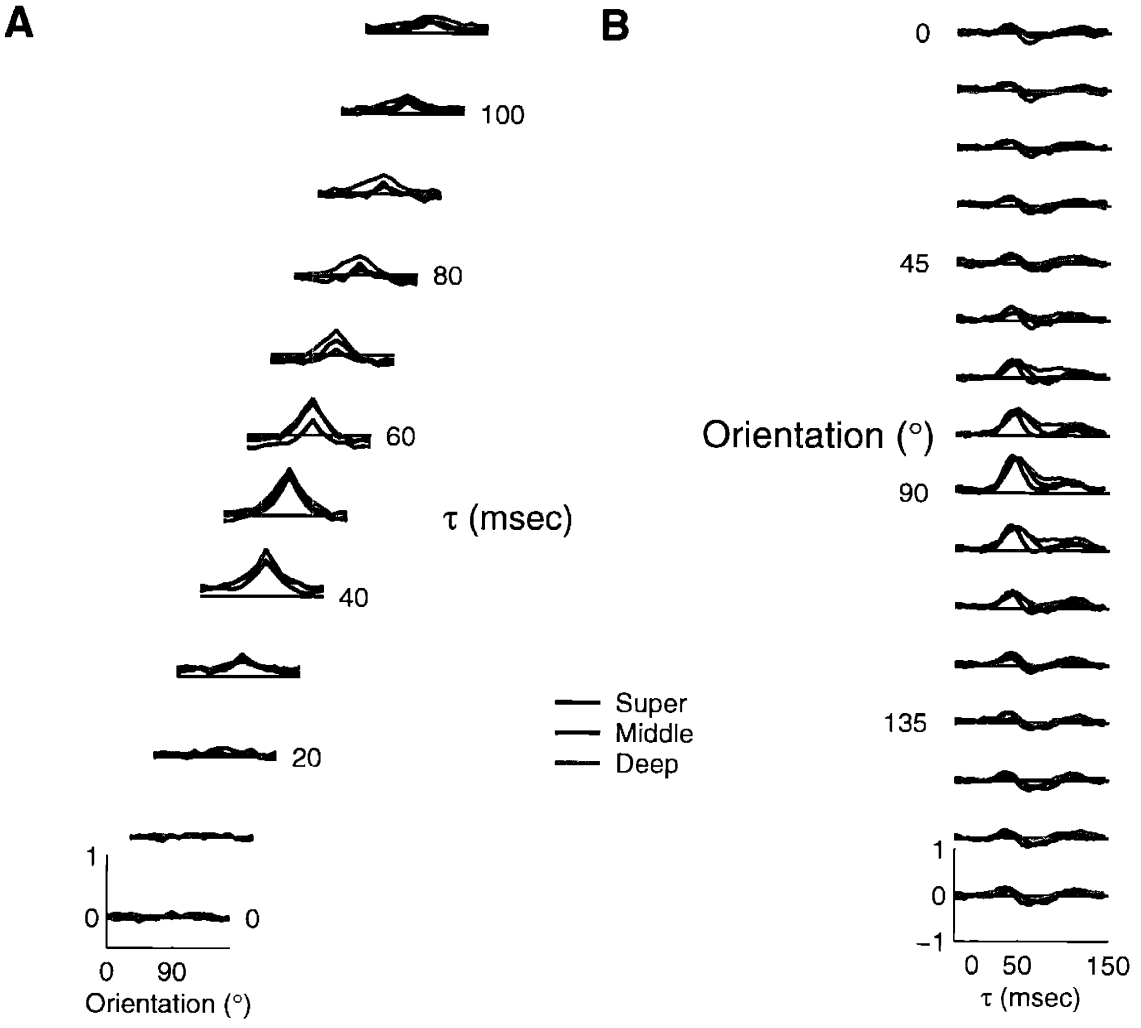
A
100
80
60
40
20
τ (msec)
1
0
0
0 90
Orientation (°)
Super
Middle
Deep
B
0
45
90
135
Orientation (°)
1
0
−1
0 50 150
τ (msec)

Figure 7 – Average dynamics of tuning as a function of laminar position. **A.** Average tuning curves of neurons recorded in superficial layers (< 600 μm; n = 20), middle layers (600 – 1200 μm; n = 44) and deep layers (> 1200 μm; n = 29). The scaling and conventions are the same as in Figures 2-3. Lines representing +/- 2 SDs have been omitted for clarity. **B.** The timecourse of responses for the three laminar groups plotted in panel **A**.

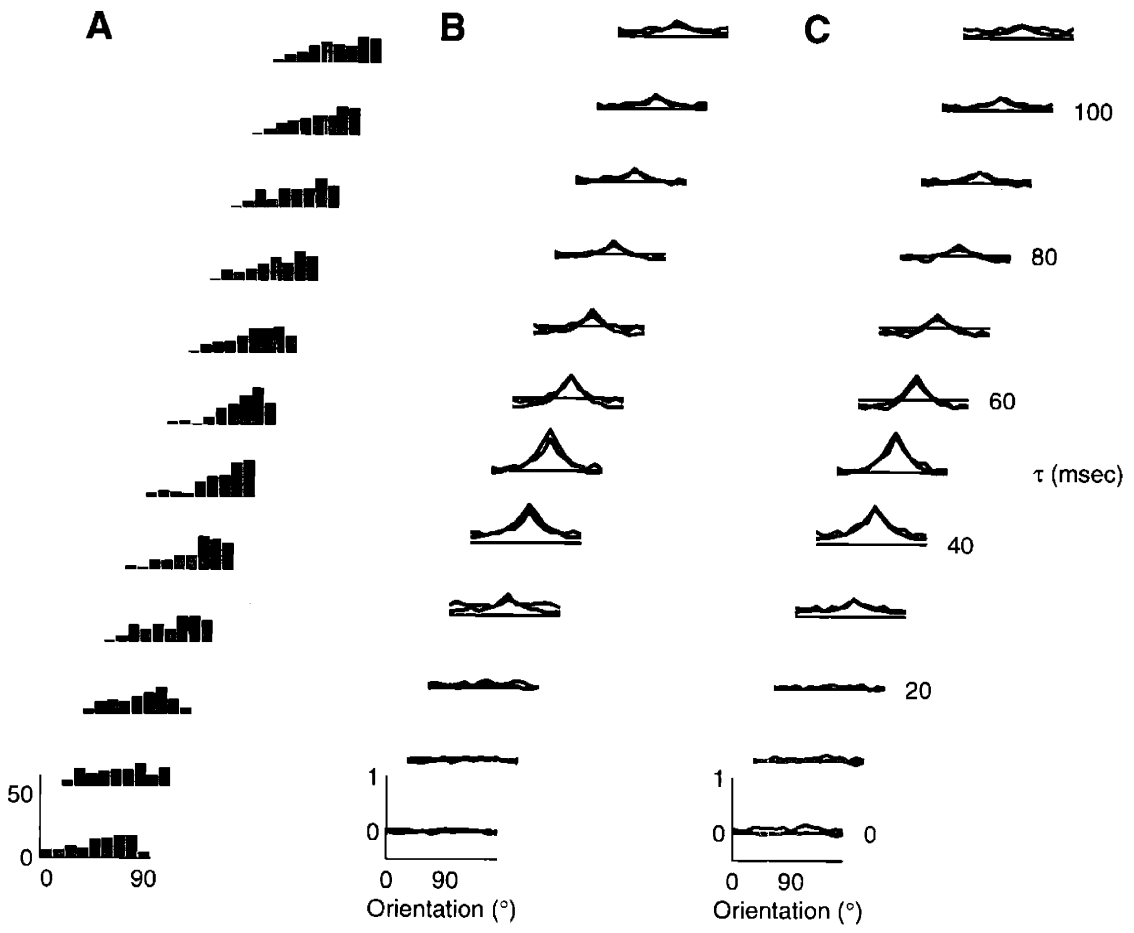
A
B
C
100
80
60
τ (msec)
40
20
50
0
0
90
1
0
0
90
Orientation (°)
1
0
0
0
90
Orientation (°)

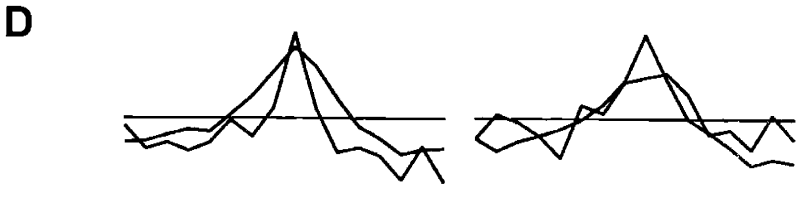
D

Figure 8 – Mexican hat tuning curves. **A** Histograms of the valley of tuning curves in the population. For each value of τ, the histogram plots the orientation with the lowest value in the tuning curve for that τ, for all units in the population (n = 93). The orientations are modulo the preferred orientation of the cell; thus 0 is the preferred orientation of the cell, and 90 is orthogonal. Values between ~22.5 and ~67.5 indicate possible Mexican hat profiles. **B** Average tuning curves for neurons identified as potential Mexican hat cells (blue; n = 24), by searching for cells with minima in the tuning curves between 22.5-45 degrees from the peak. Average tuning curves of the group of cells which consistently had minima at 90 (orthogonal) are shown for comparison (red; n = 65). **C** Average tuning curves of potential Mexican hat cells, with minima at Tdec that were significantly below the value for 90 degrees (blue; n = 20). Average of the cells that did not meet this criterion are plotted for comparison (red; n = 73). **D** Expanded views of the same curves in B (left) and C (right), for tau = 80.

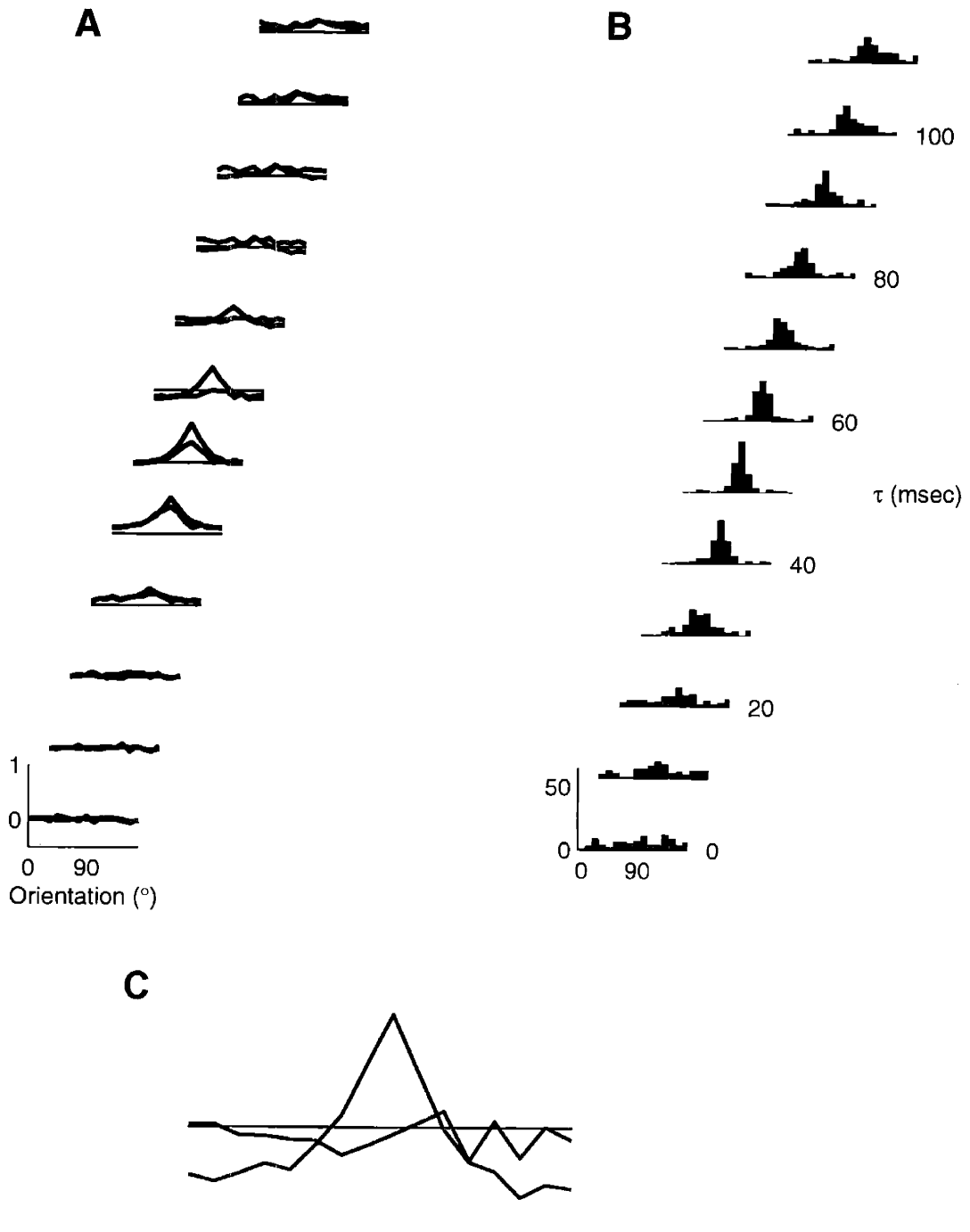
A
B
100
80
60
τ (msec)
40
20
1
0
0 90
Orientation (°)
50
0
0
0 90
C

Figure 9 – Lack of tuning curve inversions. **A.** The average tuning curves of the cells identified as potentially "inverting" (blue; n = 17), and those identified as having stable preferred orientation throughout the response (red; n = 55). All conventions and scaling are the same as in Figure 2. **B.** The histograms of the preferred orientation at each τ, for the entire population (n = 93). The preferred orientations are all relative to the preferred orientation for each cell at its peak response time, which has been aligned to 90, for ease of comparison. Thus, the height of each bin (theta) in the histograms represents the number of neurons whos preferred orientation has shifted by abs(theta-90). Tuning curve inversions would therefore be apparent as increases in the counts in the bins near the edges of the abscissa, corresponding to orientations near 0 or 180 degrees. **C.** A magnified view of the population tuning curve for tau = 80.

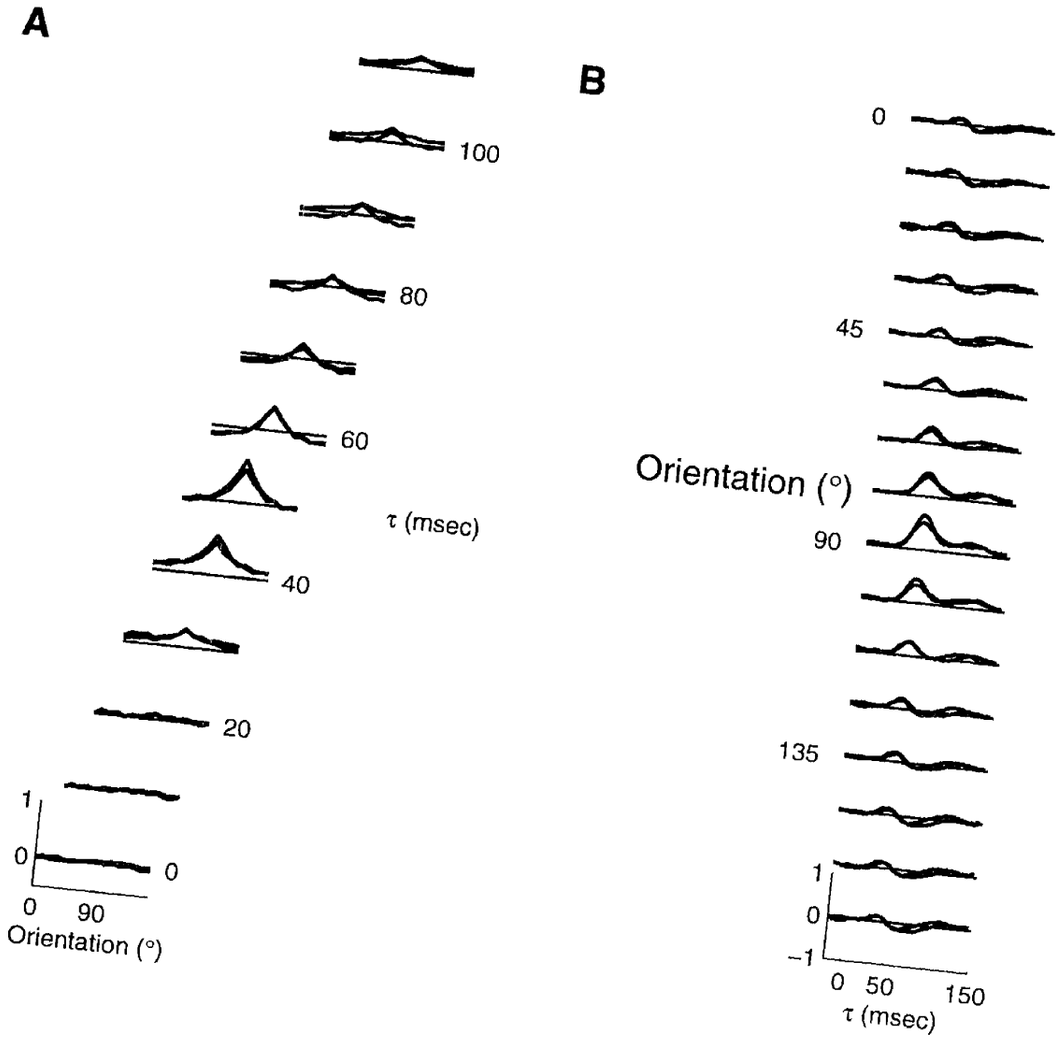
A
100
80
60
τ (msec)
40
20
1
0
0
0
90
Orientation (°)
B
0
45
Orientation (°)
90
135
1
0
−1
0
50
150
τ (msec)

Figure 10 – Orientation dynamics for pinwheel center and orientation domain neurons. **A.** For each τ, the average tuning curve for all the pinwheel neurons (red; n = 34) and orientation domain neurons (blue; n = 59) is plotted. The vertical scale is the same for all τs. The tuning curves represent the average of *normalized* individual tuning curves, with zero representing the blank response, and 1 representing the maximal response at all τs and orientations. The dashed black line represents the response to the blank stimulus for each τ. Thus, points in the tuning curve above the dashed line indicate enhancement of firing, whereas points below the dashed line represent suppression of firing.

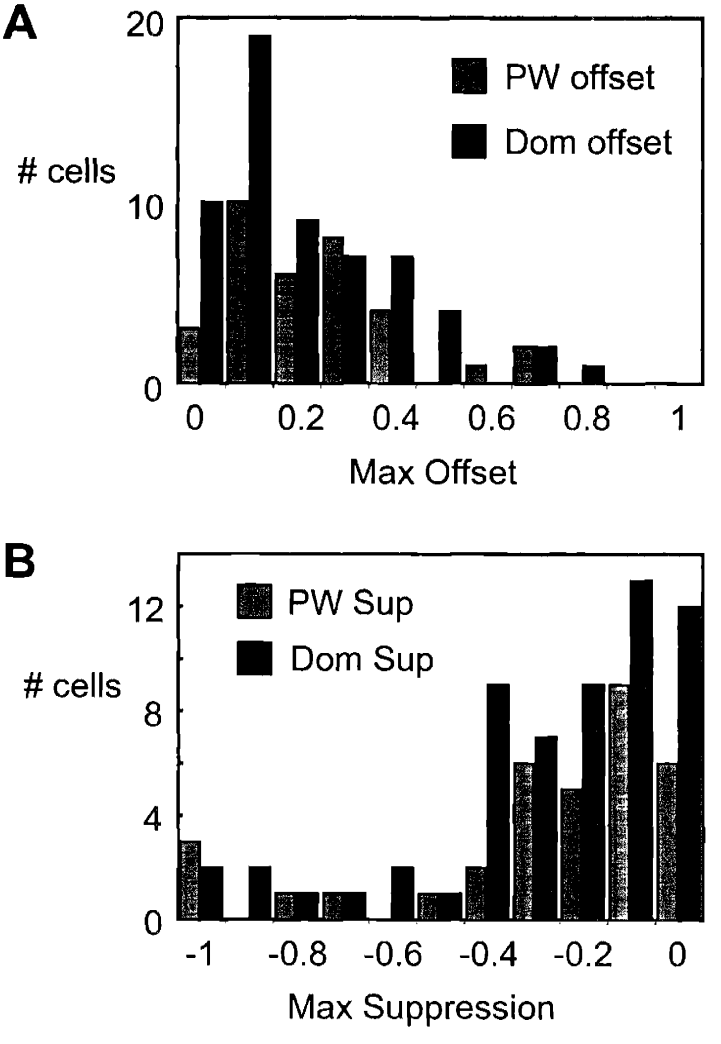
A
20
10
0
cells
PW offset
Dom offset
0
0.2
0.4
0.6
0.8
1
Max Offset
B
12
8
4
0
cells
PW Sup
Dom Sup
-1
-0.8
-0.6
-0.4
-0.2
0
Max Suppression

Figure 11 – Global suppression and enhancement do not differ between pinwheel and orientation domain neurons. Top panel is a histogram of the maximum offset of the tuning curve for pinwheel and domain neurons. Bottom panel is a histogram of the maximal suppression for pinwheel and domain neurons. There is no difference in either.

Chapter 4: Relationship of Correlated Firing in Neuron Pairs to Location in the Orientation Preference Map

ABSTRACT

Correlated spike timing in pairs of neurons is thought to be a manifestation of synaptic interactions. As such, cross-correlation analysis can provide a useful physiological measure of the functional connectivity between pairs of neurons. It has the advantages over anatomical methods that it 1) can assess the strength of connections and 2) allows physiological characterization of the connected neurons. Anatomical studies have found that local V1 connections are isotropic, regardless of location relative to the orientation preference map. It is therefore of interest to test whether the physiological correlate of connectivity follows this same rule. Recordings were made from pairs of V1 neurons at different separations, and known locations within the orientation preference map. The degree of correlation was found to corroborate the anatomical description in several respects. Correlations were found to fall off with increasing cortical separation, consistent with the density of intracortical projections. Neurons close enough to be within the range of a common pool of local projections tended to be correlated, regardless of the difference in their preferred orientations.

INTRODUCTION

The results of the intracellular experiments (Chapter 2) suggest that V1 neurons receive inputs from a spatially isotropic region of local cortex, regardless of their location with respect to the orientation preference map. Thus, neurons near pinwheel centers receive inputs from a broader range of orientations than neurons in orientation domains. Based on the analysis of the relationship of the synaptic inputs to the orientation map, in conjunction with the information derived from other anatomical and physiological studies (Malach et al., 1993; Weliky et al., 1995; Bosking et al., 1997; Kisvarday et al., 1997; Roerig and Kao, 1999; Yousef et al., 1999; Yousef et al., 2001; Roerig and Chen, 2002; Roerig et al., 2003; Tucker and Katz, 2003a, b), it is estimated that the large majority of cortical inputs arise from within a radius of less than 400 μm.

There is further experimental evidence for the spatially isotropic spread of local cortical connections. Several experiments in cortical slices have characterized the spatial pattern of synaptic inputs to single neurons. Weliky and Katz made intracellular recordings from neurons in ferret cortex slice and measured the responses evoked by stimulation of a linear array of stimulating electrodes (Weliky et al., 1995). They found that the strength of the synaptic inputs varied along the array, and concluded that the strongest inputs arise from iso-oriented cortical columns. Roerig and Chen made intracellular recordings from neurons in slices of ferret visual cortex that were aligned to the orientation preference map (Roerig and Chen, 2002). Synaptic potentials were measured in response to stimulation by photo-uncaging of glutamate at a dense matrix of sites in the slice surrounding the recorded neuron. They found that the spatial distribution of the sites that evoked synaptic potentials was roughly circular, and fell off roughly exponentially with distance from the recorded neuron. Thus, electrophysiological evidence supports the anatomical results; the local synaptic inputs to a neuron in visual cortex arise from a circular, symmetric region, with a radius less than 500 μm.

If this is so, then two neurons separated by small distances (up to ~ 700 μm) should share a substantial pool of common cortical inputs. If spike correlations reflect synaptic interactions, their probability and strength should reflect the same rules of connectivity. Specifically, correlations should be equally probable between neuron pairs at a given distance, regardless of their relative orientation preference, and position in the

orientation map, and V1 neurons located within 700 μm of each other should have the strongest correlations.

Based largely on studies of model neurons with known connections, it has been suggested that particular configurations of synaptic connections have specific signatures in the shape of cross-correlation histograms (CCHs) (Perkel et al., 1967; Aertsen and Gerstein, 1985). Two main types of synaptic interactions have been described. Direct synaptic connections between a pair of neurons will result in a peak in the CCH that is slightly displaced from zero, and may have an asymmetric shape, reflecting the shape of post-synaptic potentials. Common excitatory input to the neuron pair (from an unrecorded neuron or pool of neurons) results in a narrow peak centered at the zero offset. The width of the peak may vary, depending on the degree of synaptic jitter or bursting the neurons. Inhibitory connections have been shown to be less visible in CCHs, though they can be seen as shifted or centered troughs, or even as centered peaks (Aertsen and Gerstein, 1985). Thus, by recording the spike trains of a pair of neurons may possible to infer whether, and in what configuration, they are synaptically connected. However, the specific relationship between CCH shape and synaptic coupling has not been demonstrated empirically. For the purposes of this chapter, CCH peaks will be regarded as an indication of some (non-specific) form of synaptic interaction, or functional connectivity.

A number of previous studies have explored the functional connectivity of pairs of V1 neurons using spike train cross-correlations (Toyama et al., 1981; Michalski et al., 1983; Ts'o et al., 1986; Engel et al., 1990; Gray et al., 1990; Hata et al., 1991; Schwarz and Bolz, 1991; Nelson et al., 1992; Livingstone, 1996). These studies have assessed the influence of the receptive field properties of the neurons in the pair on the probability and strength of peaks in the CCH. The reasoning is that the rules of the connectivity of the microcircuit should be revealed in the patterns of correlated firing. T'so et al (1986) analyzed the spike correlations as a function of relative orientation preference (Ts'o et al., 1986) of pairs of V1 neurons. They found that cells with similar preferred orientations tended to show correlations, even if their receptive fields were displaced by large distances. They found that neuron pairs with large differences in preferred orientation did not have apparent spike correlation, even if their receptive fields were largely overlapping. They concluded that the correlations result from a network of very specific connections between cortical columns that share the same, or similar orientations. Hata et al (1991) reported similar findings. They found that >70 % of

correlated pairs had distances < 500 μm, and that >95 % of correlated pairs had orientation differences less than 45 degrees. Nelson et al (1992) found that CCHs were divided into three groups, based on the width of the central peaks (narrow, medium and broad). They found that narrow peaks only occurred in pairs of neurons with overlapping receptive fields, but medium or broad peaks could be found in pairs that were separated by up to 5 degrees of visual angle. Furthermore, they found that narrow peaks were 3-4 times more likely between pairs with orientation preferences within 22.5 degrees of each other. Medium width peaks had weaker orientation dependence, and broad peaks had no dependence on relative orientation.

Overall, two general conclusions have emerged from cross-correlation analysis in V1: neurons are more likely to be correlated the closer they are to each other in cortical space, and in orientation preference. However, because of the structure of orientation preference maps, these two factors are confounded – on average closer neurons will tend to have similar preferred orientations. It is therefore impossible to tell from these analyses whether it is the distance in cortical space or in orientation space that governs the functional connectivity of neuron pairs. Little evidence has been presented to discern which of these two factors is more important in determining connectivity. Only one paper has made any reference to this confound. Das and Gilbert (1999) reported that the strength of correlation fell off with distance with a similar slope both for iso-oriented and cross-oriented pairs. However, this interpretation should be viewed with caution, given that they only reported data from four iso-orientation neurons pairs with distances above 400 μm.

In order to resolve the importance of orientation difference and cortical separation on functional connectivity, pairs of neurons were recorded at identified sites in the orientation preference map. The breaks in the progression of preferred orientation at pinwheel centers provide an ideal dissociation between these two factors which allows the influence of each to be measured.

MATERIALS AND METHODS

Animal preparation

Experiments were performed on adult cats (2-3 kg) of either sex according to procedures that were approved by MIT's Animal Care and Use Committee and conformed to NIH guidelines. Animals were prepared for imaging and recording

according to procedures that have been described (Rao et al., 1997; Dragoi et al., 2000). Briefly, animals were anesthetized (1-1.5 % isofluorane in 70:30 N_2O and O_2), paralyzed with vercuronium bromide (0.2 mg/kg/hr) in a 50-50 mixture of lactated Ringer's solution and 5% dextrose, and artificially respired. Expired CO_2 was maintained at 4%; anesthesia was monitored continuously. A craniotomy and durotomy were performed over area 17, and a stainless steel chamber was mounted on the skull. The chamber was filled with agar (~2.0% in saline), covered with a circular coverglass and coated with viscous silicone oil.

Optical imaging

An orientation map was first obtained by optical imaging of intrinsic signals. Full-field, high contrast square-wave gratings (0.5 cycle/deg, 2 cycles/sec) of 4 orientations, drifting in each of 2 directions were presented using STIM (courtesy of Kaare Christian, Rockefeller University) on a 17 inch CRT monitor placed at a viewing distance of 30 cm. Images were obtained using a slow-scan video camera (Bischke CCD-5024, Japan), equipped with a tandem macro-lens arrangement, and fed into a differential amplifier (Imager 2001, Optical Imaging Inc, NY). The cortex was illuminated with 604 nm light, and the focus was adjusted to ~500 μm below the cortical surface during imaging. Care was taken to obtain reference images of the surface vasculature several times over the course of the imaging session to detect any shift of the cortex relative to the camera, and increase the accuracy of electrode penetrations.

Extracellular spike recordings

Recordings were made with arrays of paralene-coated tungsten electrodes with resistences between 2 and 4 Mohms, tested at 10 KHz (FHC). Arrays consisted of 4-7 electrodes mounted onto a thin stainless steel plate with dental acrylic. Arrays were fabricated by hand under a low power dissecting microscope with the assistance of custom micromachined guide tubes, which insured accurate inter-electrode separations. The error in electrode tip alignment, along the axis of the electrodes (depth) was estimated to be less than 50 μm. Signals from the electrode tip and a ground probe attached to the scalp were passed to a 1X high input impedance preamplifier (FHC) via short (~10 cm) leads. The differential signal was amplified, filtered between 100 Hz and 8 KHz, and sent to digitizer, interfaced with PC running data acquisition software

(Experimenter's Workbench, Datawave Technologies). A threshold was set manually in the data acquisition software, and a window of ~.7 msec before and 1.0 msec after each threshold crossing was digitized at 10 KHz and stored to disk. The software package allowed visualization of the threshold overlaid on 1 sec sweeps of the continuous data, as well as the digitized spike waveforms captured by the thresholding procedure. The spike waveforms were sorted offline, using a cluster cutting procedure (SpikeSort, Datawave Technologies) based on projections of different planes through the multidimensional space of waveform parameters. Typically between 1-2 clusters were defined for each electrode.

Trial timing and synchronization between stimulus presentation and data acquisition were performed using Cortex. A pair of PCs running the "two computer" version of Cortex were used; the "host" computer running in DOS controlled the timing of events as well as data I/O interface with other hardware via a CIO-DIO24 card, and a second "video" computer, running Windows XP presented visual stimuli to a CRT display, using a graphics card with 64Mb of onboard video RAM. Timing control files were written in Cortex runtime environment.

Cross-correlation of spike trains

The spike train cross-correlation was computed from the trials for each stimulus orientation independently. The raw CCH was computed by standard methods. The shuffle-corrector (the cross-correlation of all non-simultaneously recorded trials) was subtracted from each raw CCH, as is standard in the literature (Perkel et al., 1967; Aertsen et al., 1989). The further normalization step, of subtracting firing-rate correlations, was also made to avoid peaks unrelated to neural synchronization (Brody, 1998, 1999a). To do this, the cross-correlation was computed between the smoothed firing rate for each trial, and this was subtracted from the spike time CCH. This procedure is very similar to those previously proposed to correct for potential artifacts arising from slow variations in excitability (Brody, 1999b). The strength of correlation was calculated as the amplitude of the firing-rate adjusted CCH at the zero time bin. The CCHs were normalized by the number of spikes such that the value in each bin is equal to the percentage of all spikes. Thus, correlations between different stimulus conditions, with different numbers of spikes, can be directly compared. Strength measures that compute the area under the curve of the central peak showed qualitatively similar trends as those computed from the height.

RESULTS

Recordings were made from pairs of neurons at different cortical separations and locations in the orientation map, and cross-correlation histograms were computed from their spike trains. Figure 1 shows an example of the recordings, and the data processing used. Figure 1A shows the raster plots of the responses of two neurons to the grating stimulus. Figure 1B is a schematic representation of the cross-correlation procedure. Figure 1C shows the raw cross-correlation histogram (CCHraw) in blue, and the shuffled CCH (CCHshuf) in red. The CCHshuf is the mean CCH of all non-simultaneous trials (also sometimes called the shift-predictor). The difference between the CCHraw and the CCHshuf is formally the cross-covariance CCOV of the spike trains, but in keeping with the more common notation in the literature, it will be termed the shuffle-subtracted CCH (CCHsub) here. The purpose of subtracting the CCHshuf is to remove the potential confound of spike synchronization attributable to the common stimulus, rather than to common neural interactions (Perkel et al., 1967). The CCHsub is by far the most commonly used metric of spike synchronization in the neurophysiology literature. However, it has recently been noted that non-stationarities in firing rate on slow timescales, which are not corrected by the shuffle subtraction, can introduce peaks in the CCH unrelated to neural interactions (Brody, 1998, 1999a). Therefore a further normalization procedure was used to correct for possible slow firing rate changes; the CCHsub computed from the time-averaged firing rate (rather than individual spike times) was subtracted from the CCHsub (Figure 1D). The necessity and details of this procedure are discussed in the Appendix. The resulting firing rate adjusted CCH (CCHFRadj) was used to assess the degree of correlated firing in the remainder of the analysis in this chapter, and will simple be referred to as the CCH for the sake of clarity.

Based on tracer studies, and the subthreshold tuning curves measured intracellularly (see Chapter 2), it was expected that the pattern of correlations would be consistent with isotropic input pools to both neurons, regardless of position in the orientation map. To directly test this hypothesis, electrode arrays were constructed that consisted of a circle of six electrodes surrounding a central electrode with a radius of ~500 μm. The array was centered either on a pinwheel center, or on the center of an orientation domain. With such an arrangement, the region of local cortex that putatively provides common input to the central neuron and each of the surrounding neurons

should represent a wide range of orientations if the center neuron is located at a pinwheel center, and a much narrower range if the center neuron is in an orientation domain. If the degree of functional connectivity is based on an orientation-specific rule, the center neuron should only show CCH peaks with one or two of the surrounding neurons when the array is centered on a pinwheel center. However, if the degree of correlation depends on the intracortical separation, then the center neuron should on average have equal correlation strength with all of the other neurons.

Figure 2 A and B show the CCHs between the center neuron and each of the surrounding neurons for arrays centered on an orientation domain (A) and a pinwheel center (B). In both cases, there is a central peak in all of the CCHs, indicating that the center neuron is functionally connected with each of the neurons, regardless of the relative orientation preference of the two neurons, or the specific location in the orientation map. Both the shape of the CCH peaks, and their magnitudes are qualitatively similar for each neuron pair in both cases.

In total, 653 neuron pairs were analyzed, culled from a substantially larger pool, based on the absence of line noise in the recordings, the quality of the optical signal, and adequate spike numbers collected. Neuron pairs recorded on the same electrode were not included for analysis. Each neuron pair was classified based on the intracortical separation and difference in preferred orientation. By analyzing these two factors separately, it is possible to dissociate which factor determines the functional connectivity of a pair of neurons. Neuron pairs separated by less than 700 μm were considered to have potential common inputs mediated by local cortical connections, whereas neurons separated by more that 1 mm could only have received common inputs by long-range connections. Within these two groups, neuron pairs were divided into four bins of preferred orientation difference, equally spaced between 0 and 90. CCHs were averaged across all of the neurons in each bin (Figure 3). For locally connected pairs, the average strength of the correlation (peak height) shows no systematic relationship to orientation difference (red bars in Figure 3A). This pattern is consistent with the local functional connectivity being mediated by spatially isotropic inputs, rather than orientation specific connections. For long-range neuron pairs, the average correlation strength is weaker for all orientation differences. There is a gradual decline in correlation strength, with no correlation for pairs with near orthogonal orientation preferences (blue bars in Figure 3A), suggesting that there may be a broad orientation specificity to the long-range interactions. Figure 3B-C shows the average

CCHs for each of the groups. Tracer studies of long-range connections have found that the long-range lateral connections in layer II/III are orientation specific (Bosking et al., 1997; Kisvarday et al., 1997), though the degree of specificity is unsettled. The lack of tight orientation selectivity of correlation strength may indicate that there is some source of synaptic interaction other than the layer II/III patchy lateral connections, such as ascending layer IV axons, feed-back or commisural connections which is not orientation specific. It may also result from the fact that a substantial portion of neurons are near pinwheel centers in the population, and the long-range connection patterns of these neurons has not been studied with anatomical tracer injections.

Another advantage of cross-correlation analysis of functional connectivity over anatomical methods is that the stimulus conditions under which the connectivity is expressed can be assessed. An anatomical projection form one neuron to another may be misleading if it is activated rarely, or only under certain stimulus configurations. The analysis above indicated that nearby neurons interact, regardless of their orientation preferences, but this leaves open an important question. When are they correlated? Is there a fixed probability of correlated firing, regardless of the inputs or activity of the cortical network? Or are there specific stimulus conditions that activate the functional connectivity? This question is important because it reveals the network interactions, ie what is the source of the functional connectivity? It is also relevant to the potential population representations of the stimulus and to the question of how sharp orientation tuning is generated and maintained.

The CCHs were calculated independently for each of the eight stimulus orientations of the stimuli used. Figure 4 shows two examples of this analysis. In panels (A, C), the CCHs for each stimulus orientation is shown. In panel (B, D), the firing rate tuning curves of the two neurons, as well as the strength of the correlation are plotted. For the pair shown in Figure4A-B, the two neurons had similar preferred orientations. The tuning curve of the correlation strength also had a similar tuning curve, peaking intermediate to the tuning curves of the two cells. It is important to note that the strength calculation has been normalized for the firing rates of the two neurons – the strength represents the percentage of spikes in the center bin regardless of the absolute number of spikes. The two neurons in this example were located <500 μm apart, in the same orientation domain, so it is not altogether surprising that they should have the strongest synaptic interaction when the stimulus activates the home column. The neuron pair shown in Figure 4C-D, the preferred orientations were close to orthogonal, and

interestingly, the correlations are strongest for the intermediate orientations, away from the peaks of the neurons' tuning curves. These neurons were also located <500 μm apart, and therefore the neurons located between them in the orientation map had intermediate preferred orientations. It is therefore interesting to know, across all cell pairs, with a wide range of positions in the orientation map, what stimulus orientations engage correlated firing.

Therefore, all of the local neuron pairs were grouped based on the difference in preferred orientation, and the tuning curves of the correlation strength were averaged. Figure 5 shows the results of this analysis. The correlation strength tuning curves were aligned to the preferred orientation of one of the cells, which is positioned at orientation zero in the plots. For neuron pairs with very similar orientations (top panel), the correlation, as expected, peaked near the neurons' preferred orientation. The correlation strength falls off, as the stimulus orientation deviates from the preferred orientation, reaching about half of the peak value at the orthogonal orientation. As the difference in orientation preference increases, the peak of the correlation strength shifts accordingly, such that the peak is generally intermediate to the preferred orientations of the two neurons. For orthogonally tuned neurons (bottom panel), the strength tuning curve is fairly flat, compared to the top panel, but there is a modest peak at 135, intermediate between the two cells' preferred orientations. The correlation strength is lowest near the preferred orientation of the two neurons. This suggests that the population that engages the functional connectivity is weakly activated by either of these stimuli. The smaller modulation depth of the strength tuning curve compared to the top panel is consistent with the structure of the orientation map. Local cell pairs with similar preferred orientations most likely sit in the same orientation column, and receive most of their common inputs from other cells in the same column – there are a limited number of orientation map locations that can have two iso-oriented cells within 700 μm of each other. Orthogonal neuron pairs, however may be found in a number of configurations, and the orientations represented in the cortical patch in between them is potentially quite diverse.

DISCUSSION

The results of the analysis of correlated firing suggest that the primary determining factor in spike train correlations is cortical separation. At least for neurons

separated by less than 700 μm, there does not appear to be an orientation-specific rule to functional connectivity. Previous studies that have reported orientation specificity of correlations have probably confounded orientation selectivity and cortical distance because they are highly correlated across the majority of V1. By specifically targeting locations near pinwheel centers, where the correlation between orientation preference and cortical space is broken, the two factors were dissociated. The orientation tuning of the strength of correlation suggests that the populations that provide common input tend to be activated most strongly by orientations intermediate to the preferred orientations of the neuron pair. This population is relatively homogeneous for iso-oriented pairs, because they are most often found in homogeneous locations in the orientation map. At the other extreme, the orientation representation located intermediate to orthogonally oriented pairs is more heterogeneous, but biased towards orientations intermediate to the preferred orientations of the cell pair.

Comparison with anatomical studies of connectivity

A number of studies have combined optical imaging of orientation preference maps with injection of tracers, in order to map the connections between neurons to the layout of cortical columns. The injections have generally been targeted to orientation domains, but one study has specifically targeted pinwheel centers. Bosking et al (1997) measured the orientation specificity of boutons labeled by biocytin injections for local (<500 μm) and long-range (>500 μm) projections. They found that the long-range connections were fairly orientation specific, the local projections were generally less specific, and often spatially homogeneous. Kisvarday et al (1997) also made biocytin injections at known locations in the orientation map and came to similar conclusions, although quantitatively, they found considerably less orientation specificity for both local and long-range projections. The authors also analyzed the connections of inhibitory neurons, and found them to be even less specific than the excitatory ones. Yousef et al (2001) made both anterograde and retrograde injections at pinwheel centers. They found that the extent of the label was smaller for these sites than for orientation domain injections, and that there was no orientation specificity of the connections. An integration of these studies yields a conclusion that there are two distinct systems of lateral connections in V1 – local and long range – that follow different rules of connectivity. There are several limitations of tracer injection studies, including the inability to resolve individual neurons, the inability (in some cases) to identify the

excitatory or inhibitory nature of the synaptic connections, and the lack of knowledge about the physiological strength of the connections. Measurements of functional connectivity provide a good complement to anatomical studies.

The patterns of functional connectivity seen here broadly confirm the anatomical studies. The correlation strength of local neuron pairs was on average stronger than the strength of long-range correlations, though there were examples of long-range pairs with strong correlations. This is consistent with the high density of local labeling, and the more sparse, patchy labeling at long range. The local correlations were not orientation specific, consistent with the general lack of specificity of local projections found in tracer studies. The long-range correlations showed weak orientation-specificity – there was no average correlation between orthogonal long-range neurons. This might indicate that some source of synaptic inputs is responsible for correlations other than the intrinsic lateral connections. An important consideration is that a significant portion of common inputs even to layer II/III neurons may arise from layer IV axons. Layer IV axons extend up to 6mm in layer II/III, and distal axons show no bias for preferred orientations (Yousef et al., 2001).

Relation to theories of synchronous firing

The mechanisms underlying correlated firing in cortex are somewhat controversial. A peak in the CCH is an indication of no more than non-independence of firing times; the mechanism must be inferred based on the features of the CCH and of the circuitry in question. Traditionally, narrow, centered peaks in the CCH (as examined in this study) were interpreted to indicate that two cells received common excitatory input. This interpretation can only be firmly supported when the underlying circuitry can be established, which is not the case in cortex, where the circuitry is particularly complex. Other potential mechanisms include mutual excitation, or common inhibitory input, though these would generally be considered to yield broader peaks. Another theory has proposed that correlations can arise from dynamic network states that specifically synchronize groups of neurons across large regions of cortex in a stimulus specific manner. As such, these correlations have been postulated to play a role in binding the firing of neurons in order to specifically signal properties of stimuli for further processing. Experimental support for this hypothesis has come from the fact that neurons at large distances, within or even between hemispheres can be precisely synchronized, and the level of synchrony is often not only stimulus-specific, but

furthermore consistent with gestalt grouping principles of the stimulus. This theory implies that such synchrony should not be constrained by the structural arrangement of the neurons involved, but rather that most or all neurons, at least within V1 should be capable of being synchronized should the stimulus properties be appropriate. Thus, our findings are generally at odds with this theory, and tend to support an interpretation of CCH peaks based on synaptic connections. However, we cannot rule out the possibility of dynamic stimulus-specific synchronization of firing for several reasons. Our stimuli were significantly different from those used in studies which have provided evidence for this theory in that we did not tailor the stimuli for the receptive fields of the neurons, and we did not alter any gestalt properties of the stimuli. Furthermore, many of the correlations which have been found to support the binding theory of correlations were found to be oscillatory, indicating a more global mechanism, whereas we did not find evidence of oscillatory firing in the present study. It is therefore possible that our experimental conditions were not appropriate to engage the network synchronization mechanisms.

Implications for the mechanisms of orientation selectivity

The results in this chapter indicate that well tuned cells in V1 can receive input from other cells with quite different orientation preferences. Furthermore, the extent to which a neuron receives input from neurons with differing orientation preferences depends on the neuron's location in the orientation map. It would seem that neurons are able to generate and maintain selective responses despite non-selective local inputs. The result is that neurons near pinwheel centers, which presumably receive a very heterogeneous pool of local inputs, are equally orientation selective as are those in the center of orientation domains, where local input is relatively homogeneously tuned for similar orientations. This suggests the possibility that the mechanisms responsible for orientation tuning in neurons in different map locations might be different. Regardless, it seems that the local inputs have little influence on the selectivity of a cell's visual response. It should be noted that the strength of the correlations measured in this study was quite small, on average, the peaks in the CCHs contained at most about 3% of a neuron's spikes. Thus, it is conceivable that local inputs to a neuron provide a small enough proportion of the excitatory drive to a neuron as to have an undetectable influence on the firing rate of a neuron, while still inducing detectable levels of correlated firing. This would be somewhat surprising, based on their relatively large number, found

in anatomical studies. One possible explanation is that the correlations detected in this study arise from common input partly, or entirely, from inhibitory neurons. Theoretical studies have shown that common inhibitory drive, as well as common excitatory drive will produce centered peaks in the CCH, though typically those arising from inhibitory input will be broader.

Still, the most parsimonious explanation is that near pinwheels, even cells with orthogonal orientation preferences can be driven by stimuli that are of intermediate orientations. In effect, this should broaden the specificity at pinwheels. Indeed, the subthreshold responses are broader at pinwheels than at orientation domains (see Chapter 2). However, by a combination of inhibition and the spike threshold, the spike output of pinwheel cells remains as sharply tuned as at orientation domains. This argues for a form of intrinsic control of excitability at the level of the cell and of the network of which it is part – in a manner similar to the homeostatic regulation of excitability in single cells in vitro or in much sparser networks.

Do pinwheel centers represent specific stimulus features?

It has been proposed that neurons near pinwheel centers may specifically represent corners, or "T junctions" (Das and Gilbert, 1999). This conclusion is based upon the findings that 1) neurons on either side of a pinwheel center have non-overlapping receptive fields, 2) neurons on either side of a pinwheel center can have correlated firing, and 3) orthogonal stimuli abutting the receptive field of a neuron can suppress its response. Thus, these authors proposed that the local connections across pinwheel centers have a net inhibitory effect, which somehow signals the presence of a junction between two orthogonal elements in a visual scene. The present results cannot directly address this specific proposal, because the receptive field locations were not adequately mapped, and because specific T-shaped stimuli were not used. Qualitatively, the receptive fields in this study were generally overlapping for all local neuron pairs, regardless of their position relative to pinwheel centers, which would argue against one aspect of the T-junction proposal. Regardless, it is interesting to consider whether some aspect of the visual scene would be represented differentially near pinwheel centers. The fact that the tuning curves of pinwheel neurons are indistinguishable from those in orientation domains implies that the first-order information about stimulus orientation is no different near pinwheel centers. However, if the output of groups of neurons is considered together, the output of a pinwheel center may be

quite different from that of an orientation domain. To the extent that correlated firing may increase the efficacy of inputs to a common postsynaptic target, the output of a pair (or more) of neurons near a pinwheel center, which would be synchronized over a wider range of stimulus configurations, would be more likely to drive a common postsynaptic targets over a range of stimulus orientations. Neurons near pinwheel centers may well integrate visual stimuli containing multiple stimulus orientations differently. For example, a plaid grating might excite a pinwheel center neuron more than it would an orientation domain neuron, because more orientations depolarize the cell. Future studies would be necessary to evaluate this possibility.

Conclusion

The analysis in this chapter indicates that the functional connectivity of pairs of neurons can be extremely non-specific. Neurons with narrow, non-overlapping tuning curves can still have strong correlated firing. It is surprising that they are able to maintain such sharp orientation tuning of their firing rates in the face of such broad connectivity with other neurons in the local cortical network. A similar conclusion was reached in the analysis of the intracellular recordings in Chapter 2. Taken together with that analysis, it appears that many neurons, due to their position in the topographical map of orientation, receive inputs from a very diverse, and sometimes quite broad, compliment of orientations. Yet, the tuning curves are uniform across the orientation map. The broad connections seem to be somehow ignored by the cells in order to generate sharp tuning. Based on the conductance measurements presented in Chapter 2, the most likely mechanistic explanation is that strong inhibition, in combination with the spike threshold, works to limit the inputs that influence the spiking of a neuron. Thus, the inputs appear to be regulated, based on the output tuning of individual cells.

REFERENCES

Aertsen AM, Gerstein GL (1985) Evaluation of neuronal connectivity: sensitivity of cross-correlation. Brain Res 340:341-354.

Aertsen AM, Gerstein GL, Habib MK, Palm G (1989) Dynamics of neuronal firing correlation: modulation of "effective connectivity". J Neurophysiol 61:900-917.

Alonso JM, Usrey WM, Reid RC (2001) Rules of connectivity between geniculate cells and simple cells in cat primary visual cortex. J Neurosci 21:4002-4015.

Bosking WH, Zhang Y, Schofield B, Fitzpatrick D (1997) Orientation selectivity and the arrangement of horizontal connections in tree shrew striate cortex. J Neurosci 17:2112-2127.

Brody CD (1998) Slow covariations in neuronal resting potentials can lead to artefactually fast cross-correlations in their spike trains. J Neurophysiol 80:3345-3351.

Brody CD (1999a) Correlations without synchrony. Neural Comput 11:1537-1551.

Brody CD (1999b) Disambiguating different covariation types. Neural Comput 11:1527-1535.

Das A, Gilbert CD (1999) Topography of contextual modulations mediated by short-range interactions in primary visual cortex. Nature 399:655-661.

Dragoi V, Sharma J, Sur M (2000) Adaptation-induced plasticity of orientation tuning in adult visual cortex. Neuron 28:287-298.

Engel AK, Konig P, Gray CM, Singer W (1990) Stimulus-Dependent Neuronal Oscillations in Cat Visual Cortex: Inter- Columnar Interaction as Determined by Cross-Correlation Analysis. Eur J Neurosci 2:588-606.

Gray CM, Engel AK, Konig P, Singer W (1990) Stimulus-Dependent Neuronal Oscillations in Cat Visual Cortex: Receptive Field Properties and Feature Dependence. Eur J Neurosci 2:607-619.

Hata Y, Tsumoto T, Sato H, Tamura H (1991) Horizontal interactions between visual cortical neurones studied by cross-correlation analysis in the cat. J Physiol 441:593-614.

Kisvarday ZF, Toth E, Rausch M, Eysel UT (1997) Orientation-specific relationship between populations of excitatory and inhibitory lateral connections in the visual cortex of the cat. Cereb Cortex 7:605-618.

Livingstone MS (1996) Oscillatory firing and interneuronal correlations in squirrel monkey striate cortex. J Neurophysiol 75:2467-2485.

Malach R, Amir Y, Harel M, Grinvald A (1993) Relationship between intrinsic connections and functional architecture revealed by optical imaging and in vivo targeted biocytin injections in primate striate cortex. Proc Natl Acad Sci U S A 90:10469-10473.

Michalski A, Gerstein GL, Czarkowska J, Tarnecki R (1983) Interactions between cat striate cortex neurons. Exp Brain Res 51:97-107.

Nelson JI, Salin PA, Munk MH, Arzi M, Bullier J (1992) Spatial and temporal coherence in cortico-cortical connections: a cross-correlation study in areas 17 and 18 in the cat. Vis Neurosci 9:21-37.

Perkel DH, Gerstein GL, Moore GP (1967) Neuronal spike trains and stochastic point processes. II. Simultaneous spike trains. Biophys J 7:419-440.

Rao SC, Toth LJ, Sur M (1997) Optically imaged maps of orientation preference in primary visual cortex of cats and ferrets. J Comp Neurol 387:358-370.

Roerig B, Kao JP (1999) Organization of intracortical circuits in relation to direction preference maps in ferret visual cortex. J Neurosci 19:RC44.

Roerig B, Chen B (2002) Relationships of local inhibitory and excitatory circuits to orientation preference maps in ferret visual cortex. Cereb Cortex 12:187-198.

Roerig B, Chen B, Kao JP (2003) Different inhibitory synaptic input patterns in excitatory and inhibitory layer 4 neurons of ferret visual cortex. Cereb Cortex 13:350-363.

Schwarz C, Bolz J (1991) Functional specificity of a long-range horizontal connection in cat visual cortex: a cross-correlation study. J Neurosci 11:2995-3007.

Toyama K, Kimura M, Tanaka K (1981) Cross-Correlation Analysis of Interneuronal Connectivity in cat visual cortex. J Neurophysiol 46:191-201.

Ts'o DY, Gilbert CD, Wiesel TN (1986) Relationships between horizontal interactions and functional architecture in cat striate cortex as revealed by cross-correlation analysis. J Neurosci 6:1160-1170.

Tucker TR, Katz LC (2003a) Recruitment of local inhibitory networks by horizontal connections in layer 2/3 of ferret visual cortex. J Neurophysiol 89:501-512.

Tucker TR, Katz LC (2003b) Spatiotemporal patterns of excitation and inhibition evoked by the horizontal network in layer 2/3 of ferret visual cortex. J Neurophysiol 89:488-500.

Weliky M, Kandler K, Fitzpatrick D, Katz LC (1995) Patterns of excitation and inhibition evoked by horizontal connections in visual cortex share a common relationship to orientation columns. Neuron 15:541-552.

Yousef T, Toth E, Rausch M, Eysel UT, Kisvarday ZF (2001) Topography of orientation centre connections in the primary visual cortex of the cat. Neuroreport 12:1693-1699.

Yousef T, Bonhoeffer T, Kim DS, Eysel UT, Toth E, Kisvarday ZF (1999) Orientation topography of layer 4 lateral networks revealed by optical imaging in cat visual cortex (area 18). Eur J Neurosci 11:4291-4308.

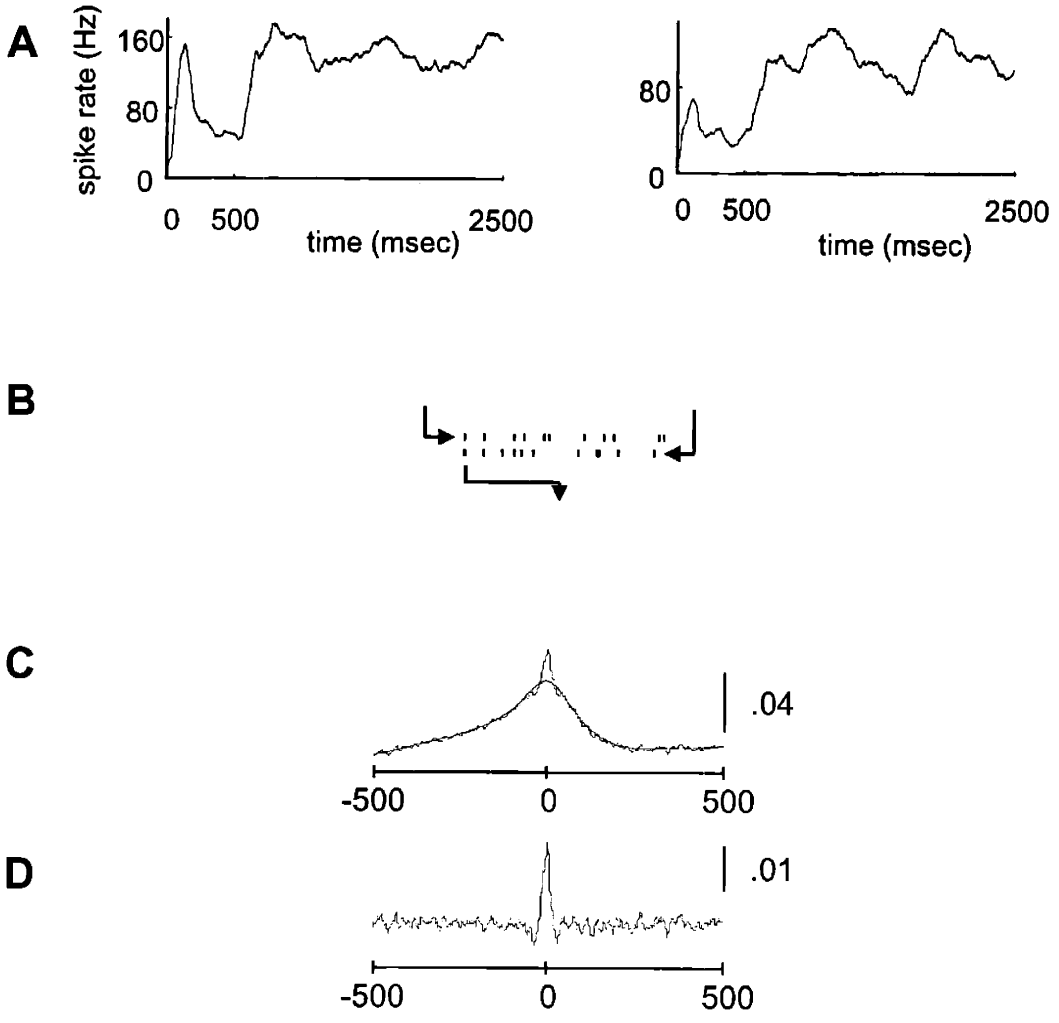
A
spike rate (Hz)
160
80
0
0
500
2500
time (msec)
80
0
0
500
2500
time (msec)
B
C
.04
-500
0
500
D
.01
-500
0
500

Figure 1. Schematic demonstration of the cross-correlation procedure. A. PSTH representation of the responses of the two neurons to the drifting grating stimulus. A stationary grating is presented at time zero, begins drifting at 500 msec, and drifts for 2 secs. The cross-correlation is computed only from the spikes recorded during the drifting phase of the stimulus. B. Raster plot of the responses. Each row depicts the spike times of a single trial. The arrows represent the correlation procedure. C. The shuffle-subtracted CCH is plotted in blue between time lags ranging from –500 to +500 msec. The shuffle-subtracted firing rate correlation is plotted in red. D. The result of subtracting the CCHFR from the CCHshuf.

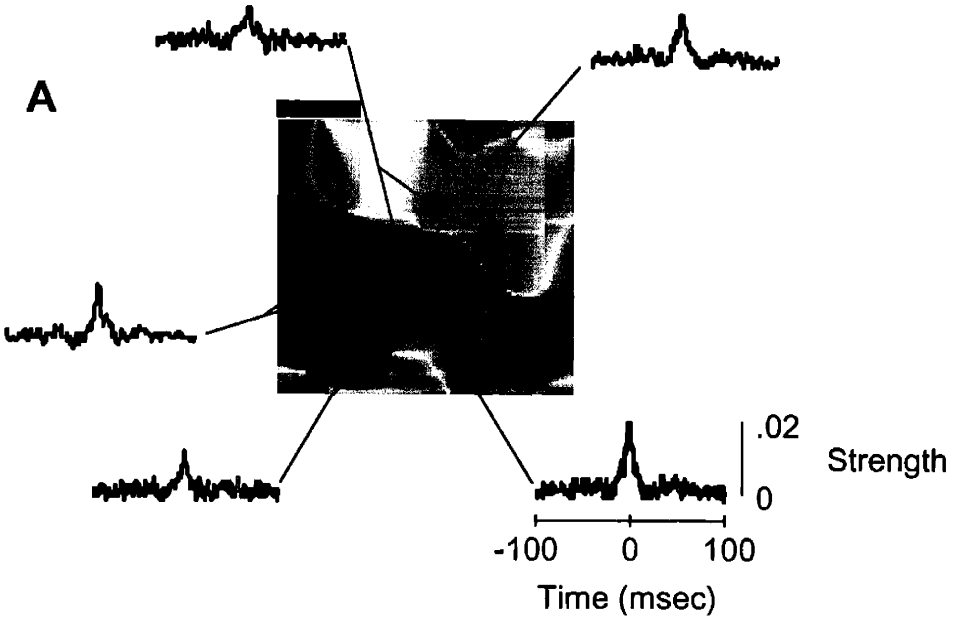
A
.02
0
Strength
-100
0
100
Time (msec)

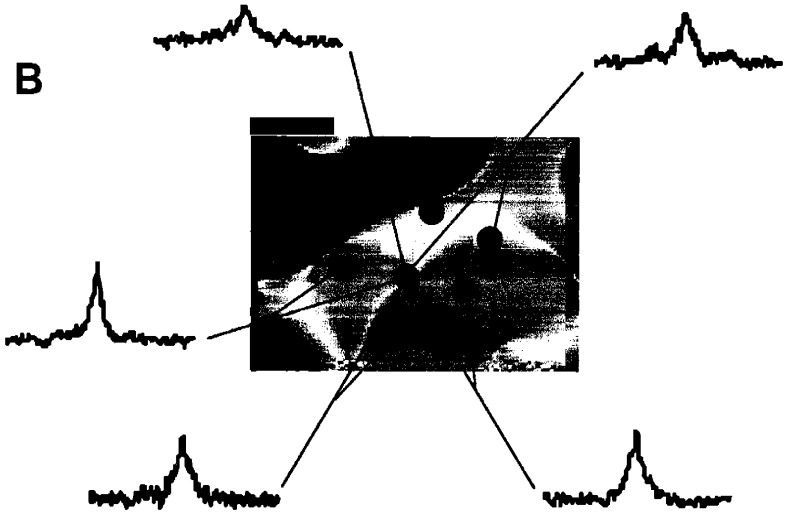
B

Figure 2. Neurons are correlated with their neighbors, regardless of map location. A. Example of recordings from a circular array centered on an orientation domain. The position of each recording site in the orientation preference map is indicated by the cross. The CCHs on the periphery are computed from the spikes of the center neuron and the recording site closest to the CCH graph. The CCHs are computed from time lag −100 to 100 msec. The vertical scale for each CCH is the same, so their heights can be directly compared. The black scale bar represents 500 μm of cortical space. B. CCHs computed between the center neuron, located in a pinwheel center, and each of the surrounding recording sites. All conventions are as in A.

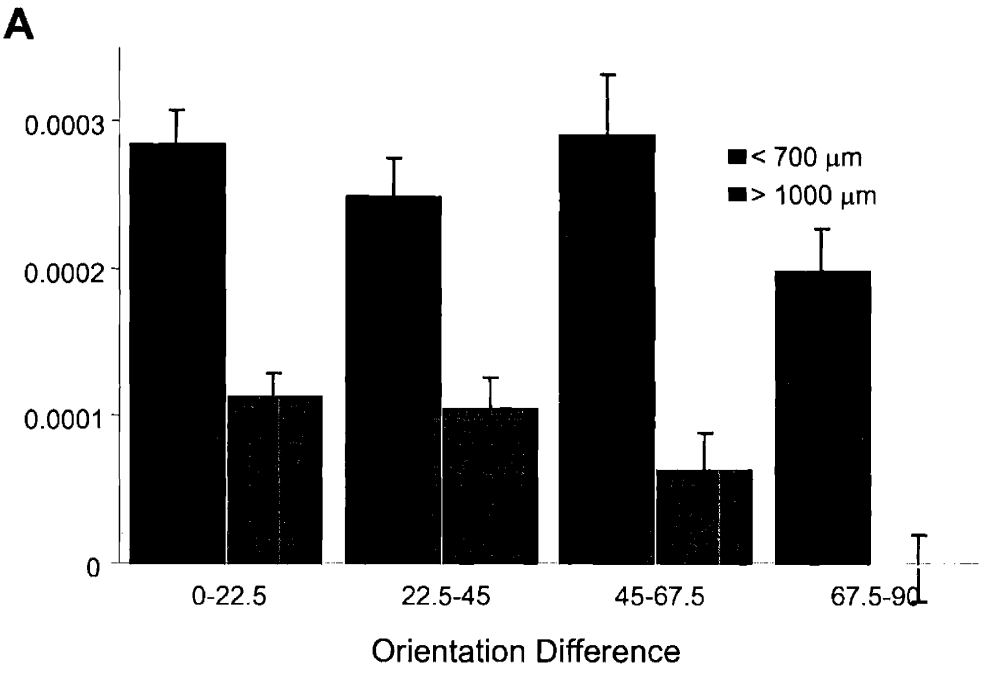
A
0.0003
0.0002
0.0001
0
< 700 μm
> 1000 μm
0-22.5
22.5-45
45-67.5
67.5-90
Orientation Difference

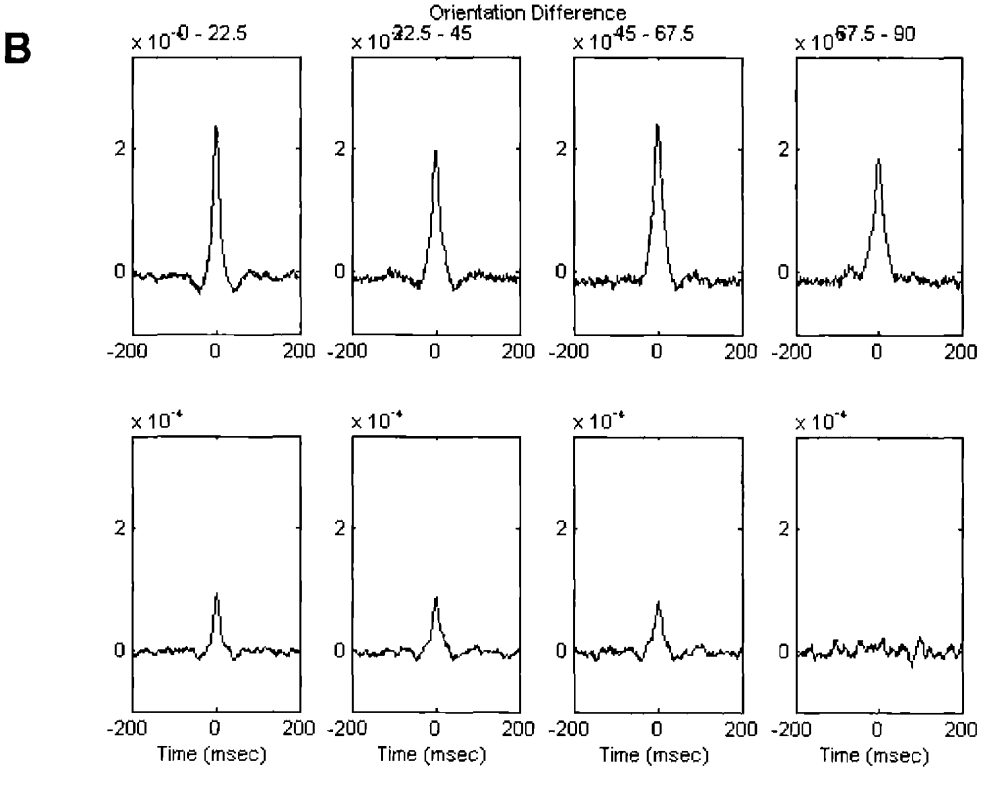
B
Orientation Difference
0 - 22.5
22.5 - 45
45 - 67.5
67.5 - 90
Time (msec)

Figure 3. Correlations between local neuron pairs do not depend on the relative preferred orientations of the neurons. A. Average CCHs of all of the neuron pairs located within 700 μm of each other, for each of four ranges of relative orientation preference. From left to right at the CCHs for neuron pairs with orientation differences between 0-22.5 (n = 120), 22.5-45 (n = 115), 45-67.5 (n = 57), and 67.5-90 (n = 59). B. Averages CCHs of neuron pairs separated by more than 1 mm on the cortex. From left to right at the CCHs for neuron pairs with orientation differences between 0-22.5 (n = 160), 22.5-45 (n = 79), 45-67.5 (n = 47), and 67.5-90 (n = 16).

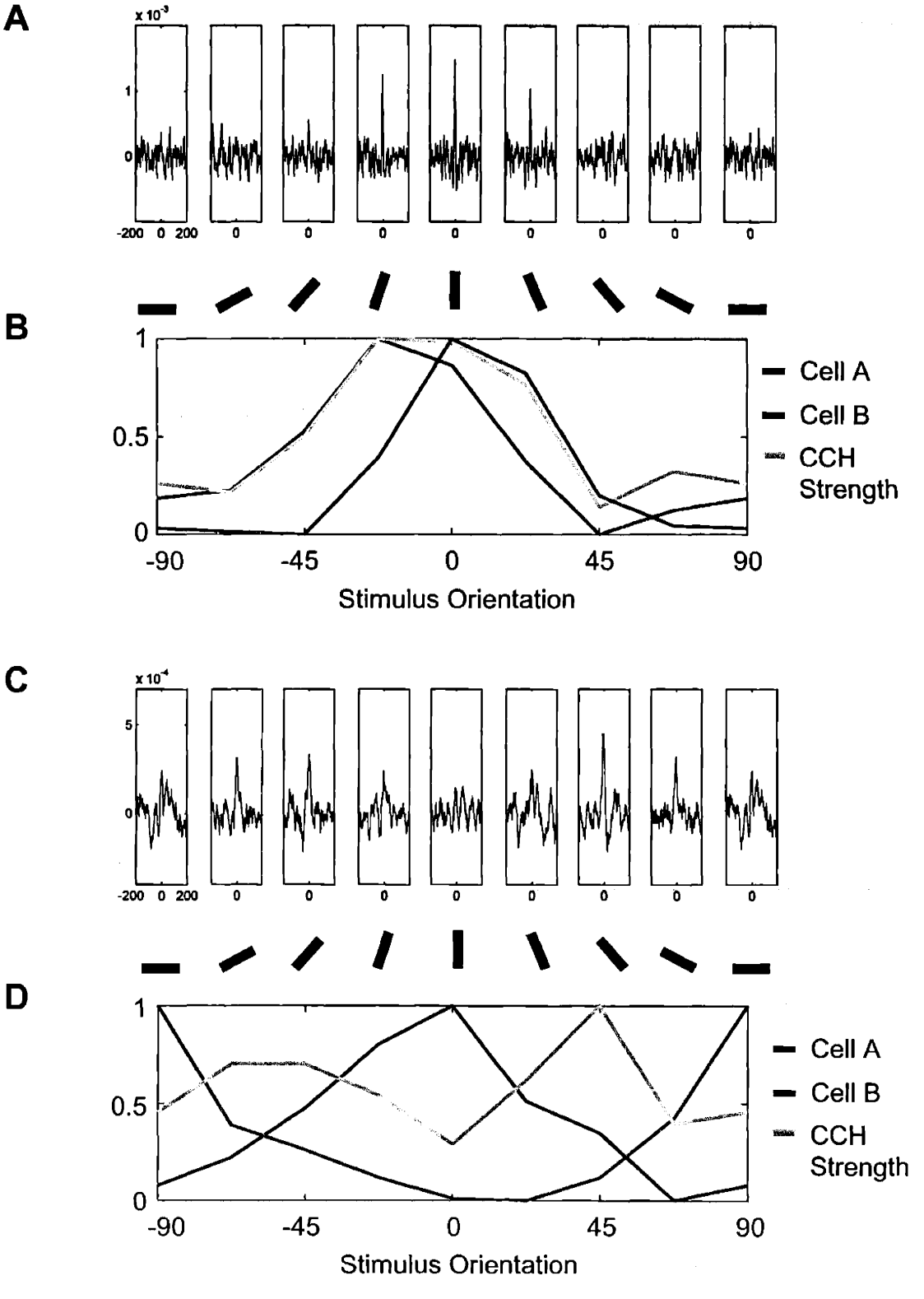
A
x 10^-3
1
0
-200 0 200
B
1
0.5
0
-90
-45
0
45
90
Stimulus Orientation
Cell A
Cell B
CCH
Strength
C
x 10^-4
5
0
-200 0 200
D
1
0.5
0
-90
-45
0
45
90
Stimulus Orientation
Cell A
Cell B
CCH
Strength

Figure 4. Orientation specificity of the strength of correlation for an example neuron pair. A. The CCHs computed for each of eight stimulus orientations, covering 180 degrees. The vertical and horizontal scales are indicated on the left-most plot. The stimulus orientations are in register with the label in panel B. B. The firing rate tuning curves of the two neurons are plotted in red and blue, and the strength of the correlation is plotted in gold. All three curves have been scaled to one, to facilitate visual comparison.

Orientation Difference

0 – 22.5

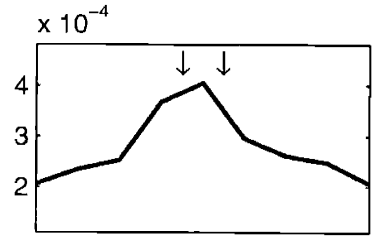

22.5 – 45

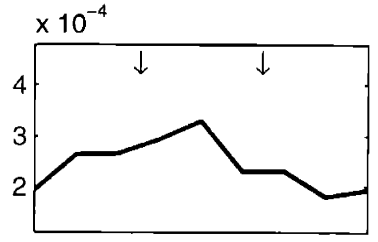

45 – 67.5

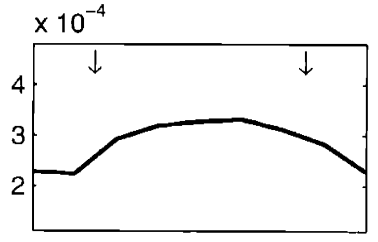

67.5 – 90

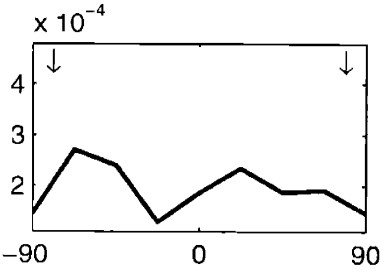

Figure 5. Orientation specificity of correlation strength. Each panel plots the average correlation strength as a function of the stimulus orientation. From top to bottom, the panels plot the average of all neuron pairs falling within the orientation difference bins indicated to the left. Each plot has been aligned to the preferred firing rate orientation of cell a. Thus the preferred orientation of the second cell in each pair moves progressively from the edges (0 and 180) in towards the center (90) from top to bottom, as indicated by the arrows on each plot. Only neurons located within 1 mm of each other were included in this analysis.

Chapter 5: Conclusions and discussion

Summary of results

The goal of this thesis was to gain a better understanding of the role of local cortical connections in shaping the orientation selectivity of responses in V1. The results presented in Chapter 2 demonstrate that the orientation tuning of subthreshold membrane depolarizations of V1 neurons shows a close correspondence with the orientation representation in the local region of cortex surrounding them. This strongly suggests that, to a large extent, the input tuning curves of V1 neurons represent inputs from the local cortical network, assuming spatially isotropic rules for local connectivity. The possible mechanisms that could account for the translation of membrane potential responses into spike responses, across the orientation map, were also considered. The simplest interpretation of this analysis is that input-output transformation of V1 neurons is best explained by strong inhibition that balances excitation and keeps the membrane potential below threshold. Chapter 3 examined the influence of location in the orientation map on the temporal integration of inputs. The reverse-correlation analysis indicates that the temporal development of the orientation selectivity of spike responses does not vary systematically as a function of map location. This result suggests that the filtering of inputs occurs just as rapidly as the responses themselves. Chapter 4 studied the consequences of the superposition of isotropic input regions onto the orientation map for the correlations in the spike times of pairs of neurons. It was found that neurons within ~700 μm of each other tend to have correlated spike trains regardless of their relative preferred orientations. Furthermore, the orientations that elicit correlated firing tend to be those intermediate to the preferred orientations of the two neurons. These result provides further confirmation for the rule of isotropic local connectivity suggested in Chapter 2. They also imply that although the orientation information passed on by individual neurons does not depend on map location, the information carried by ensembles of neurons may depend on proximity to pinwheel centers.

Implications for the mechanisms that generate orientation selectivity

The mechanism(s) that generate orientation selectivity have been controversial. At the crux of the debate has been the question of the degree to which convergent thalamic inputs to layer IV V1 neurons is sufficient to account for the selectivity of these

neurons (the Hubel and Wiesel Model). It must be kept in mind that the contestant models are exclusively concerned with the initial emergence of orientation selectivity in thalamic recipient layer IV cells in the cat. The experiments described here do not directly address this issue. The results however, are important regardless of the model that initially provides the selectivity in simple cells.

Integration of inputs

The broader issue that this thesis addresses, which is implicit in the orientation selectivity debate, is how the different inputs to a neuron are integrated to produce its response properties. What mechanisms are used by V1 neurons to produce constant orientation tuning across the orientation map, despite the diversity of inputs they receive (as a consequence of the pinwheel structure of the map)? Most previous models of orientation selectivity have assumed a canonical mechanism that shapes the orientation tuning of all V1 neurons. This thesis emphasizes that regardless of the form of the model, a single scheme of the inputs involved cannot account for orientation tuning in all neurons.

Most computational or analytical models of orientation tuning have assumed identical orientation tuning of inputs to all neurons (Ben-Yishai et al., 1995; Somers et al., 1995). Recently, a model has been introduced which include the pinwheel arrangement in the model architecture, and assumes isotropic local connections (McLaughlin et al., 2000). This model has successfully demonstrated that with a model neurons in a network with realistic orientation map organization can be orientation selective near pinwheel centers. The model also point to the important role of inhibition for orientation tuning in pinwheel cells, as suggested by the results here. As shown in this thesis, future models will need to incorporate the orientation map structure in order to model the behavior of all V1 neurons.

Relationship between local cortical connections and response properties

In order to address the issue of how anatomical inputs shape response properties, the patterns of anatomical connections need to be known. Fortunately, substantial work has described the connections in V1. This thesis does not present any new anatomical results, but rather makes assumptions of the patterns of connectivity, based on the work of others. The description of connectivity patterns in V1 is fairly

consistent across a number of studies, from several labs, and using different techniques. There has been no demonstration to date of different local connection patterns near pinwheel centers (Yousef et al., 2001), or of any inhomogeneity of local projections in general across the orientation map. Unpublished results from this lab have confirmed that small injections of tracers label an isotropic zone of cells, regardless of the location of the injection site relative to pinwheel centers. Previous in vitro physiological experiments have generally confirmed the isotropic nature of local connections (Weliky et al., 1995; Roerig and Chen, 2002). Taken together, previous work supports the assumption that the structure of local connections is isotropic, with a roughly gaussian falloff. It should be noted, however, that the direct anatomical confirmation that individual neurons receive connections with this same pattern, regardless of map location, is still missing.

All of the analysis in this thesis has aimed to characterize the relationship between responses of V1 neurons and the local pattern of connections. The influence of the inputs from other input sources, most notably thalamocortical projections to layer IV and VI neurons, and long-range intracortical projections in layers II/III have been ignored. The finding that there is a strong relationship between the pattern of local inputs and the subthreshold neural responses provides a good justification for these simplifications. The close relationship between the behavior of individual neurons and the inputs from the local cortical network is not surprising, given previous estimates of the magnitude of local inputs on V1 neuron response (Ferster et al., 1996). The analysis of the local inputs may therefore provide a reasonable estimate of the responses of individual V1 neurons. Future work should be directed towards identifying, and modeling the inputs arising from different sources. For instance, it would be interesting to test whether the thalamocortical projections reflect the pinwheel structure, and might be different for pinwheel center and orientation domain layer IV neurons. Similarly, it would be interesting to know whether the long-range intracortical inputs to individual neurons varies as a function of location in the orientation map.

Conclusion

This thesis has demonstrated that the orientation selectivity of the inputs to V1 neurons varies with the orientation selectivity of the orientation representation in the local cortical region surrounding them, but the selectivity of the spike outputs does not. Neurons near pinwheel centers receive very broadly tuned synaptic inputs, but filter

them such that the orientation tuning of the firing rate responses, throughout the entire duration of the response, is narrowly tuned. Thus the input-output transformation that neurons perform varies systematically with their location relative to the pinwheel map. Inhibition is demonstrated to play a crucial role in regulating this transformation, particularly in neurons near pinwheel centers, where the transformation is most dramatic. Thus the cortical circuit as a whole appears to regulate its connections to generate useful responses from all cells, despite the constraints imposed by the pinwheel structure of the orientation preference map.

REFERENCES

Ben-Yishai R, Bar-Or RL, Sompolinsky H (1995) Theory of orientation tuning in visual cortex. Proc Natl Acad Sci U S A 92:3844-3848.

Ferster D, Chung S, Wheat H (1996) Orientation selectivity of thalamic input to simple cells of cat visual cortex. Nature 380:249-252.

McLaughlin D, Shapley R, Shelley M, Wielaard DJ (2000) A neuronal network model of macaque primary visual cortex (V1): orientation selectivity and dynamics in the input layer 4Calpha. Proc Natl Acad Sci U S A 97:8087-8092.

Roerig B, Chen B (2002) Relationships of local inhibitory and excitatory circuits to orientation preference maps in ferret visual cortex. Cereb Cortex 12:187-198.

Somers DC, Nelson SB, Sur M (1995) An emergent model of orientation selectivity in cat visual cortical simple cells. J Neurosci 15:5448-5465.

Weliky M, Kandler K, Fitzpatrick D, Katz LC (1995) Patterns of excitation and inhibition evoked by horizontal connections in visual cortex share a common relationship to orientation columns. Neuron 15:541-552.

Yousef T, Toth E, Rausch M, Eysel UT, Kisvarday ZF (2001) Topography of orientation centre connections in the primary visual cortex of the cat. Neuroreport 12:1693-1699.